NASA CR 54520

FINAL REPORT

DEVELOPMENT OF A DISPERSION STRENGTHENED NICKEL BASE ALLOY USING THE HIGH INTENSITY ARC PROCESS

by

H. M. McCullough and M. Ortner

prepared for

NATIONAL AERONAUTICS AND SPACE ADMINISTRATION

August 21, 1967

CONTRACT NAS 3-7275

Technical Management
NASA Lewis Research Center
Cleveland, Ohio
Airbreathing Engines Division
F. Harf - Project Manager
M. Quatinetz - Research Advisor

DEVELOPMENT OF A DISPERSION STRENGTHENED NICKEL BASE ALLOY USING THE HIGH INTENSITY ARC PROCESS

by
H. M. McCullough and M. H. Ortner

ABSTRACT

Alloy powders having a nominal composition 60 Ni-20 Co-10 Mo-10W and containing dispersions of thoria, yttria, alumina, magnesia, and lanthana were prepared and evaluated. Based upon their dispersion characteristics, thoria and yttria dispersions were selected for larger scale preparation. Scaleup procedures were developed for powder preparation and billets containing 0, 2, 4, and 7 volume percent thoria and yttria were prepared and evaluated by density and microhardness measurements as well as optical and electron metallography before and after thermal stability tests. The best of the billets produced contained 4% thoria. The yttrium-containing billets evidenced particle growth and inhomogeneous distribution. Clad billets without a dispersion oxide and containing 4% thoria were extruded to bar. The thoria dispersion was stable to the thermal stability test and to the extrusion process. The stress to rupture of this alloy was exceptionally low.

TABLE OF CONTENTS

Section		Page
1	SUMMARY	1
2	INTRODUCTION	4
3	GENERAL PROCESS DESCRIPTION AND PROCEDURE	6
3.1	Preparation of Electrodes	6
3.2	The Arc Vaporization (Hierarc) Process	7
3.3	Hydrogen Reduction and Metal Powder Preparation	12
3.4	Pressing and Sintering of Billets	17
4	EXPLORATORY EXPERIMENTAL AND ANALYTICAL RESULTS	22
4.1	Electrode Composition and Arc Vaporization	22
4.2	Investigation of Various Oxide Dispersions	28
4.3	Establishment of Sintering Cycles	38
5	FINAL POWDER PRODUCTION, SINTERING, AND EXTRUSION	41
5.1	Preparation of Alloy Powders Containing Thoria	41
5.2	Preparation of Alloy Powders Containing Yttria	47
5.3	Pressing and Sintering of Billets	47

TABLE OF CONTENTS (Cont'd.)

Section		Page
5.4	Evaluation of the As-Sintered Billets	49
5.5	Extrusion of Sintered Billets	59
5.6	Stress Rupture Testing	74
6	DISCUSSION OF RESULTS	87
7	CONCLUSIONS	91
8	RECOMMENDATIONS	93
APPENDIX		94

LIST OF ILLUSTRATIONS

Figure No.	Title	Page
1	Mixer	8
2	Extrusion Press	9
3	Harper Furnace for Baking Electrodes	10
4	Typical Electrodes	11
5	Arc Chamber for Production of Submicron Oxide Powders	13
6	Vaporization Head	14
7	Schematic of the Arc System	15
8	Fume Collector	16
9	Hydrogen Reduction Retort and Hayes Furnace	18
10	Dry Box with Tube Reduction Retort	19
11	Flow Chart for Metal Powder Preparation by the Arc Process	20
12	Nickel Alloy Containing ThO_2	29
13	Thorium Oxide Dispersion in Nickel Alloy Prepared from Electrodes Containing Thorium Oxalate (Run #76)	31
14	Nickel Alloy Containing ZrO_2	32
15	Linde B Alumina in Nickel Base Alloy	33
16	Electron Micrograph of Nickel Alloy Containing La_2O_3	35
17	Electron Micrograph of Nickel Alloy Containing Y_2O_3	37

LIST OF ILLUSTRATIONS (Continued)

Figure No.	Title	Page
18	Microstructure of Alloy Powder Sintered for 3 Hours in Hydrogren at Various Temperatures (ZrO_2 Dispersion - Unetched)	39
19	Microstructures of Specimens (Run 73) Sintered at 1425 and 1450°C	40
20	Microstructure of Control Billet (No Dispersoid) as Sintered and After 100 Hour Thermal Stability Test	52
21	Microstructure of Billet Containing 2^{V}/o Thoria as Sintered and After 100 Hour Thermal Stability Test	53
22	Microstructure of Billet Containing 4^{V}/o ThO_2 as Sintered and After 100 Hour Thermal Stability Test	54
23	Microstructure of Billet Containing 7^{V}/o Thoria as Sintered and After 100 Hour Thermal Stability Test	55
24	Microstructure of Billet Containing 2^{V}/o Y_2O_3 as Sintered and After 100 Hour Thermal Stability Test	56
25	Microstructure of Billet Containing 4^{V}/o Y_2O_3 as Sintered and after 100 Hour Thermal Stability Test	57
26	Microstructure of Billet Containing 7^{V}/o Y_2O_3 as Sintered and After 100 Hour Thermal Stability Test	58
27	Electron Micrograph of Control Billet as Sintered	60
28	Electron Micrograph of Control Billet After 100 Hour Thermal Stability Test	61

LIST OF ILLUSTRATIONS (Continued)

Figure No.	Title	Page
29	Electron Micrograph of Billet Containing 2^{V}/o ThO_2 as Sintered	62
30	Electron Micrograph of Billet Containing 2^{V}/o ThO_2 After 100 Hours Thermal Stability Test	63
31	Electron Micrograph of Billet Containing 4^{V}/o ThO_2 as Sintered	64
32	Electron Micrograph of Billet Containing 4^{V}/o ThO_2 After 100 Hour Thermal Stability Test	65
33	Electron Micrograph of Billet Containing 7^{V}/o as Sintered	66
34	Electron Micrograph of Billet Containing 7^{V}/o ThO_2 After 100 Hour Thermal Stability Test	67
35	Electron Micrograph of Billet Containing 2^{V}/o Y_2O_3 as Sintered	68
36	Electron Micrograph of Billet Containing 2^{V}/o Y_2O_3 After 100 Hour Thermal Stability Test	69
37	Electron Micrograph of Billet Containing 4^{V}/o Y_2O_3 as Sintered	70
38	Electron Micrograph of Billet Containing 4^{V}/o Y_2O_3 After 100 Hour Thermal Stability Test	71
39	Electron Micrograph of Billet Containing 7^{V}/o Y_2O_3 as Sintered	72
40	Electron Micrograph of Billet Containing 7^{V}/o Y_2O_3 After 100 Hour Thermal Stability Test	73

LIST OF ILLUSTRATIONS (Continued)

Figure No.	Title	Page
41	Extruded Billets	77
42	Microstructure of as Extruded Billet Without a Dispersion Oxide	79
43	Microstructure of as Extruded Billet Containing 4% Thoria Dispersion	80
44	Electron Micrograph of the Extruded Control Billet Without a Dispersion Oxide	81
45	Electron Micrograph of the Extruded Billet Containing 4% ThO_2	82
46	Location of Specimens in Test Material	83
47	1/4-Inch Creep - Rupture Specimen	84
48	Stress-Rupture Results for Thoriated and Control Material of the 60Ni-20 Co-10Mo-10W Alloy at 2000F	90

LIST OF TABLES

Table No.	Title	Page
1	Chemical Composition of Electrode and Fume Product	23
2	Analysis of Electrodes and Resultant Reduced Powders Using Various Carbons	25
3	Electrode and Product Analysis From Electrodes Containing 10% Black Pearl	27
4	A Comparison of Chemistries of the Electrodes and Product for 3 and 10 Electrode-Size Mixes Containing Thorium Oxide	42
5	Chemistry of Electrode and Reduced Powder for Standard Alloy Without a Dispersion Oxide	43
6	Analyses of Electrode and Reduced Powder for Nominal 2^{v}/o Thoria Alloy	44
7	Analyses of Electrode and Reduced Powder for Nominal 4^{v}/o Thoria Alloy	45
8	Analyses of Electrode and Reduced Powder for Nominal 7^{v}/o Thoria Alloy	46
9	Chemical Analyses of Blended Lots of Alloy Powder Containing Yttria	48

LIST OF TABLES (Continued)

Table No.	Title	Page
10	Billet Weights and Densities	50
11	Knoop Hardness (50 KG Load) of As-Sintered and Thermal Stability Specimens	51
12	Research and Technology Division Experimental Metallurgical Plant Wright-Patterson Air Force Base, Ohio - Extrusion Data Sheet	75
13	Research and Technology Division Experimental Metallurgical Plant Wright-Patterson Air Force Base, Ohio - Extrusion Data Sheet	76
14	Density and Hardness Measurements of Extruded Section	78
15	Results of Stress-Rupture Tests at 2000°F	86

DEVELOPMENT OF A DISPERSION STRENGTHENED NICKEL BASE ALLOY USING THE HIGH INTENSITY ARC PROCESS

by H. M. McCullough and M. Ortner

1. SUMMARY

The application of the high intensity arc process to the preparation of a multicomponent alloy powder containing a homogeneous submicron dispersion was successfully demonstrated. The nominal composition of the alloy selected for evaluation was 60 Ni- 20 Co- 10 Mo- 10 W containing 2, 4, and 7 volume percent dispersion oxide.

The major effort was devoted to the development of an electrode composition which:

1. was sufficiently strong to withstand the very high thermal shock during vaporization,

2. overcome the inherent vaporization problems encountered when combining two groups of metals, namely Ni-Co and Mo-W, having widely different vaporization characteristics,

3. permitted vaporization of the dispersion oxide to submicron particles homogeneously dispersed in the oxide fume product,

4. provided the desired composition of the final alloy.

In the development of high strength electrodes for vaporization, it was necessary to use binder and carbon containing a higher sulfur content than desired. A method was developed to reduce residual sulfur in the condensed fume product to less than 30 ppm.

In preliminary studies, electron microscopic evaluation of pressed and sintered specimens revealed that the high intensity arc process, at the present state-of-the-art, did not provide submicron particles when Al_2O_3, MgO, La_2O_3 or ZrO_2 were utilized as the dispersion oxide. ThO_2 and Y_2O_3, however, appeared to be satisfactory.

It became necessary to readjust the electrode composition on scaling up the process, in order to obtain the desired end product composition, and also to readjust the electrode composition as the dispersion oxide content was changed. No other difficulties were encountered in preparing the thoria and yttria-bearing powders. The yttria, however, was slightly more difficult to vaporize than the thoria-bearing material.

Sintered densities of all billets were 90% or more of theoretical density. Microscopic results showed differences in apparent porosity between the surface and core of the billets and, on several of the billets, a definite macroetch ring could be seen visually. No definite conclusions have been reached as to the possible causes for these differences in structure.

Electron micrographs of billet sections revealed that the best dispersion was obtained in the alloy containing $4^{v}/o$ thoria. The $2^{v}/o$ and $7^{v}/o$ thoria billets contained large oversized dispersion particles. The oversized thoria particles are attributed to incomplete vaporization of the thoria contained in the electrode and/or agglomeration of fine thoria particles at the molten anode face which are ejected from this molten surface by the effluent vapor stream and carried through to the product collection system.

Contrary to preliminary results, the billets containing yttria displayed a gross reaction between the yttria and one or more of the alloy components of the system, yielding extremely large particles in the sintered billets. This interaction is not understood, nor can the inability to duplicate the preliminary results be explained at this time.

The billets containing $4^{v}/o$ thoria and the control billet (no dispersion) were extruded to 1/2 inch diameter for stress rupture testing. The thoria-bearing billet extruded satisfactorily, but the control billet was oxidized, possibly due to faulty canning.

Preliminary stress rupture testing indicated stress levels far below the target strength; consequently, further testing was discontinued. However, the effect of the thoria in increasing the life to rupture was apparent.

2. INTRODUCTION

The demand for iron, nickel and cobalt base alloys to withstand the temperature and stress regimes of future jet engine and space applications is becoming increasingly critical. In previous years, emphasis was placed on the development of Fe, Ni, and Co-based alloys in which the high temperature strength was developed by utilizing solid solution, and precipitation strengthening mechanisms. Unfortunately, increased operating temperatures and extended service requirements have exceeded the strengthening capabilities of these mechanisms since their effects are temperature dependent. Consequently, other methods must be pursued to realize the strengths required for advanced applications.

The most promising approach for achieving improved high temperature strengths is the utilization of the dispersion strengthening mechanism where insoluble, hard ultrafine particles are uniformly incorporated in a metal matrix. Although this type of strengthening is not new, it has not been utilized to a great extent due to the difficulty inherent in the preparation of ultrafine dispersion particles, and in the incorporation of these particles into a metal matrix in a completely random and homogeneous manner. Previous attempts to achieve good dispersions have been made by mechanical mixing of individual powders, co-precipitation and selective reduction, vapor deposition and reduction, and other methods.

Progress in the dispersion strengthening of metals has advanced to the stage where several alloys are commercially available; i.e., SAP aluminum and TD nickel. The development of TD nickel has demonstrated the feasibility of producint an alloy having high temperature stress-rupture capabilities in excess of the best cast or wrought processed alloy. As a result, a number of alloy systems are being studied utilizing powders prepared by various methods.

The purpose of this investigation was to further develop a specific method, namely, the high intensity arc (Hierarc)[1] process, for the preparation of a superalloy metal powder containing a homogeneously dispersed

---

[1] U.S. Patents
2,616,842 - Arc Process for the production of fume, 11/4/52, C. Sheer and S. Korman
2,960,726 - Process for fabricating electrodes, 11/22/60, C. Sheer
3,255,283 - Method for electrode fabrication, 6/7/66, R. Weidman

oxide, having an average particle size of <0.1 micron and an average interparticle spacing of less than 1.0 micron, and ultimately, to prepare sufficient material for stress rupture testing. The over-all objective of this program was to develop and evaluate nickel base alloys, dispersion strengthened by oxide additions, with the goal of producing a material having 3000 hour stress rupture strength of 15,000 psi at 2000°F.

The high intensity arc process could provide the following advantages in the preparation of complex alloys containing a dispersed phase:

a. Dispersion particles less than 1000 angstroms in diameter can be achieved.

b. Homogeneous distribution of dispersion particles is accomplished by vapor phase mixing in the arc plasma.

c. Any alloy composition whose oxides can be hydrogen reduced can be prepared by this method.

d. The method of powder preparation is relatively simple.

A matrix composition of 20 Co-10Mo-10W-balance Ni with 3 to 8 volume percent dispersion of zirconia or thoria was selected for this study for the following reasons:

a. To provide a high strength solid solution alloy in which the dispersed phase can be fully evaluated without influence of secondary reactions.

b. To provide a very stable dispersed phase for further strengthening.

The program was separated into three tasks. In Task I, the utilization of the Hierarc Process to prepare a complex alloy powder containing a dispersoid phase of thoria and zirconia was to be demonstrated. In Task II the parameters were to be determined to scale up the process to prepare a sufficient quantity of powder to press and sinter extrusion billets containing 2, 4, and 7 volume percent dispersion oxide. Under Task III several billets were to be extruded to 1/2" diameter bar stock for stress rupture testing at 2000°F.

3. GENERAL PROCESS DESCRIPTION AND PROCEDURE

3.1 Preparation of Electrodes

The basic premise of the high intensity arc process is the preparation of a submicron oxide by the vaporization of an electrode and the condensation and collection of the resulting oxide particles.

The approach selected to prepare submicron oxides was the homogeneous electrode technique. In this method, all of the alloying constituents, as metal or oxide powders, or combinations of the two, are thoroughly mixed with carbon and an organic binder, extruded, and baked to provide an electrically conductive electrode having sufficient strength to withstand the high thermal stresses encountered during arcing. The constitution of the electrode varies, particularly in the carbon content, because of the wide variation in the vaporization characteristics of different materials.

In this program, homogeneous electrodes were prepared using nickel and cobalt metal powders and oxides of tungsten, molybdenum and the dispersoid. Because of the significant differences in the vapor pressure-temperature relationships of the Ni-Co and MoW groups, it was necessary to develop both electrodes having adequate strength and electrode compositions having satisfactory overall vaporization characteristics.

The types of raw materials are dictated to a large extent by purity, availability, particle size, and density. Generally, irregularly shaped, high density, minus 200 mesh powders are desirable for the preparation of electrodes. The purity level of the raw materials is important, particularly with regard to the carbon. Certain impurities in carbon will carry over into the product, and the higher the carbon content of the electrode, the greater the concentration of impurity in the product. Consequently, low ash contents are necessary. Lists of the raw materials used in this program and their chemical analyses are given in Appendix A.

To prepare the electrodes, appropriate amounts of -200 mesh nickel and cobalt metal powders and molybdenum oxide, tungsten oxide, and the dispersion oxides were mixed with carbon and binder until the mix was thoroughly blended and wetted. A Lancaster Countercurrent Batch Mixer having a capacity of 1/10 cu. ft. was utilized to prepare electrodes for the development and evaluation studies. Sufficient material could be processed in this mixer to provide

three electrodes, 1 inch in diameter by approximately 30 inches long. A similar mixer having a capacity of 5/8 cu. ft. was utilized for preparation of electrodes for the scale-up studies and for the preparation of powders for the billets. Sufficient material could be processed in this mixer to provide ten electrodes, 1 inch diameter by approximately 30 inches long. The larger mixer had a slower mixing action and a heavier roller than the smaller mixer, consequently, mixing times were approximately twice as long in the larger unit.

The mix was evacuated after charging into the chamber of the extrusion press, and extruded at a pressure of approximately 2000 psi at a 4.1 reduction. After extrusion, the electrodes were heated in stainless steel tubes in a Harper, Globar-heated box furnace at 100°C per hour to 900°C, held four hours at 900°C, and then cooled at the natural rate of the furnace to 200°C before removal. Figures 1, 2, 3, and 4 are photographs of the 1/10 cu. ft. Lancaster Mixer, the extrusion press, baking furnace, and typical electrodes produced by this procedure.

3.2 The Arc Vaporization (Hierarc) Process

The Hierarc Process utilizes a high intensity electric arc as the energy source. The process material is incorporated into the anode, vaporized, and collected by condensation of the effluent vapors. One of the most important features of the high intensity arc is that the material to be vaporized is incorporated into the arc anode and all of the constituents are vaporized simultaneously. This permits direct application of a major fraction of the arc energy to the process material, thus achieving highly efficient energy transfer. When the high intensity mode of arc operation is used, the anode material is rapidly vaporized in the form of a plasma of ionized gas with a peak temperature of approximately 7000°C. The electrode is rotated to promote uniform burning at the anode face, and the arc gap is maintained by an electrically driven feed which is manually controlled. The graphite cathodes are fed in the same manner since these too are consumed due to the high temperatures generated.

The anode feed rates, which are governed by the rate of vaporization, vary depending upon the carbon content of the electrode and the power required for vaporization; the less the carbon content of the electrode and/or the higher the power, the greater the rate of vaporization. Because of the different vaporization modes of the materials used in this program, the maximum power level available, 40 kw, was used to vaporize all of the electrodes processed.

As soon as the plasma cools below the dew point, rapid condensation occurs to form extremely fine particles. This fine state of subdivision is due to the high

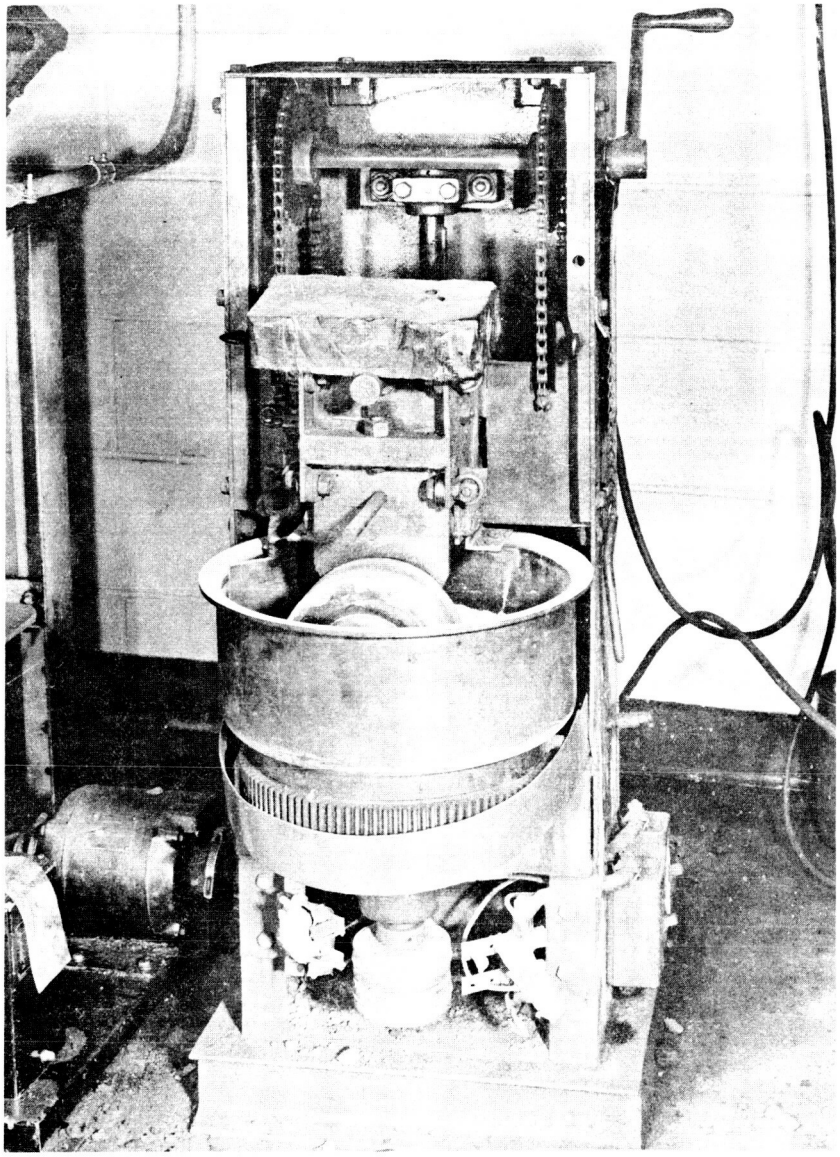

FIGURE 1

MIXER

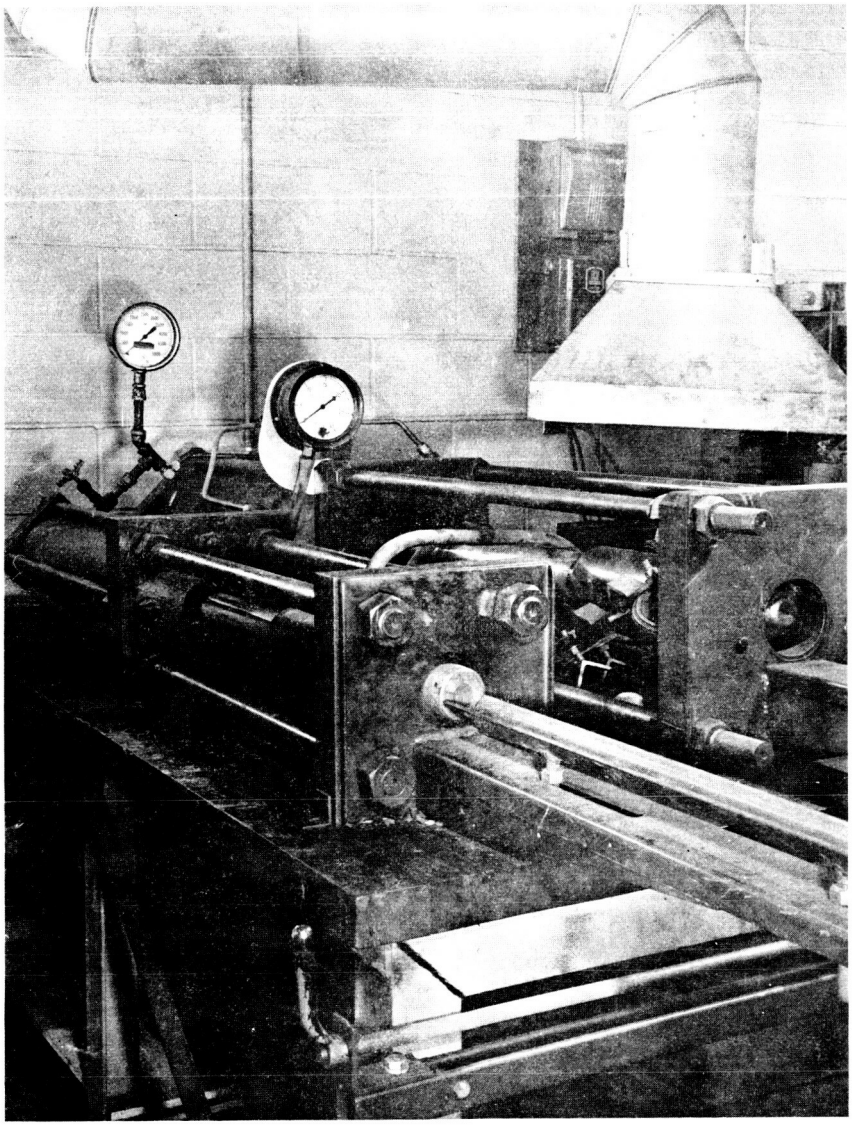

FIGURE 2

EXTRUSION PRESS

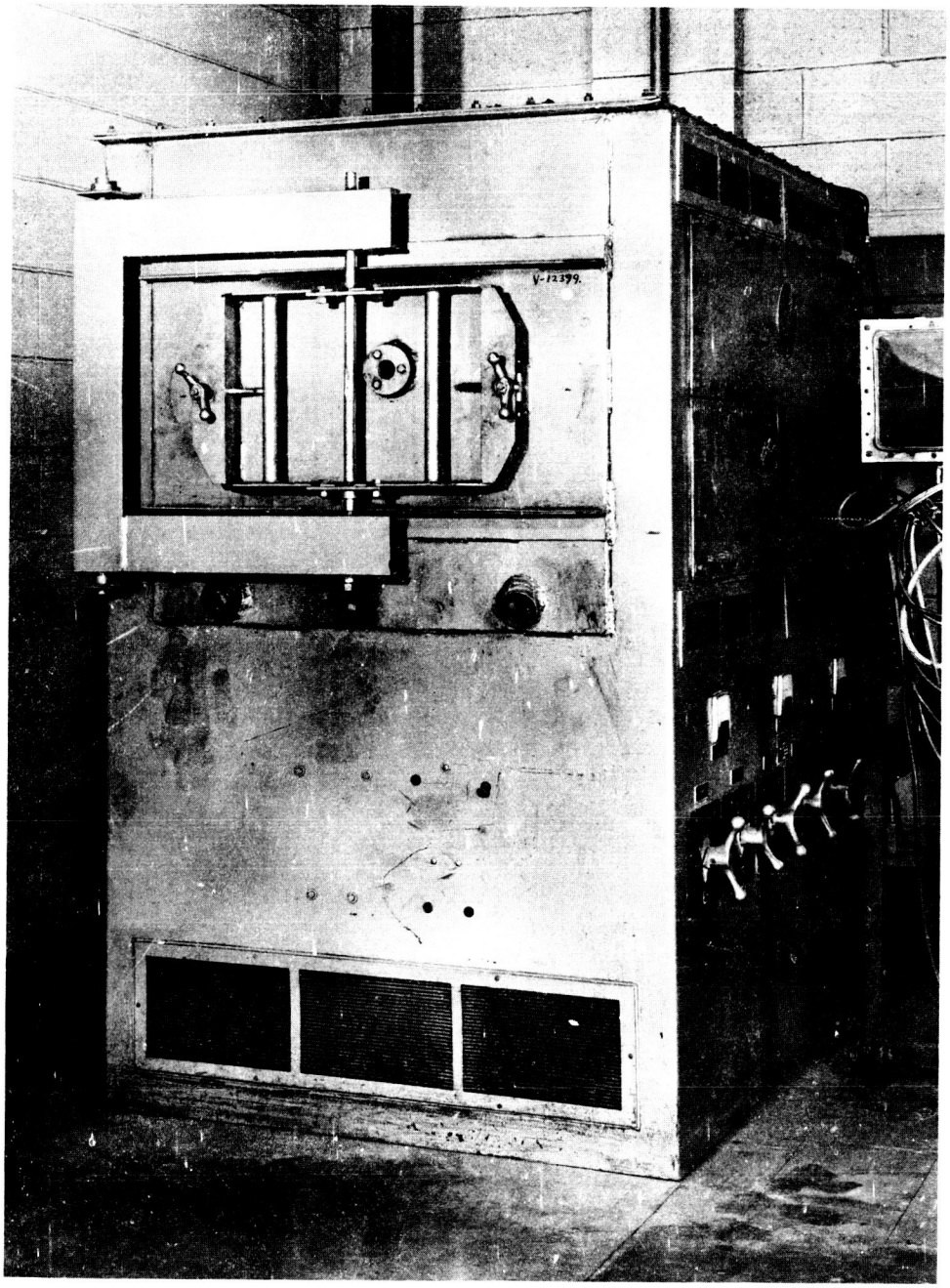

FIGURE 3

HARPER FURNACE FOR BAKING ELECTRODES

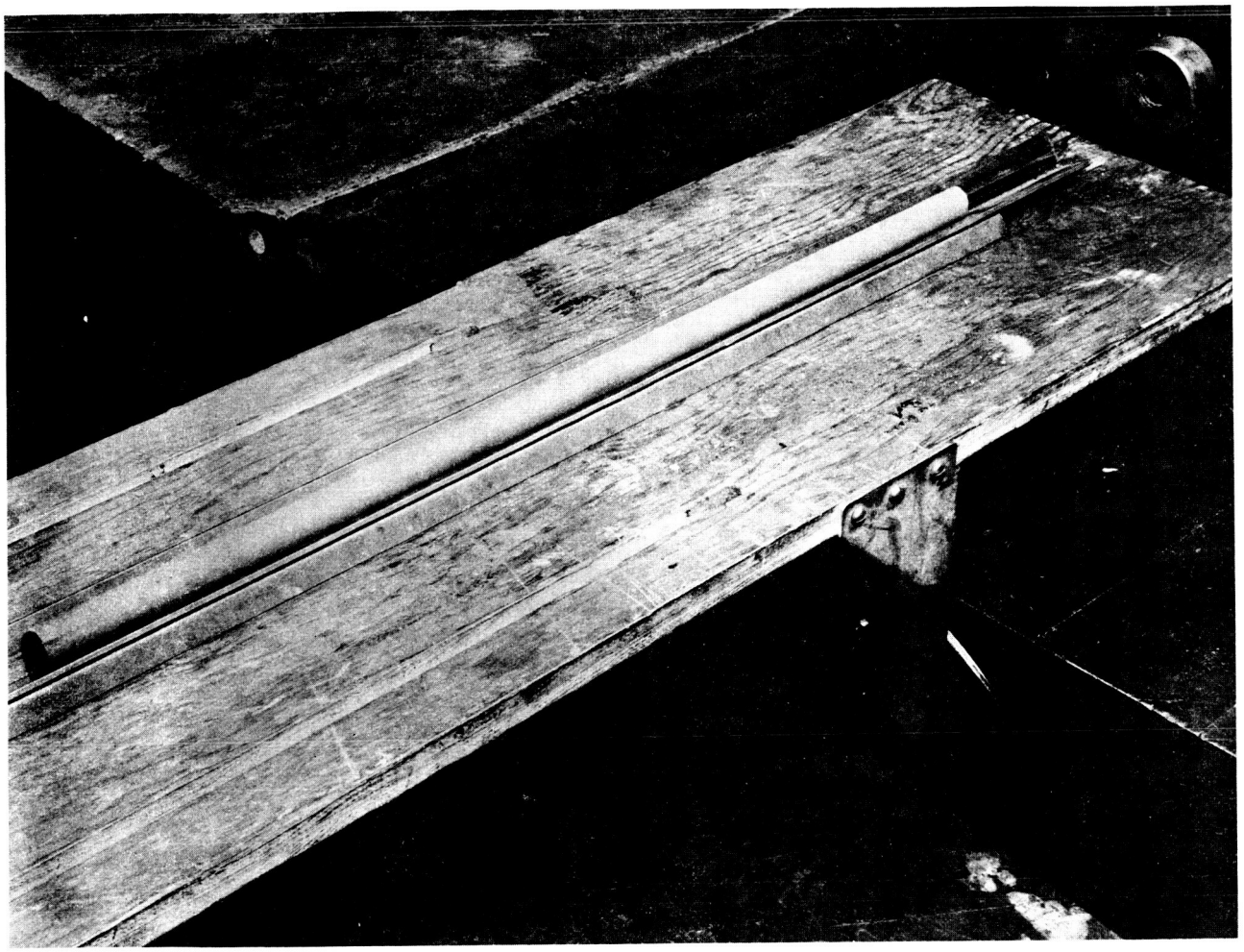

FIGURE 4

TYPICAL ELECTRODES

density of positive ions and free electrons which present nucleation sites for a large number of individual particles, and to the large temperature gradient along the plasma which permits rapid cooling of these particles so that they have little time to grow.

The vaporization of the homogeneous electrode (covaporization) provides a completely homogeneous mixture of all the electrode constituents and this homogeneity persists upon condensation of the plasma. Control of particle size can be maintained to a certain extent by quenching the plasma with an air jet, and particle sizes from 100-500 angstroms are readily achieved. Figures 5 and 6 are photographs of the arc chamber and the anode-cathode mechanisms, respectively. Figure 7 is a schematic of the arc operation.

The condensed fume is exhausted from the chamber by a high velocity air stream created by an exhaust blower on the discharge side of the bag collector. After leaving the chamber, the condensed fume passes through several cyclone collectors and is finally collected in a reverse jet bag collector in the form of agglomerates held together by electrostatic forces. The fume is collected in the container at the bottom of the bag collector shown in Figure 8. The submicron fume product contains all of the alloy constituents homogeneously blended by vapor phase mixing.

To further define the term "vaporization" as it is used in this report, when an arc is struck between the baked electrode (anode) and cathode (graphite rod) at high current density, the temperatures generated at the anode face are sufficient to convert material at the anode face to a true vapor. Under ideal conditions, the transition from solid-to-liquid-to-vapor is so rapid that transformation of all of the material to the vapor phase occurs if the electrode has sufficient strength to withstand the thermal shock. If the transformation to the vapor phase is slow, however, an excess liquid phase accumulates which will drip from the electrode or be ejected as shot from the anode face. If the electrode has poor thermal shock qualities, solid chips will break off the electrode and drop to the chamber floor. Therefore, the vaporization characteristics of an electrode are determined primarily by the degree of melting and by the thermal shock resistance of the electrode formulation.

3.3 Hydrogen Reduction And Metal Powder Preparation

The reduction of the submicron alloy oxide fume was carried out under a hydrogen atmosphere, in a conventional batch type Inconel retort containing 5 trays, in a Hayes box type furnace. The retort and its carriage are so designed that the reduced powder can be discharged into an argon atmosphere

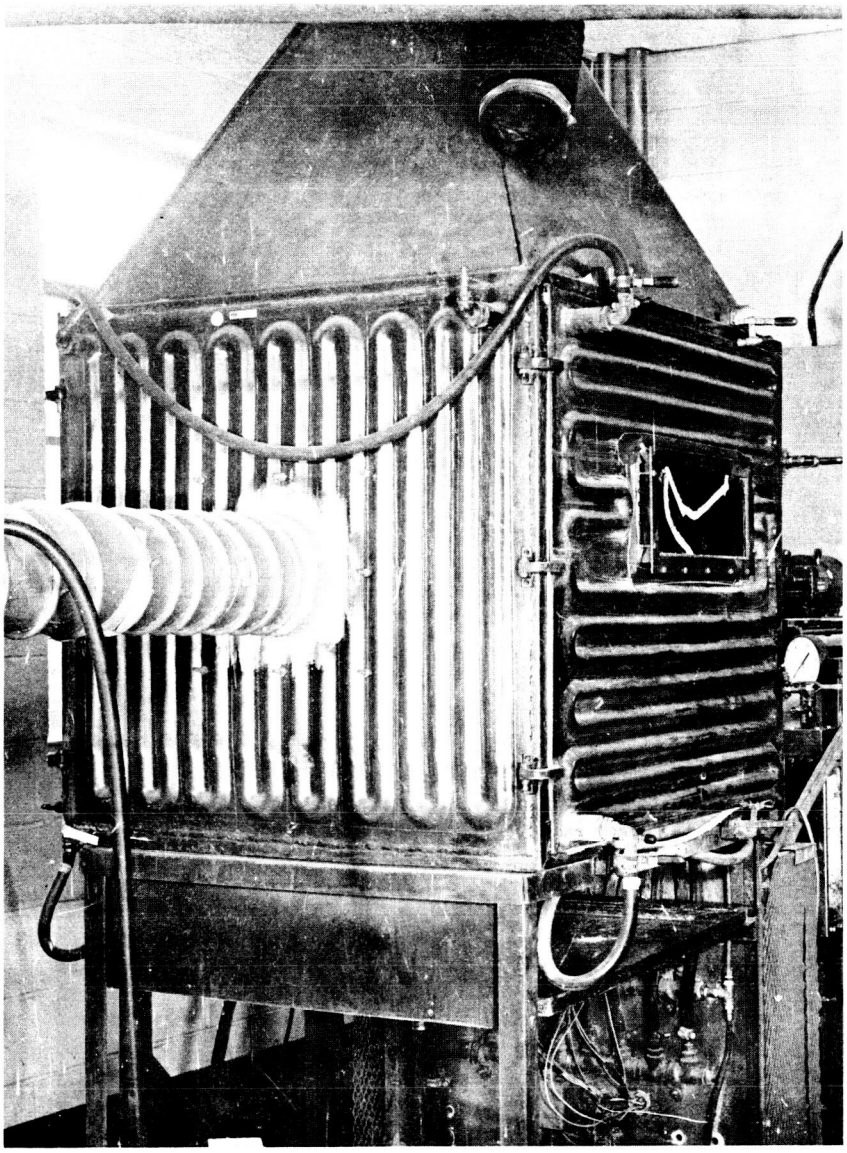

FIGURE 5

ARC CHAMBER FOR PRODUCTION
OF SUBMICRON OXIDE POWDERS

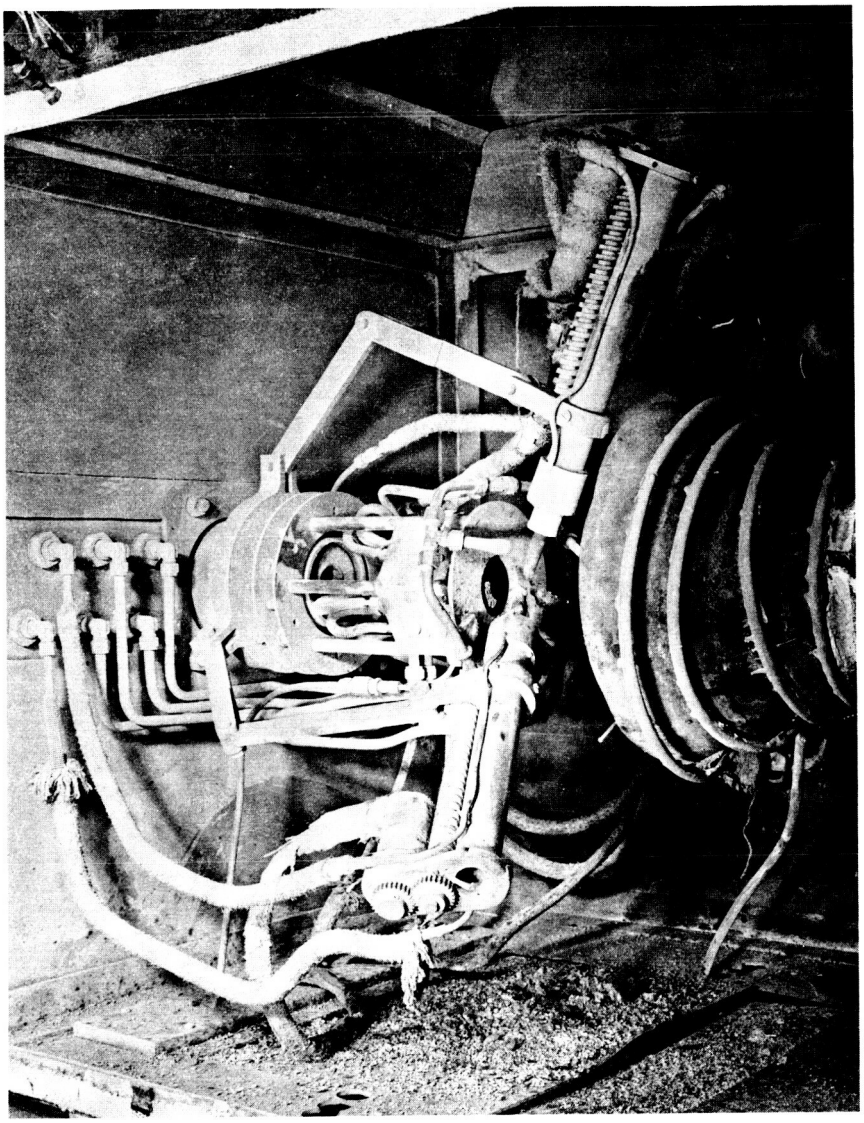

FIGURE 6

VAPORIZATION HEAD

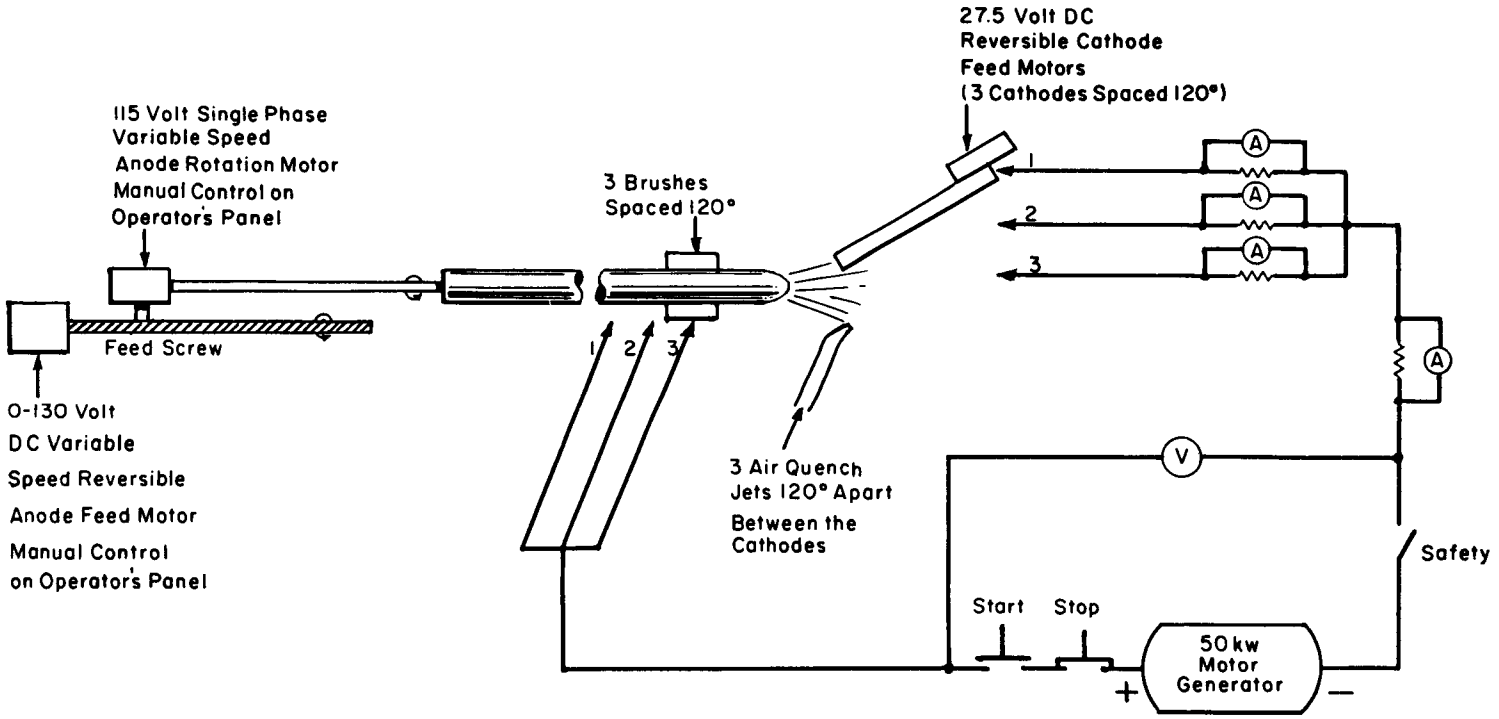

FIGURE 7

SCHEMATIC OF THE ARC SYSTEM

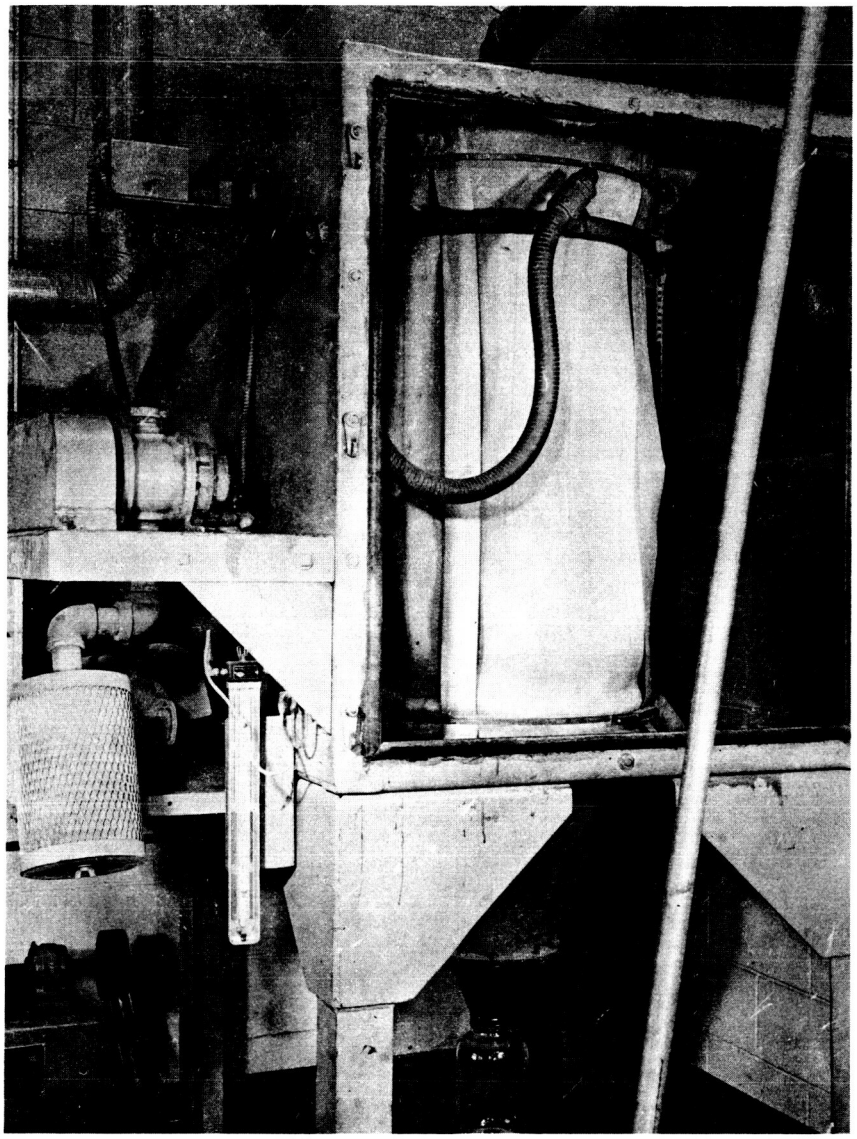

FIGURE 8

FUME COLLECTOR

receptacle which can be detached and taken into an argon atmosphere drybox. The maximum capacity of the retort is approximately 1500 grams of oxide fume yielding about 1100 grams of reduced metal powder per charge.

The reduction conditions of time, temperature, hydrogen flow rate, depth of powder bed, etc., are dictated by the properties desired in the reduced metal powders. The cycle utilized for the alloy powder for this program was: ambient to 650°C in 15 hours; hold at 750°C for 3 hours including the 15 minutes required for heating from 650° to 750°C; then cool. The hydrogen flow rate was approximately 50 cu.ft/hr., and the depth of the oxide powder bed was maintained at 1/4". This cycle is considerable longer than necessary, but was established as a matter of convenience since a shorter cycle could not be effected with this equipment within a normal working day.

The reduction of small quantities of powder was carried out in a 2" diameter Inconel tube furnace which was attached to a drybox. Reduced specimens were taken directly into the drybox under an argon atmosphere. Approximately 10 grams of oxide could be reduced per charge in this furnace. The cycle utilized in the small tube retort was a 1-hour hold at 800°C after reaching temperature in approximately 1 hour.

Figures 9 and 10 show the large reduction retort, and the drybox with the small reduction tube, respectively. The reduced powder from the retort consisted of loosely sintered agglomerates which were readily broken up by brushing on a 100 mesh screen. Three batches of electrodes (a total of 30 electrodes) were required to prepare about 2500 grams of reduced metal powder of a given dispersion content for pressing a billet preform. The three lots were combined after reduction and tumbled for several hours, then screened through -270 mesh to break up any large agglomerates formed as a result of tumbling. The powders were maintained under an argon atmosphere during tumbling and screening. Figure 11 shows a flow chart of the overall process for making metal powders by this process.

3.4 Pressing and Sintering of Billets

The blended powder lots were prepressed under argon in a 2-1/2 inch diameter die under a load of 4000 psi using a 50 ton Dake Press. After pressing, the ejected preformed billet was bagged in rubber tubing, evacuated, and sealed for hydrostatic pressing under a 40,000 psi loat at Kawecki Chemical Corporation.

The pressed billets were sintered individually in a resistance heated, vertical

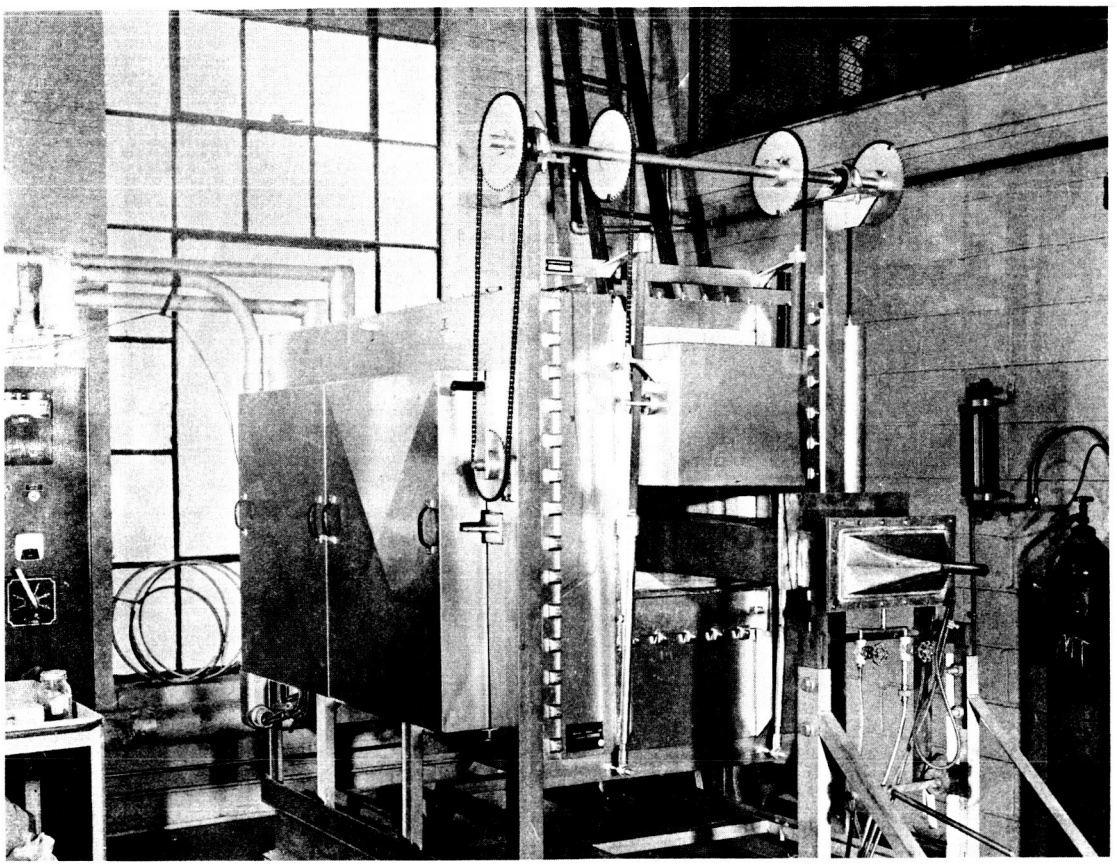

FIGURE 9

HYDROGEN REDUCTION RETORT
AND HAYES FURNACE

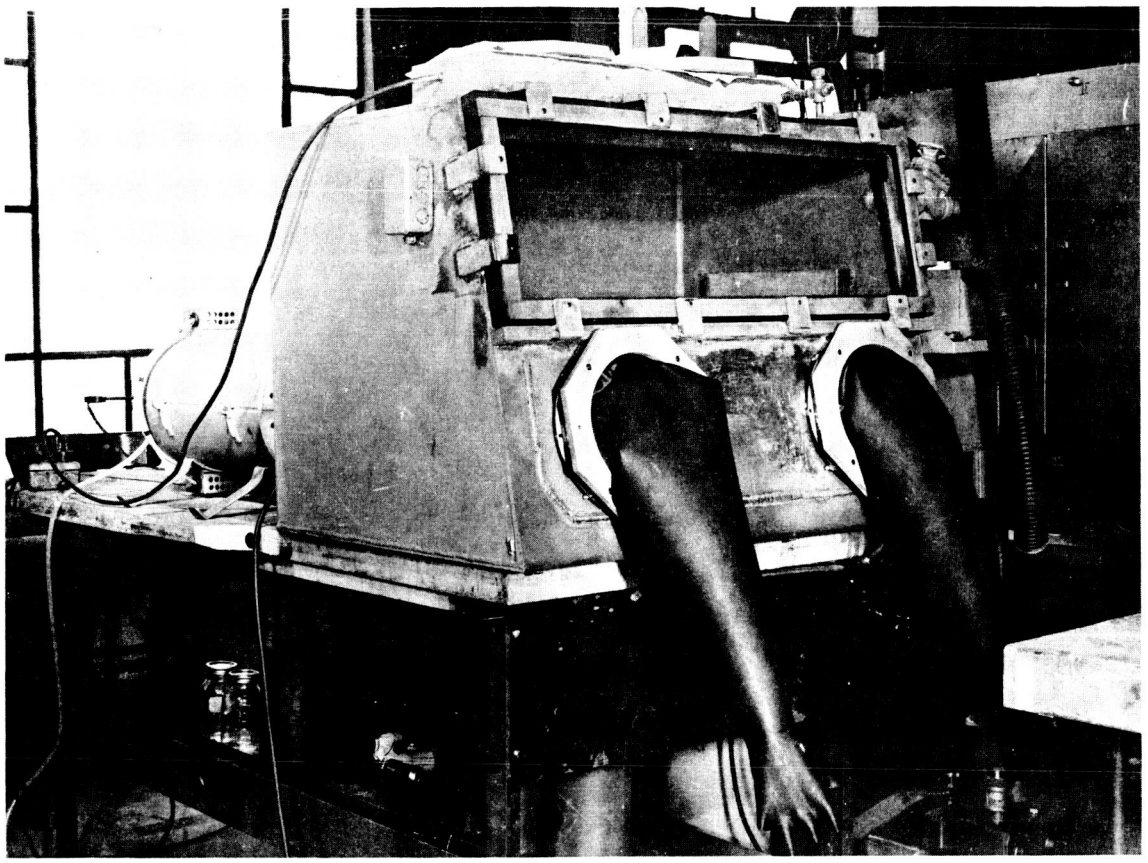

FIGURE 10

DRY BOX WITH TUBE REDUCTION RETORT

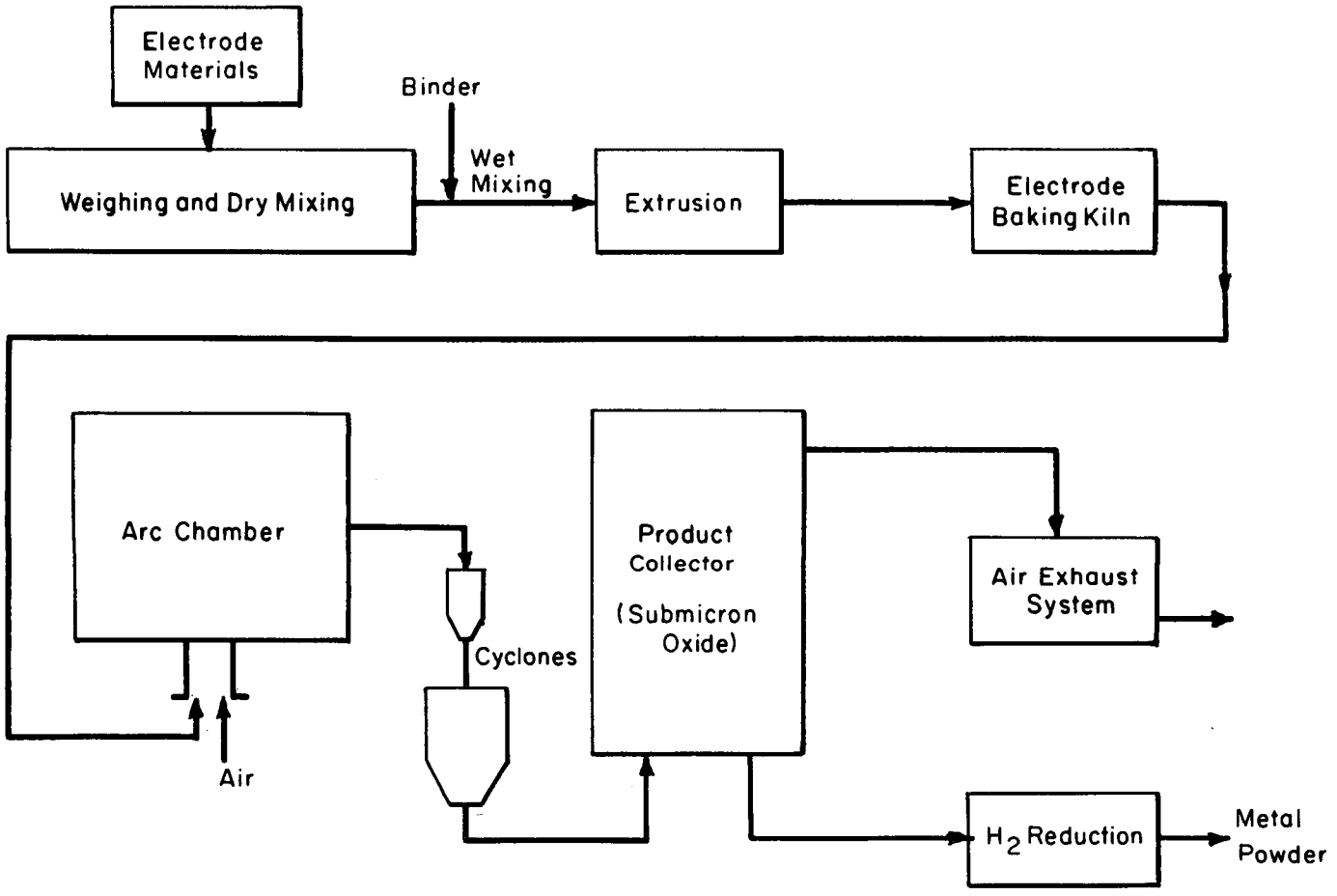

FIGURE 11

FLOW CHART FOR METAL POWDER PREPARATION
BY THE ARC PROCESS

alundum tube furnace in a hydrogen atmosphere. The sintering cycle was established in this furnace by using two billets prepared from powder which was chemically out-of-specification. The cycle established was 4 to 5 hours to a temperature of 1350°C with a two hour hold at temperature. The billets were furnace cooled overnight under hydrogen.

For the preparation of evaluation specimens, metal powders were compacted in a Carver press, bagged, evaculated, and isostatically pressed to the desired load in a 1-inch diameter isostatic chamber. Sintering was performed in a Globar type alundum tube furnace in a hydrogen atmosphere or in a Model 1064 Brew vacuum furnace.

4. EXPLORATORY EXPERIMENTAL AND ANALYTICAL RESULTS

4.1 Electrode Composition and Arc Vaporization

A major effort was devoted to the development of an electrode formulation which provided an electrode having adequate strength and vaporization characteristics, and desired purity levels in the product. Many problems arose in the selection of materials, particularly carbon, of adequate purity from which strong electrodes could be fabricated which would withstand thermal shock and provide a sufficient quantity of vaporized product. The two basic groups of elements, Ni-Co and Mo-W, which have widely different vaporization characteristics, had to be incorporated into a homogeneous electrode in the proper ratio and with the proper carbon content to fulfill the requirements of vaporization and strength, and yield a high purity oxide fume of the desired composition. The Mo-W group does not vaporize as effectively as the Ni-Co group when combined into a homogeneous electrode. Furthermore, it appears that the Ni-Co group promotes reduction of MoO_3-WO_3 at the arc-anode interface forming molten drops of Mo-W metal which do not vaporize sufficiently rapidly and ultimately drop to the bottom of the chamber.

In the initial attempts to improve the vaporization characteristics of the homogeneous electrode, carbon contents between 5 and 50 percent were studied using small mixes (3 electrodes per mix). Table 1 lists some typical analytical results of electrode composition versus fume product composition from electrodes made with varying carbon contents.

Several runs in Table 1 are listed as two-step electrode fabrication. In the two-step method, one or more of the constituents is premixed with the binder, and cured and crushed prior to being mixed with the remainder of the mix. This method frequently improves electrode strength and burning characteristics. No improvements in vaporization were realized in this system within the limited studies made. In addition to poor and inconsistent electrode strengths, considerable melting and dripping occurred at the anode face during vaporization with electrodes containing low carbon contents. Electrodes containing up to 10 percent carbon dripped profusely and burned so rapidly that the maximum feed rate of the electrode was inadequate to maintain a continuous arc. Electrodes containing between 10 and 30 percent carbon dripped and ejected fine shot; the dripping decreased with increasing carbon content; and electrodes containing 30 to 50 percent carbon ejected fine shot.

TABLE 1

CHEMICAL COMPOSITION OF ELECTRODE
AND FUME PRODUCT

	Run No.	20	21	22	23[1]	24	25[2]	31	32[3]
ELECTRODE[5]	Ni	48.7[4]	49.8	48.1	46.6	34.1	77	48.2	52
	Co	--	--	--	--	12.0	--	--	--
	Mo	21.2	20.6	21.2	22.1	18.6	10	21.4	23
	W	22.9	22.4	23.0	23.8	21.8	10	23.1	25
	ZrO_2	7.2	7.1	7.2	7.5	14.3	3	7.3	--
	Carbon Equiv.[6]	4.7	4.3	7.6	10.6	1.1	5	50	5
PRODUCT[5]	Ni	74	84.5	86	93.5	57.3		73	54.3
	Co	--	--	--	--	11.0	Not	--	--
	Mo	12.9	5.1	8.9	4.5	7.8	Analyzed	11.8	17.6
	W	12.4	8.1	3.8	1.54	20.2		13.1	24.2
	ZrO_2	1.68	2.06	1.28	.52	3.8		2.1	3.9

Runs 25 through 30 not analyzed due to poor burning or weak electrodes.

(1) Two-step procedure for MoO_3 and WO_3.
(2) Two-step procedure for NiO, MoO_3, WO_3, and ZrO_2. (NiO used instead of Ni metal powder)
(3) Two-step procedure for Ni only.
(4) All values weight percent.
(5) Analysis of oxide calculated to reduced metal equivalent.
(6) Percent carbon given based on actual weight of metals and oxides used in electrode formulation.

The electrodes containing 50 percent carbon appeared to have the best overall vaporization characteristics but the amount of oxide fume produced per unit weight of electrode was very low due to the high carbon content. Also, the collection system becomes overheated within a short time due to the high volume of hot CO gas formed.

Concurrent with the studies to improve electrode strength and vaporization, the carbon purity versus oxide fume product purity was investigated, particularly with regard to sulfur and SiO_2. The existence of sulfur in the final product was somewhat surprising considering the extremely high arc temperatures, for it was thought that sulfur and similar elements would either be removed by oxidation to a gaseous product or be diluted to a negligible concentration. It was established, however, that sulfur does react quite readily with certain elements during condensation of the vapor; and the concentration in the product increases as the amount of carbon in the electrode is increased.

Dual approaches were studied for sulfur removal. One was to employ high purity materials, e.g. G-38 graphite. This led to reduction of sulfur levels in the product from 300-500 ppm to 30-70 ppm. However, the strengths of the electrodes reverted to powder during baking.

The other approach to sulfur removal was calcination of the oxide fume product in air prior to reduction. A series of experiments revealed that calcining at 600°C for 4 hours in air effectively removed sulfur to less than 30 ppm.

Since stronger electrodes resulted when the higher sulfur-bearing (.063%) carbon and binder were used, a series of electrodes was made using different carbons. (See Appendix A for analyses of carbons.) The sulfur contents of the fume products were all reduced to less than 30 ppm after calcination. As a result of these experiments, it appeared that the electrodes prepared with Thermax carbon were the strongest.

Next, a series of runs was conducted using 40% or 50% Thermax carbon, 10% Black Pearl or 10%G-48 carbons in the electrode formulations to determine the effect of the SiO_2 ash content upon the SiO_2 content of the product fume. The 10% content was chosen to compensate for its higher sulfur content and to facilitate sulfur removal during subsequent calcination of the fume prior to reduction. Furthermore, the lower carbon would improve the yield per unit weight of electrode vaporized. Table 2 lists typical data from these studies.

TABLE 2

ANALYSIS OF ELECTRODES AND RESULTANT REDUCED POWDERS USING VARIOUS CARBONS

	52		58		62		64	
Run No.	Electrode	Reduced Powder	Electrode	Reduced Powder	Electrode	Reduced Powder	Electrode	Reduced Powder
Nickel	28.5	56.3	11.0	48.9	11.0	36.8	11.0	41.4
Cobalt	13.5	27.4	4.6	21.3	4.6	14.6	4.6	15.9
Molybdenum	24.0	5.4	35.7	10.8	35.7	18.0	35.7	19.3
Tungsten	24.0	4.4	38.7	10.2	38.7	16.6	38.7	14.5
Zirconia	10.0	2.1	10.0	2.3	10.0	7.9	10.0	6.0
Silica		~4		~5		.023		.015
Sulfur		<30ppm		<30ppm		<30ppm		<30ppm
Carbon	50% Thermax		40% Thermax		10% Black Pearl		10% G-48	

The silica contents of the powders prepared from electrodes which contained Thermax carbon were exceptionally high. Although it was expected that the powder produced using Thermax would be higher in silica than those from the G-48 or Black Pearl carbons, a material balance taking into account the SiO_2 content of all the materials used could not account for more than 1% of the SiO_2 found in the products of Runs 52 and 58. The source of the excess silica found was not determined in this series of experiments.

Since it was somewhat difficult to prepare electrodes using graphites (G-38 and G 48) due to their poor wetting characteristics with the binder, all subsequent electrode preparations were made using the Black Pearl carbon. Vaporization of the electrodes containing the lower carbon contents was also improved. For the same electrode compositions considerably more molybdenum tungsten and zirconia were converted to fume product for the electrodes containing 10% carbon (Runs 62 and 64) than those containing 40 and 50% carbon (Runs 52 and 58). The over-all yield was also approximately doubled.

Several runs were made with minor variations in electrode chemistry to produce fume product for reduction, sintering and electron microscopic evaluation. Table 3 shows the electrode and reduced powder compositions. Runs 73 and 74 were identical to illustrate the reproducibility of the process when all variables are held constant.

The good control of composition is reflected in Runs 72, 73, and 74 in Table 3. The electrode chemistry of Run 73 was modified slightly in comparison to Run 72 to compensate for the high molybdenum and tungsten and low cobalt in the product. Run 74 was prepared identically to 73, and the chemical analyses of the two runs are considered identical within the experimental error of the analytical methods used.

The spectrograph analysis of reduced powder from Run 74 indicates a silicon content slightly higher than that desired. The source of the silicon was ultimately determined to be the decomposition of transite heat shields surrounding the anode. The relocation of these shields completely eliminated silicon problems.

Although not clearly evident in Table 3, it was found that, when the amount of dispersion oxide is altered in an otherwise fixed electrode chemistry, the vaporization characteristics of the electrode are also modified and result in a variation in the analysis of the powder product. Consequently, it was necessary to readjust the electrode chemistry to obtain the desired alloy composition for each dispersion content which was studied.

TABLE 3

ELECTRODE AND PRODUCT ANALYSIS
FROM ELECTRODES CONTAINING 10% BLACK PEARL

	66		67		71		72		73		74	
	E	P	E	P	E	P	E	P	E	P	E	P
Nickel	15.6	42.0	20.7	49.9	24.1	65.7	24.1	55.3	23.5	59.4	23.5	58.4
Cobalt	5.6	13.4	6.9	14.4	7.3	16.6	7.3	15.2	7.8	16.9	7.8	16.2
Molybdenum	40.4	16.5	37.4	12.5	37.4	6.4	37.4	11.5	36.2	9.0	36.2	9.5
Tungsten	34.9	22.7	32.0	20.2	29.0	8.6	29.0	14.4	27.7	9.8	27.7	10.5
ZrO_2	3.5	3.0	3.0	2.7								
ThO_2					2.2	1.3	2.5	2.0	4.9	2.6	4.9	2.7
Total Oxygen										1.08		1.17

E = Metal equivalent of electrode
P = Reduced metal powder

by spectrographic analysis

Al	.01	.01
Cr	.001	.003
Cu	.01	.02
Fe	.08	.08
Mg	.015	.015
Mn	.015	.015
Si	.3	.3

4.2 Investigation of Various Oxide Dispersions

The original plan of this program was to study thoria and zirconia as dispersion oxides. It was found that zirconia would not provide an ultrafine dispersion oxide, but that thoria appeared to be satisfactory. Effors were then redirected to investigate other oxides as a substitute for zirconia.

The basic electrode composition of run 74, Table 3 was utilized for preparation of powders containing the various oxides. The resultant fume products were reduced in a 2-inch diameter Inconel tube which was heated externally by a resistance-wound tube furnace. Approximately 15 grams of oxide fume in a molybdenum boat was heated in a hydrogen atmosphere to 800°C (approximately 1 hour to temperature) and held for 1 hour at temperature. The reduced powder was cooled in hydrogen for approximately 1 hour, the system flushed with argon, and the powder taken directly into the argon atmosphere drybox without exposure to the air. The Inconel tube was attached to the drybox, and was isolated from the drybox by an O-ring sealed, threaded cap which was secured from within the box.

All powders were precompacted into pellets 1/2-inch diameter by 1/4-inch thick. The pellets were wrapped in one mil Teflon foil, bagged, evacuated, and isostatically pressed at 25 TSI. Sintering was performed in a hydrogen atmosphere for 3 hours at 1300°C.

The results obtained for the dispersion oxides investigated are presented in the following paragraphs.

Thoria

American Potash Company Grade 112H thorium oxide was utilized to prepare the evaluation specimens. The electrode and product compositions are listed as runs 73 and 74 of Table 3. A typical structure of this material is shown in the electron micrograph of Figure 12.

A study was made of the utilization of thorium oxalate for the preparation of powders since it was suspected that thorium oxalate would be dispersed into finer particles than thoria during mixing, and then convert into still finer particles during baking of the electrode when the oxalate was decomposed to the oxide. It was found, however, that there was no apparent difference in the vaporization characteristics between the thorium oxide and thorium oxalate electrodes. An electron micrograph of a pressed and sintered specimen pre-

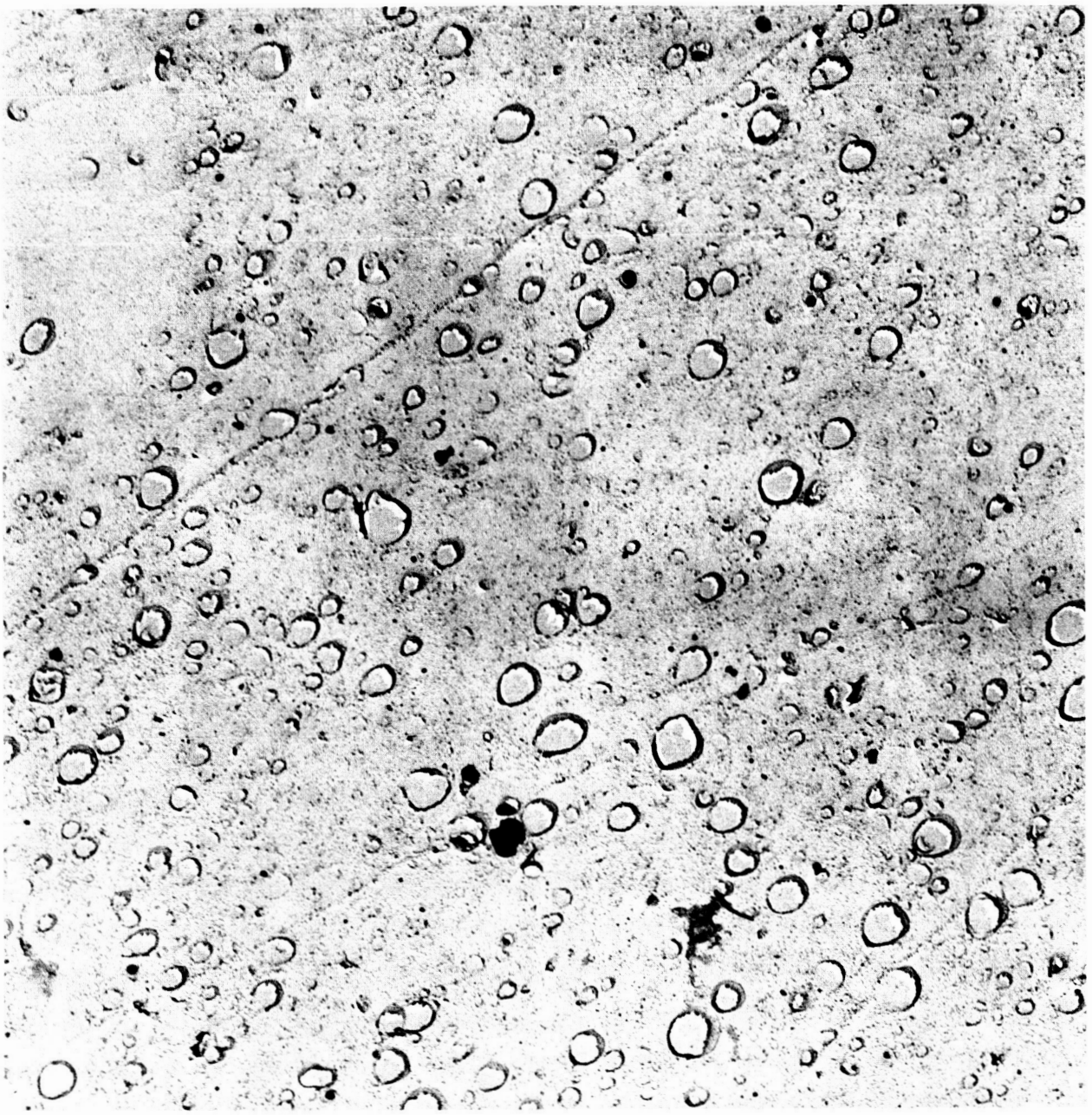

16,000 X

FIGURE 12 NICKEL ALLOY CONTAINING ThO_2

pared with thorium oxalate is shown in Figure 13. A close comparison of the thoria particle sizes reveals that the alloy prepared with the oxalate has a slightly larger over-all dispersion particle size than the one prepared with the oxide. No further studies were made with the oxalate addition.

Zirconia

The vaporization characteristics of electrodes containing zirconia were very similar to those containing ThO_2, and the tan-colored oxide fume product obtained was identical with the fume without a dispersion and with the fume containing thoria.

Electron micrographs of pressed and sintered pellets revealed large particles which, for the most part, were concentrated in the grain boundaries and at grain boundary triple points. A representative structure is shown in Figure 14. Although there were some small particles, the majority of the dispersion was well in excess of the 0.1 micron average particle size desired. There also appeared to be a second phase in the grain boundaries.

Other studies in this laboratory revealed that ZrO_2 does not always vaporize readily in the high intensity arc to form discrete solid submicron particles, but that hollow spheres are often formed. Needless to say, this was surprising to find that zirconia was anomalous with all other oxide systems previously studied.

As a result of these findings no further experiments were made using ZrO_2 as the dispersion.

Aluminum Oxide

The vaporization of electrodes containing Linde B (0.05 micron) alumina and Alcoa Grade A-10 (-200 mesh) alumina yielded a fume product which was dark gray in color rather than the characteristic tan color obtained for fume containing ThO_2.

Upon reduction at 800°C in hydrogen, the powder was extremely fine, incompletely reduced, and quite pyrophoric upon exposure to air. Powder reduced at 850°C and 900°C was not pyrophoric but still quite fine. This powder was extremely difficult to press and sinter, since pressed pellets would split upon ejection from the die or shatter from thermal shock when introduced into the sintering furnace.

An electron micrograph of a sintered pellet is shown in Figure 15. Although

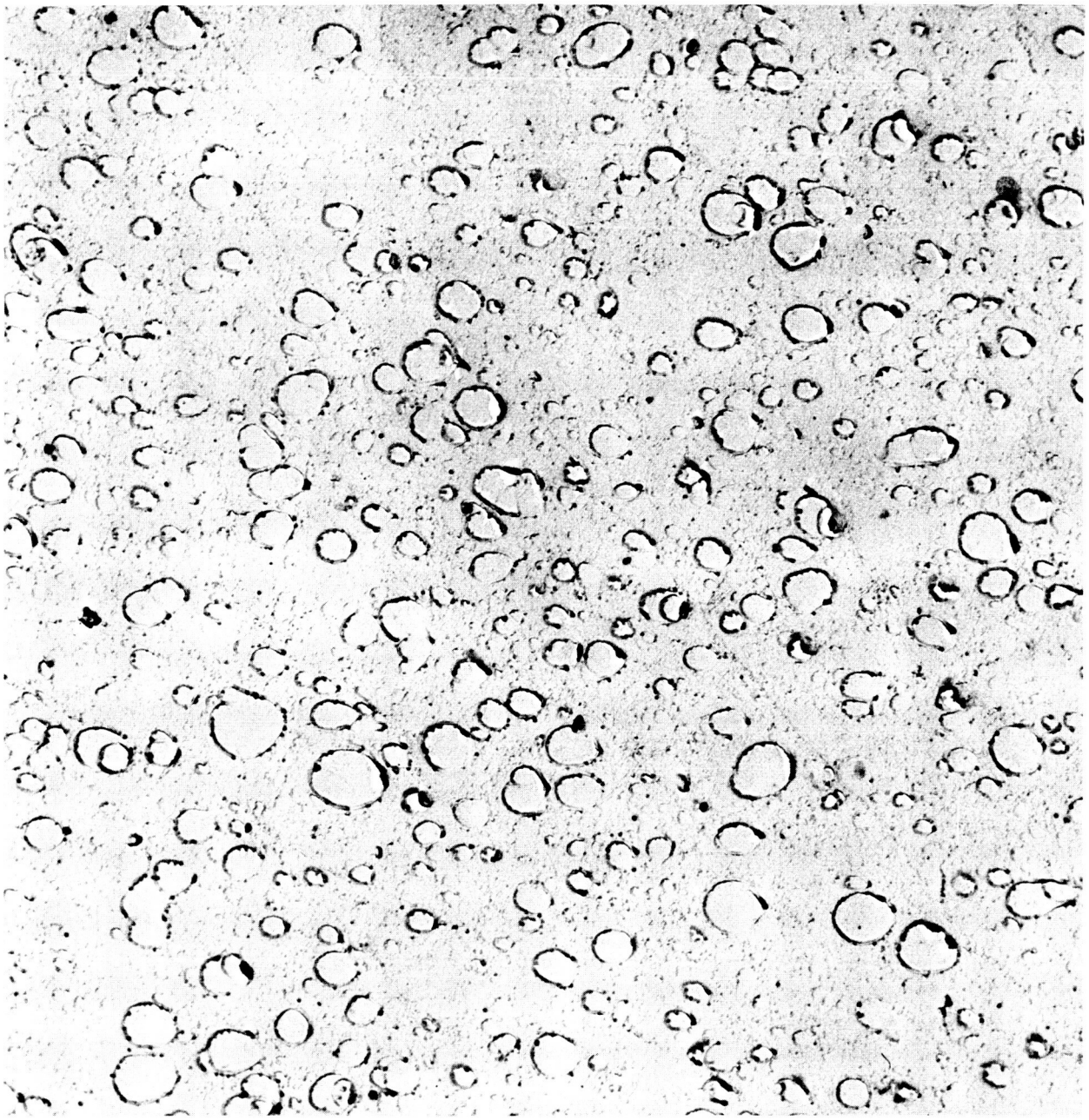

16,000 X

FIGURE 13

THORIUM OXIDE DISPERSION IN NICKEL ALLOY
PREPARED FROM ELECTRODES CONTAINING
THORIUM OXALATE
(Run #76)

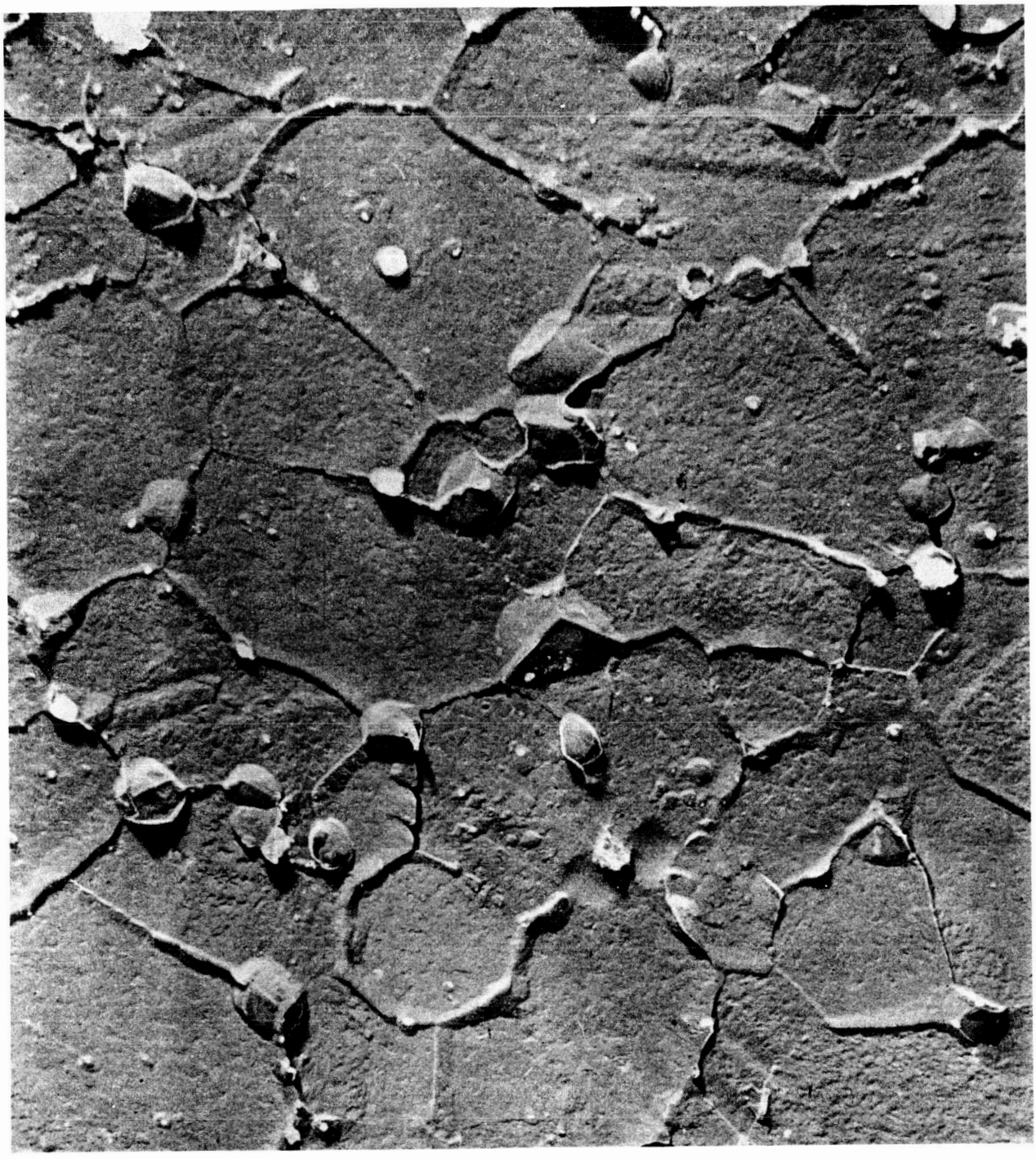

16,000X

FIGURE 14

NICKEL ALLOY CONTAINING ZrO_2

16,000 X

FIGURE 15

LINDE B ALUMINA IN NICKEL BASE ALLOY

a few small particles are evident, there appears to have been a gross reaction between alumina and one or more of the alloy constituents. It is suspected that the reaction began during the vaporization step since the color of the fume product was unusual. It also appears that this reaction product may have been molten at the sintering temperature.

Magnesium Oxide

Electrodes containing magnesia (-200 mesh) vaporized similarly to those containing zirconia and thoria; however, the metal powder obtained by reduction at 800°C was similar in color to that containing alumina. It was extremely fine, appeared to be only partially reduced, and was very pyrophoric when exposed to air. Pressed pellets exhibited poor thermal shock resistance and split during introduction to the sintering furnace. Sintered pellets appeared to have undergone melting at the 1300° and 1350°C sintering temperature. Since these powders reacted in the same manner as those containing alumina, no further work was performed with this system.

Lanthanum Oxide

Electrodes containing lanthana vaporized rather poorly, resulting in heavy slagging and low product yield; however, sufficient material was obtained for evaluation.

Fume product was reduced in hydrogen at 800°, 900°, and 1000°C for 1 hour. Powder reduced at 800°C was slightly pyrophoric, but the powder reduced at 900° and 1000°C was not pyrophoric upon exposure to air.

Sintered pellets prepared from the powder reduced at 800°C showed considerable grain growth with large inclusions in the grain boundaries and practically no structure within the grains. The sintered pellets prepared from powder reduced at 1000°C showed a considerable decrease in the amount of inclusions indicating a more complete reduction at the higher temperature.

Electron micrographs of sintered specimens prepared from powder reduced at 1000°C indicated a non-homogeneous distribution of particles, and there was some evidence that the particles were rejected to the grain boundaries. However, it does appear that the particles are quite small as can be seen in the electron micrograph of Figure 16.

Although this system appeared to have some potential, it was not considered

FIGURE 16 16,000X.

ELECTRON MICROGRAPH OF NICKEL ALLOY CONTAINING La_2O_3

further due to the poor vaporization rates initially obtained and the high temperatures required for complete reduction. Since no apparent reaction occurred between the lanthana and metal constituents, this alloy system may be worthy of future consideration.

Yttrium Oxide

Electrodes containing yttria vaporized fairly well although not as readily as the electrodes containing thoria. Powder reduced in hydrogen at 800°C was only slightly pyrophoric, and powders reduced at 900° and 1000°C were non-pyrophoric upon exposure to air.

Electron micrographs of sintered specimens showed that the Y_2O_3 particles were reasonably well dispersed but that the particle size was slightly larger than that desired. An electron micrograph of the sintered alloy containing yttria is shown in Figure 17.

Since there did not appear to be any reaction between yttria and the other alloy components during processing, and since the reduction temperature was approximately the same as that for the alloy containing thoria, yttria was selected as the second oxide for further study.

It had been established in a corporate-sponsored program that, in certain electrode compositions, the utilization of submicron dispersion powders rather than dispersion oxides having larger particle sizes yielded smaller and more uniform particles in the product. In other electrode compositions no benefit was observed. Therefore, based on the preliminary results in preparing an alloy powder containing yttria as the dispersion, it was felt that the utilization of a submicron yttria powder rather than a coarser granular powder for the preparation of the electrode might enhance the vaporization of yttria and provide a smaller particle size in the product. A considerable effort was made to vaporize yttria to provide a submicron yttria powder for subsequent use in preparing alloy electrodes.

Numerous runs were made in which the carbon content and binder content (which affects extrusion pressure) of the mix was varied to provide an electrode which would yield submicron powder upon arc vaporization. All combinations produced almost total slagging and the small amount of submicron powder obtained was gray in color. Calcination of this product in air to temperatures up to 1000°C did not produce the characteristic white oxide. One small lot, however, was obtained in which the submicron powder appeared reasonably clean but the over-all yield was only 1 percent.

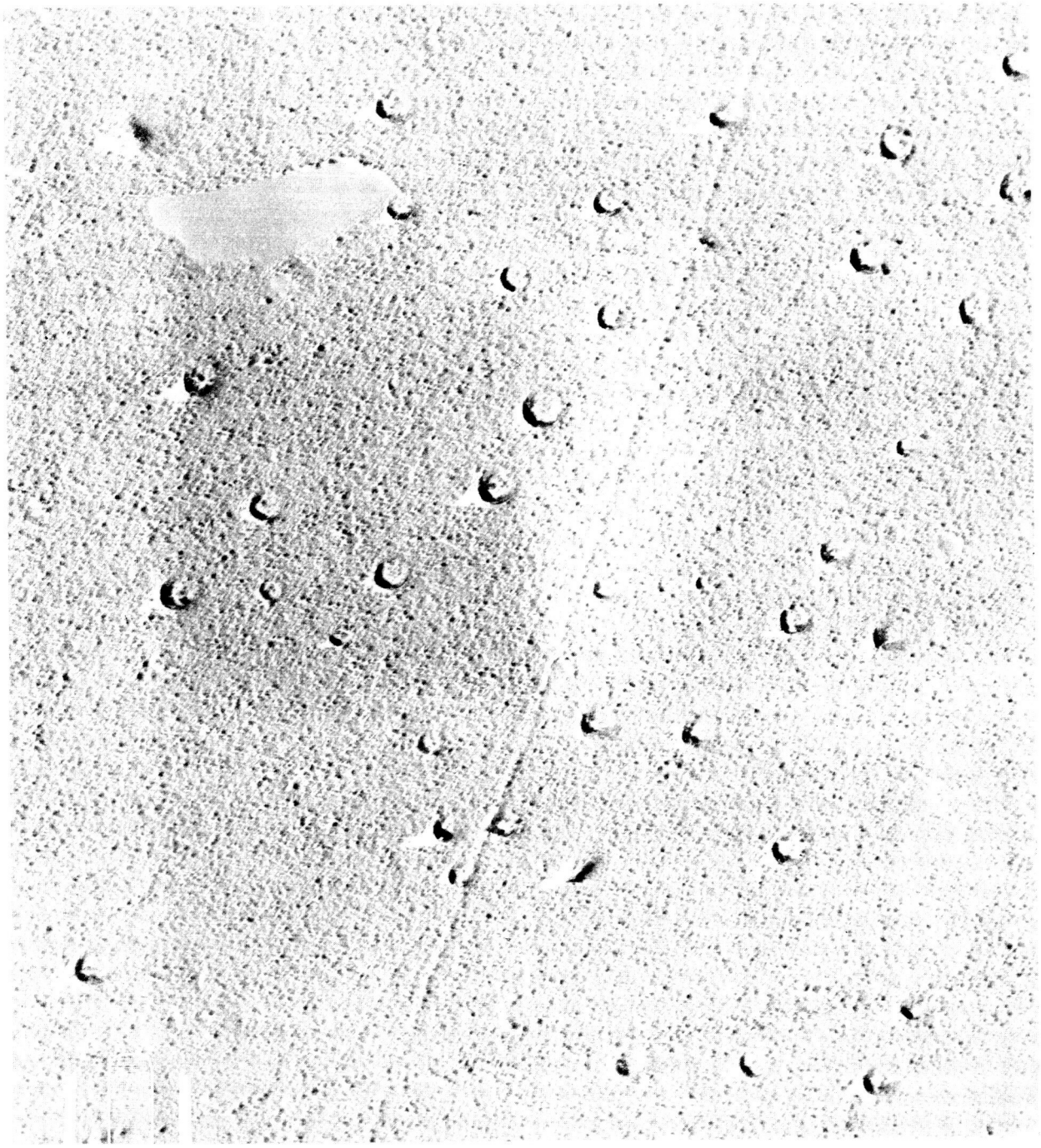

16,000X.

FIGURE 17

ELECTRON MICROGRAPH OF NICKEL ALLOY
CONTAINING Y_2O_3

In view of the difficulties encountered in the preparation of submicron yttria, this approach was abandoned and the "as received" yttria was incorporated into the homogeneous electrode in the same manner as the thoria.

4.3 Establishment of Sintering Cycles

The evaluation of sintering characteristics was made with pellets 1/2" diameter by 1/4" thick. A few specimens 1" diameter by 1" long were made from lots reduced in the large retort where sufficient powder was available. All powders were precompacted in a die at a load sufficient to provide a pellet which could be handled without breaking. The pellet was wrapped in a one mil-thick Teflon foil, bagged in a thin rubber tube, evacuated, and isostatically pressed at 25 tsi. All specimens for evaluation were pressed at this load since no significant differences were observed in the density or microstructure of sintered pellets pressed at loads between 20 and 50 tsi within the limits of the other variables investigated. The pressed specimens were then sintered in hydrogen for various times and temperatures, and some specimens were vacuum sintered for comparative purposes.

It was determined that densities between 90 and 95 percent of theoretical could be achieved by sintering in hydrogen for 3 hours at 1250° - 1300°C. (Theoretical density was assumed to be 10.2 gms/cc.) Typical microstructures of as-sintered specimens are shown in Figure 18. No significant difference was observed with the alloys containing zirconia, thoria, or yttria.

A cursory examination was made of specimens sintered at higher temperatures. Figure 19 shows the microstructures of specimens sintered at 1425° and 1450°C. The latter specimen was at temperature for 20 minutes when it began to deform.

There did not appear to be a significant difference among the microstructures obtained by vacuum sintering or sintering in hydrogen, or any effect due to presintering at a lower temperature, within the limits of the variables studied. From the data obtained, it appeared that adequate densities could be obtained for subsequent working (extrusion) by sintering for 3 hours at 1250° - 1300°C in a hydrogen atmosphere.

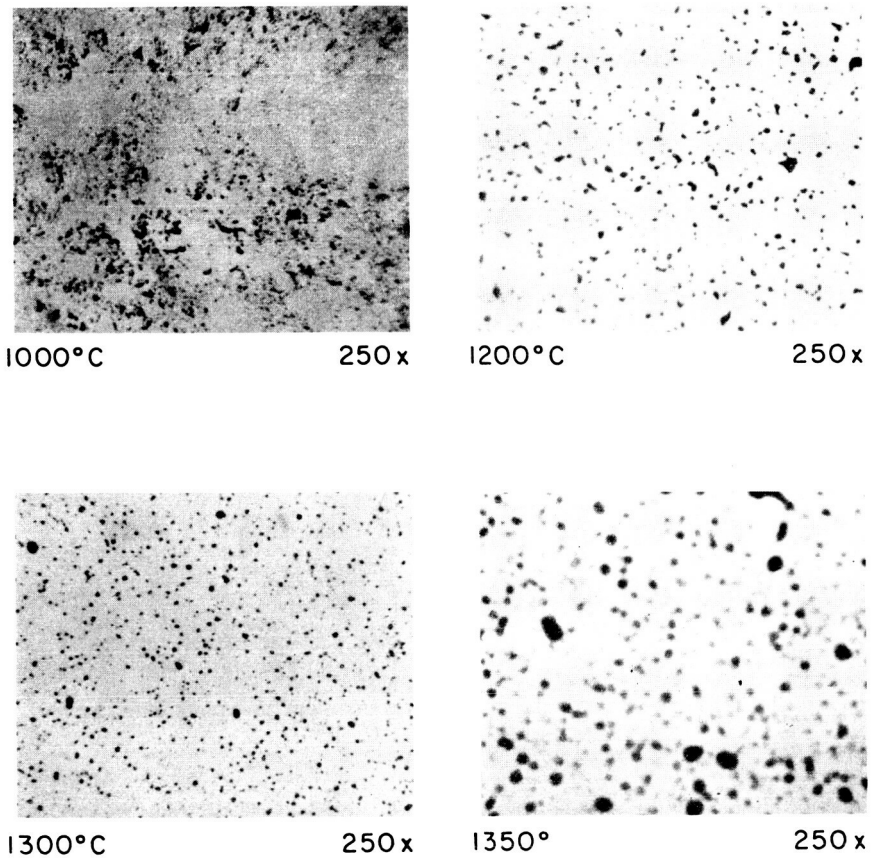

FIGURE 18

MICROSTRUCTURE OF ALLOY POWDER SINTERED FOR 3 HOURS IN HYDROGEN AT VARIOUS TEMPERATURES
(ZrO_2 Dispersion - Unetched)

1425°C 250×

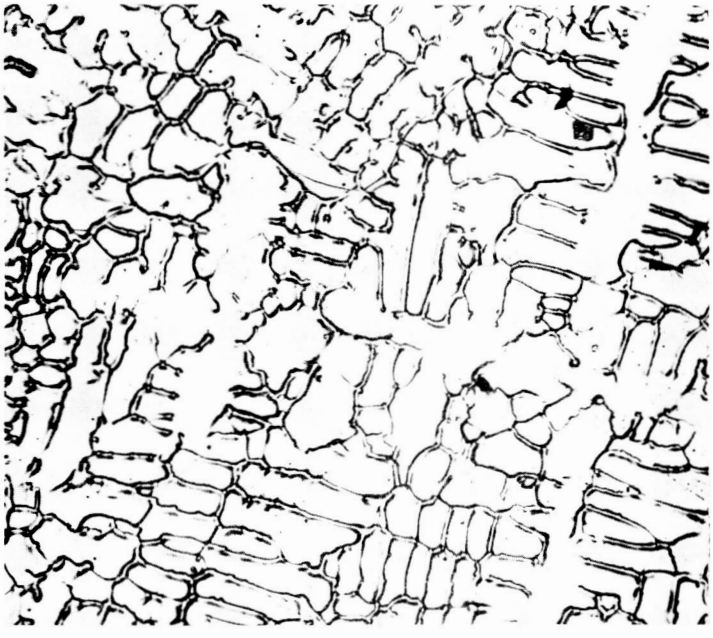

1450°C (melted) 250×

FIGURE 19

MICROSTRUCTURES OF SPECIMENS (RUN 73)
SINTERED AT 1425 AND 1450°C

5. FINAL POWDER PRODUCTION, SINTERING, AND EXTRUSION

5.1 Preparation of Alloy Powders Containing Thoria

There were no severe problems associated with scaling up the process to produce a sufficient quantity of powder containing thoria for preparation of the billets. The main problem, which was somewhat surprising, was that the electrode composition established for a 3-electrode size mix did not translate directly to a 10-electrode size mix, i.e., the desired product composition was not obtained. The reason for this is not understood. The only process change was the utilization of a larger mixer with a slower mixing action which was compensated by longer mixing times. The extrusion pressures were the same for both mix sizes. The compositions of the scaled-up mixes had to be adjusted to provide the desired product composition. Table 4 compares the chemical analyses of the three electrode mix with the equivalent scaled-up ten electrode mix and the adjusted 10 electrode mix. It was also found that increasing amounts of molybdenum and tungsten were required with increasing thoria contents in order to obtain the desired base alloy composition. The electrode composition had to be readjusted for each thoria content. Once the desired electrode composition was obtained, reproducibility of product composition was realized. Tables 5, 6, 7, and 8 list the chemistries of the electrodes and reduced metal powders obtained from individual runs, and the analyses of the blends used for the various thoria contents. All analyses have been converted to a 100 percent metal basis exclusive of thoria for a more direct comparison of electrode versus product chemistry.

Numerous chemical analyses were made during processing to establish the desired chemical composition. Analysis of these data revealed that a very good approximation could be made of the over-all powder chemistry by analyzing for tungsten and the dispersion oxide only. This method of control was adopted for small changes in electrode composition in the interest of minimizing the time lag between runs; thus, the lack of complete data in Tables 5 - 8. There are several inconsistencies in the individual run analyses when compared to the blend analyses. The inconsistencies arose since only one analytical determination was made for the individual runs, whereas three determinations were made of the blended material. Also, greater care was taken in performing the analyses for the blended material.

The average product yield for this alloy composition was approximately 20%, the primary loss being slagging during vaporization. It is obvious that if the yield could be improved as a result of improved vaporization, the electrode

TABLE 4

A COMPARISON OF CHEMISTRIES OF THE ELECTRODES AND PRODUCT FOR 3 AND 10 ELECTRODE-SIZE MIXES CONTAINING THORIUM OXIDE

	3 Electrode Mix		3 Electrode Mix Scaled to 10 Electrode Mix		10 Electrode Mix Adjusted	
	Electrode*	Product	Electrode*	Product	Electrode*	Product
Ni	24.8	61.2	24.8	54.5	29.2	59.7
Co	8.2	17.0	8.2	16.8	10.8	18.8
Mo	38.1	10.0	38.1	16.7	30.7	10.4
W	29.2	11.0	29.2	12.0	29.2	10.5
ThO_2**	4.9	2.7	4.9	3.4	2.5	2.1

* Analysis of electrode converted to 100% metal basis excluding ThO_2 for direct comparison with product analysis.

** Target thoria content of product 2%

TABLE 5

CHEMISTRY OF ELECTRODE AND REDUCED POWDER
FOR STANDARD ALLOY WITHOUT A DISPERSION OXIDE*

Electrode	Ni	Co	Mo	W	Si	S
112	29.7	10.5	30.8	29.0	-	-
113	29.7	10.5	30.8	29.0	-	-
114	29.7	10.5	30.8	29.0	-	-
Product						
112		(Not Analyzed)				
113		(Not Analyzed)				
114		(Not Analyzed)				
Reduced Powder, Blended						
	61.3	18.3	10.6	9.5	-	55 ppm
Specifications						
	60	20	10	10		

*Analyses converted to 100% metal basis.

TABLE 6

ANALYSES OF ELECTRODE AND REDUCED POWDER FOR NOMINAL 2v/o THORIA ALLOY*

	Ni	Co	Mo	W	ThO_2	SiO_2	S
Electrode							
92	29.9	10.5	30.9	28.7	2.4	-	-
93	29.2	10.8	30.7	29.2	2.5	-	-
94	29.2	10.8	30.7	29.2	2.5	-	-
Product							
92	59.7	18.8	10.4	10.5	2.1	-	-
93	60.8	-	-	9.8	2.0	-	-
94	60.0	-	-	9.7	2.0	-	-
Reduced Powder, Blended							
	61.2	17.0	10.9	10.4	2.1	0.07	25 ppm
Specification							
	60	20	10	10			

*Analyses converted to 100% metal basis exclusive of thoria.

TABLE 7

ANALYSES OF ELECTRODE AND REDUCED POWDER
FOR NOMINAL 4 V/o THORIA ALLOY*

	Ni	Co	Mo	W	ThO_2	Si	S
Electrode							
99	29.3	10.5	30.4	29.4	5.7	-	-
100	29.3	10.5	30.4	29.4	5.7	-	-
101	29.6	10.5	30.4	29.5	5.9	-	-
Product							
99	58.6	20.3	-	9.3	3.6	-	-
100	-	-	-	9.6	3.5	-	-
101	-	-	-	8.9	3.4	-	-
Reduced Powder, Blended							
	60.8	17.5	11.7	9.9	3.5	0.03	50 ppm
Specification							
	60	20	10	10			

*Analyses converted to 100% metal basis exclusive of thoria.

TABLE 8

ANALYSES OF ELECTRODE AND REDUCED POWDER FOR NOMINAL 7 v/o THORIA ALLOY*

Electrode	Ni	Co	Mo	W	ThO_2	Si	S
110	22.8	7.7	34.8	34.8	12.3	-	-
111	22.3	7.6	34.1	36.0	12.0	-	-
Product							
110	-	-	-	8.5	8.4	-	-
111	-	-	-	7.8	7.7	-	-
Reduced Powder, Blended	62.4	19.0	9.7	8.9	7.7	0.005	45 ppm
Specification	60	20	10	10			

*Analyses converted to 100% metal basis exclusive of thoria.

composition would approach more closely that of the product, and the necessity for process control would be minimized.

5.2 Preparation of Alloy Powders Containing Yttria

Identical electrode mixes were utilized for the preparation of powders containing yttria and for the powders containing thoria at the respective volume percentage of dispersion oxide. Only check analyses were made on the first run to insure proper yttria content. Three mixes for each yttria composition were prepared, the reduced powders were blended, and chemical analyses were made of the blended lots. The analyses are shown in Table 9.

5.3 Pressing and Sintering of Billets

Each lot of powder was preformed under an argon atmosphere in a 2-1/2 inch diameter die under a load of 4000 psi. Upon ejection the preforms were wrapped with 1/2 mil Teflon sheet, bagged in 20 mil rubber tubing, and the tubing was evacuated before sealing off the ends. The preforms were then bagged again to insure absolute tightness against oil leakage during subsequent hydrostatic pressing.

Hydrostatic pressing was performed at Kawecki Chemical Company, Boyertown, Pennsylvania. The billets containing 2, 4, and 7 volume percent thoria, the control billet (i.e., no dispersion), and two scrap billets (prepared from powders out of chemical specification) were processed in one loading at a pressure of 40,000 psi. Upon stripping the bag, the billet containing 7^{v}/o thoria had broken in several places and the pieces were displaced sufficiently to render the compact unsatisfactory for further processing.

The damaged 7 percent thoria billet was crushed to -60 mesh powder, oxidized to break up the coarser material, and re-reduced to metal powder for subsequent pressing. The re-reduced powder was coarser than that obtained from the first reduction.

The 2, 4, and 7 volume percent yttria billets, a small billet containing 2 percent yttria prepared using submicron yttria, and the reclaimed 7 volume percent thoria billet were pressed in the same manner as described above. All of the yttria-containing billets compacted satisfactorily.

Sintering was carried out under hydrogen in a resistance heated, Alundum tube furnace. The two scrap billets were sintered first to verify the heating cycle

TABLE 9

CHEMICAL ANALYSES OF BLENDED LOTS
OF ALLOY POWDER CONTAINING YTTRIA

Nominal v/o Y_2O_3	Ni	Co	Mo	W	Y O	S
2	56.8	18.8	9.5	11.1	1.2	25 ppm
4	58.6	17.1	8.9	11.4	1.9	53 ppm
7	58.2	16.4	8.1	10.3	3.8	35 ppm
Specification						
	60	20	10	10		

previously established for billets pressed in a 2-inch diameter die. The sintering cycle used was a 4 - 5 hours to 1350°C and a 2-hour hold at temperature. The billets were furnace cooled overnight in hydrogen. Table 10 lists the densities and weights of the billets after the various processing steps.

5.4 Evaluation of the As-Sintered Billets

A 1/4-inch thick slice was cut from the top of each billet. This slice was cut into radial segments for thermal stability tests and electron and light microscopic evaluations. The thermal stability test consisted of heating the sample at 1225°C for 100 hours in a dry hydrogen atmosphere.

Microhardness measurements were made on a segment of each composition in the as-sintered condition, and after the 100 hour thermal stability test. These data are listed in Table 11. A wide scatter in hardness values was obtained, but several consistent patterns resulted. The average hardness increased with increasing thoria content, all values being greater than those for the alloy without a dispersion. Contrary to expectations, however, average hardness values for the alloys containing Y_2O_3 were less than the average value for the alloy without a dispersion.

The $2^V/o$ and $4^V/o$ thoria dispersion specimens exhibited a 1/4-inch wide peripheral band upon etching. A second slice was taken from these two billets and the band was not evident on the specimen containing $2^V/o$ thoria, but persisted on the $4^V/o$ thoria specimen to the same width. Hardness values were also taken on these second slices and are given in Table 11. Small segments cut from the $4^V/o$ thoria billet revealed a difference in density between the core and ring, the core having a density of 9.44 gm/cc and the ring 9.68 gm/cc. This difference was further reflected in micrographic examination which revealed less porosity in the outer ring. This porosity variation, however, was noted in all the billet sections to a varying degree although the hardness measurements did not entirely reproduce the differences noted in porosity.

Figures 20 through 26 show optical micrographs of the thoria and yttria alloys in the as-sintered condition and after the thermal stability treatment for 100 hours at 1225°C. There did not appear to be any significant change in the structures as the result of this thermal treatment, except for the alloy containing $7^V/o$ ThO_2. Since this material was reprocessed, it is not representative, and the change in microstructure was probably due to contamination. The micrographs for the alloys containing Y_2O_3 dispersion indicate that a gross reaction took place between the Y_2O_3 and one or more of the alloy constituents during processing. This was not evident during the

TABLE 10

BILLET WEIGHTS AND DENSITIES

Billet	Powder Tap Density (g/cc)	Green Density (g/cc)	Green Billet Weight (gms)	Sintered Density (g/cc)	Sintered Billet Weight (gms)
Control	1.74	5.5	2450	9.14	2432
2 v/o ThO_2	1.47	5.4	2092	9.55	2080
4 v/o ThO_2	1.38	5.5	2645	9.60	2630
7 v/o ThO_2	1.81	5.2	1680	9.31	1670
2 v/o Y_2O_3	1.26	4.9	2104	8.96	2050
4 v/o Y_2O_3	1.30	4.5	2868	9.02	2807
7 v/o Y_2O_3	1.12	4.8	2694	8.71	2640

TABLE 11

KNOOP HARDNESS (50 GM LOAD) OF
AS-SINTERED AND THERMAL STABILITY SPECIMENS

Location of Hardness Measurement	No Dispersion	2v/o ThO_2 1st Slice	2v/o ThO_2 2nd Slice	4v/o ThO_2 1st Slice	4v/o ThO_2 2nd Slice	7v/o ThO_2	2v/o Y_2O_3	4v/o Y_2O_3	7v/o Y_2O_3
As Sintered									
1	274	322	390	368	426	328	204	303	216
2	274	394	385	351	343	344	204	285	201
3	248	322	322	307	322	351	185	244	253
4	220	426	322	517	351	341	204	263	212
5	224	336	309	517	336	300	201	274	204
6	231	322	315	517	343	322	212	226	235
7	216	322	368	468	385	362	195	253	204
8	227	303	385	493	426	330	208	224	224
After Thermal Stability Test									
1		330		394		322	219	288	204
2		355		351		336	226	293	212
3		330		424		303	212	282	231
4		346		424		322	186	280	225
5		321		446		336	184	262	240
6		307		492		322	151	241	255
7		315		517		322	192	202	212
8		310		468		322	175	229	191

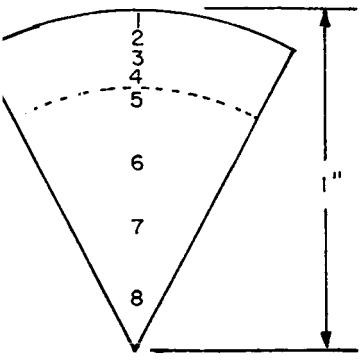

Relative Location of Hardness Measurements

Note: 1st slice 1/4" from top of billet
2nd slice 1/2" from top of billet

Control Billet

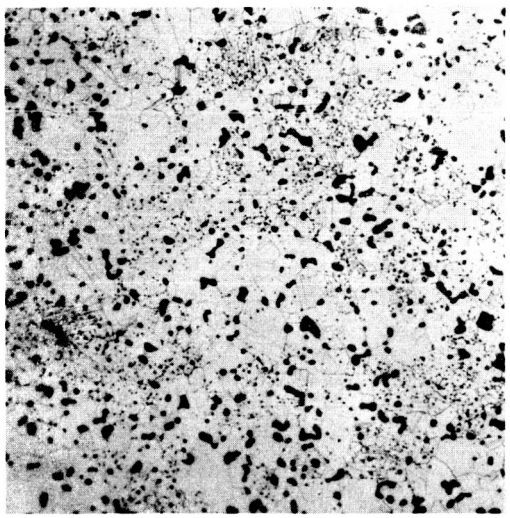

As Sintered 100x

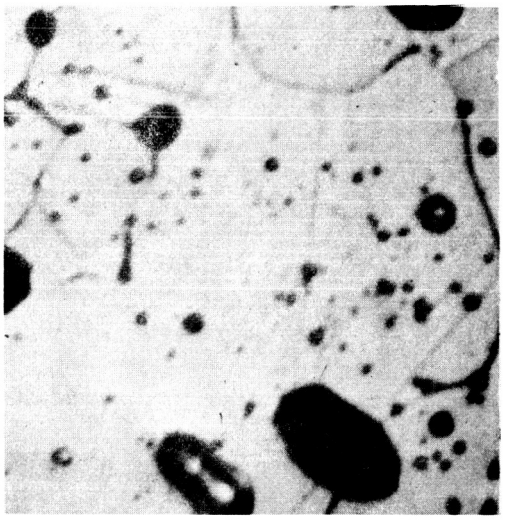

1000x

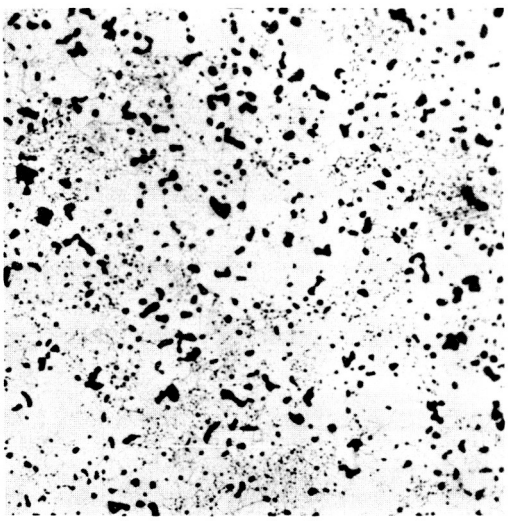

100 Hours at 1225°C 100x

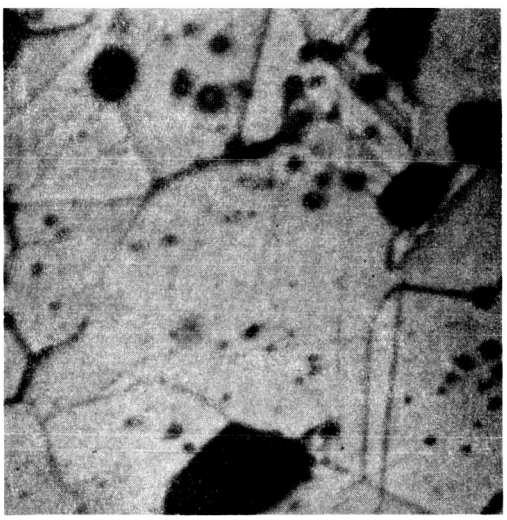

1000x

FIGURE 20

MICROSTRUCTURE OF CONTROL BILLET
(NO DISPERSOID) AS SINTERED AND AFTER
100 HOUR THERMAL STABILITY TEST

2% Thor

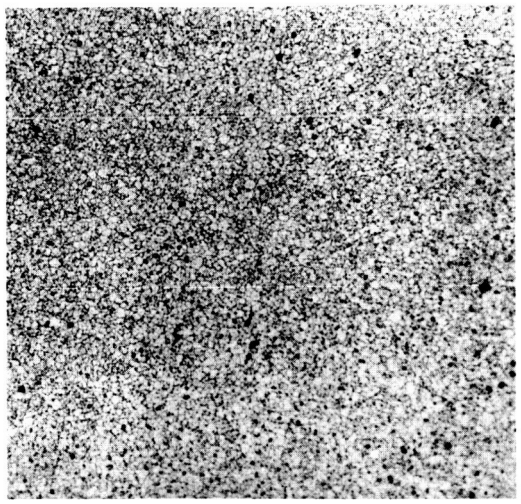

As Sintered 100x

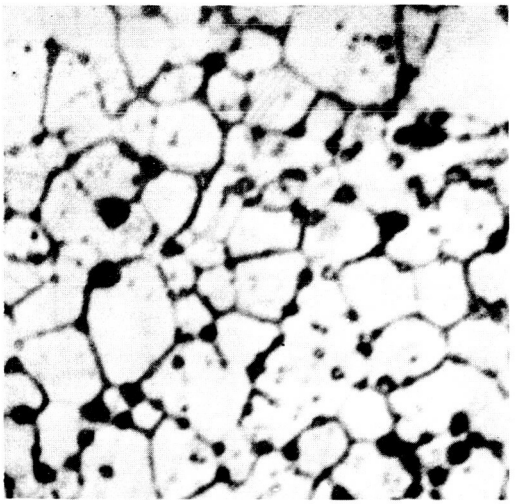

1000x

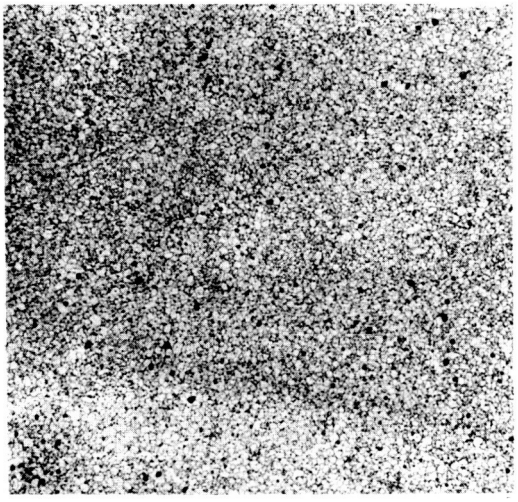

100 Hours at 1225°C 100x

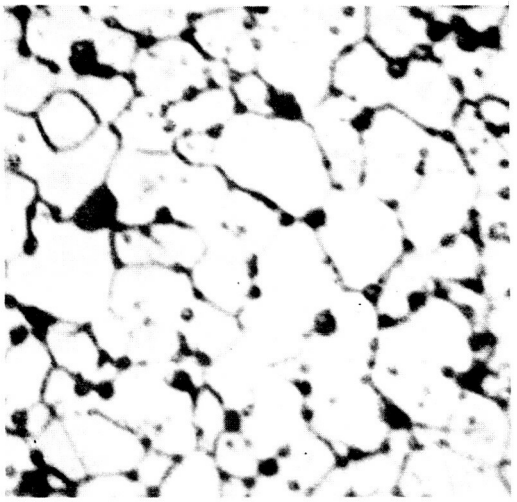

1000x

FIGURE 21

MICROSTRUCTURE OF BILLET CONTAINING 2 v/o THORIA AS SINTERED AND AFTER 100 HOUR THERMAL STABILITY TEST

4 % Thor

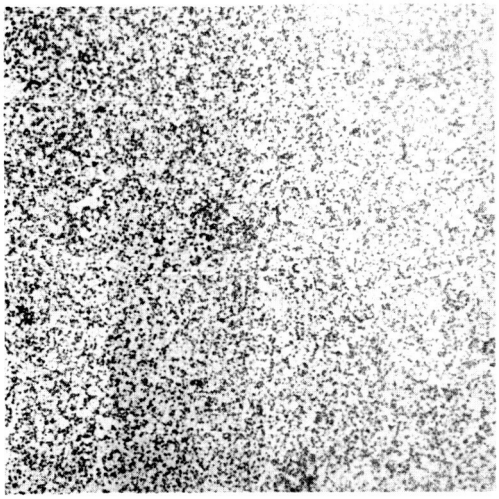

As Sintered 100x

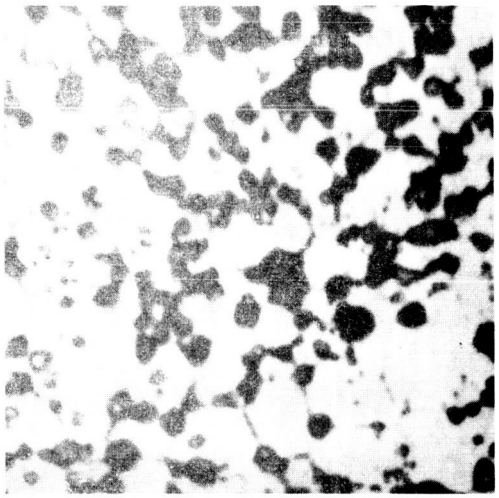

1000x

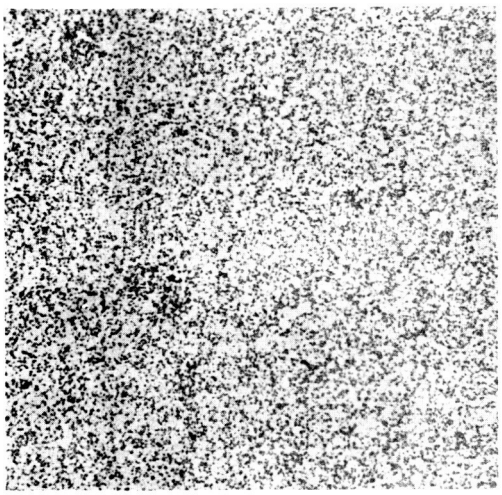

100 Hours at 1225°C 100x

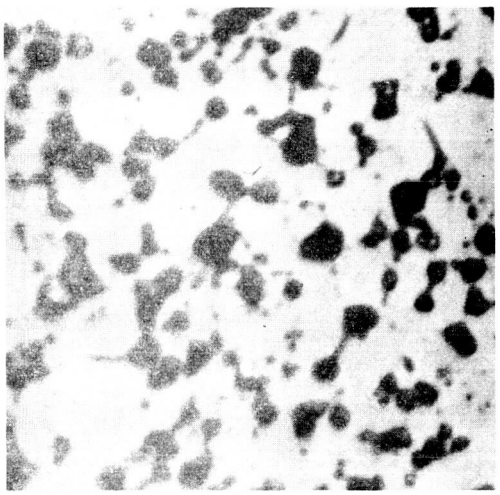

1000 x

FIGURE 22

MICROSTRUCTURE OF BILLET CONTAINING
4 ^{v}/o ThO_2 AS SINTERED AND AFTER 100 HOUR
THERMAL STABILITY TEST

7% Thor

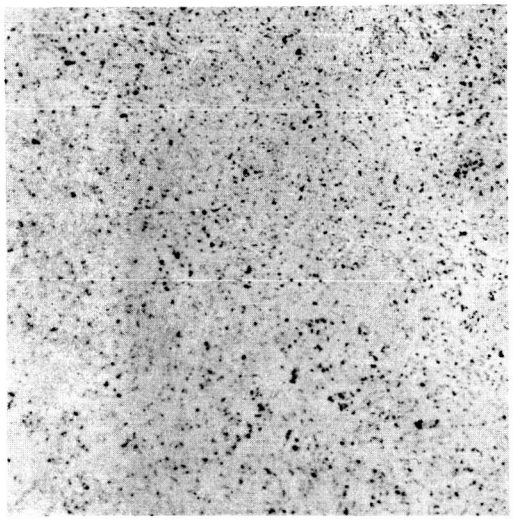

As Sintered 100x

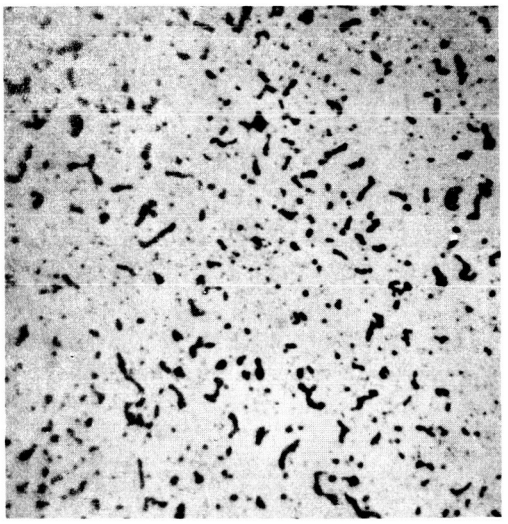

1000x

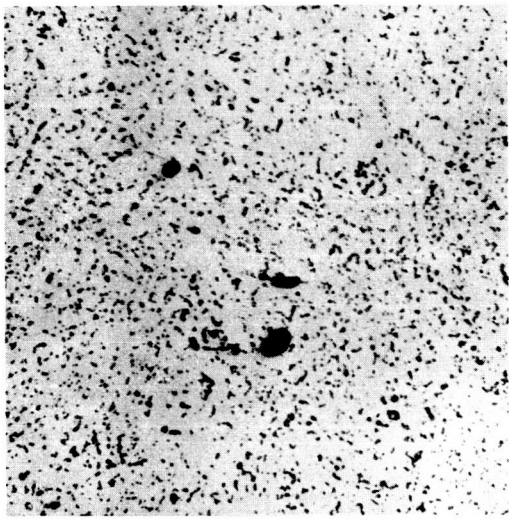

100 Hours at 1225°C 100x

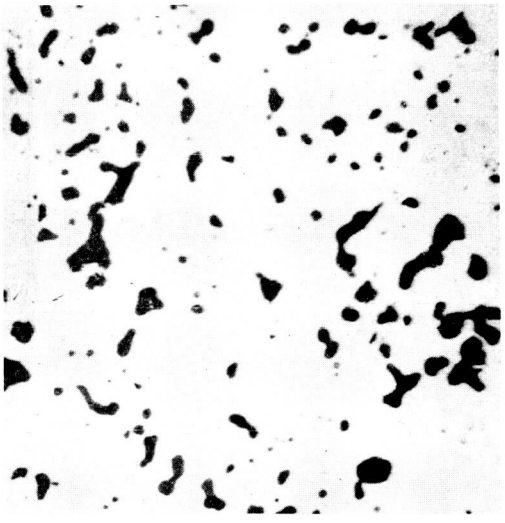

1000x

FIGURE 23

MICROSTRUCTURE OF BILLET CONTAINING 7 ^{V}/o THORIA AS SINTERED AND AFTER 100 HOUR THERMAL STABILITY TEST

2V% Y_2O_3

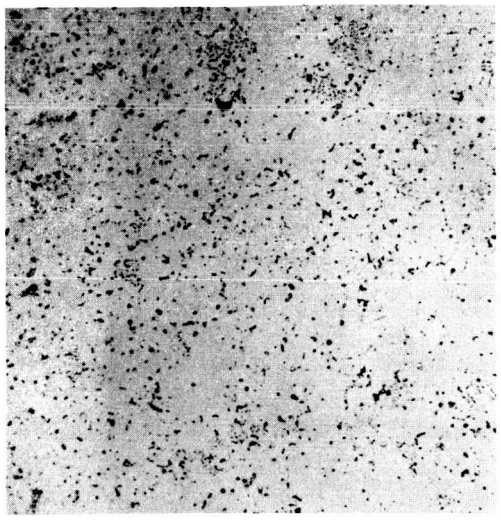

As Sintered 100 x

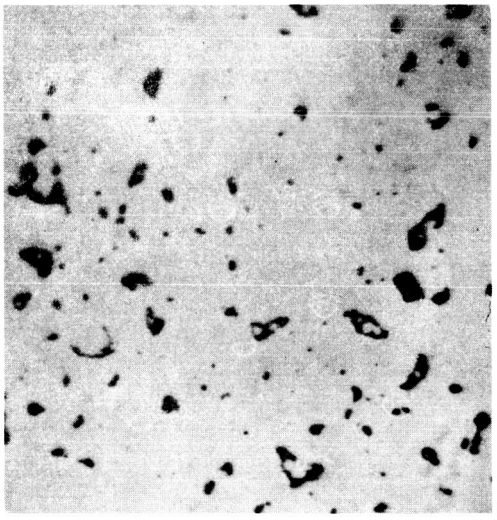

1000 x

2V % Y_2O_3

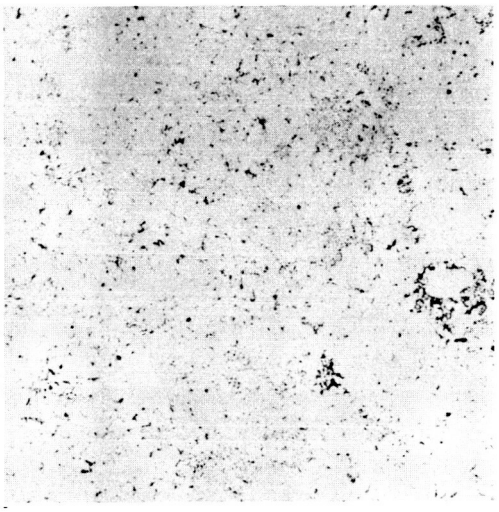

100 Hours at 1225°C 100 x

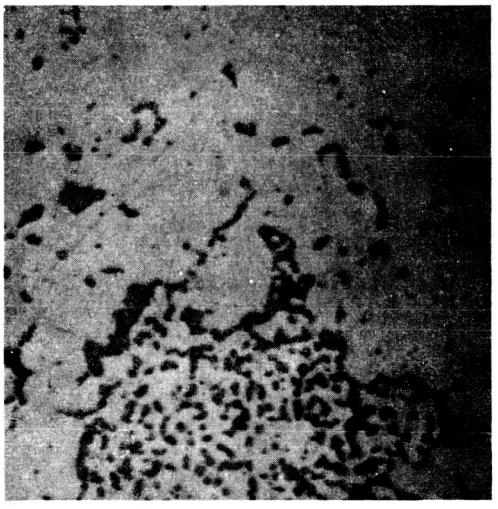

1000 x

FIGURE 24

MICROSTRUCTURE OF BILLET CONTAINING
2 $^{v}/_{o}$ Y_2O_3 AS SINTERED AND AFTER 100 HOUR
THERMAL STABILITY TEST

4 V% Y_2O_3

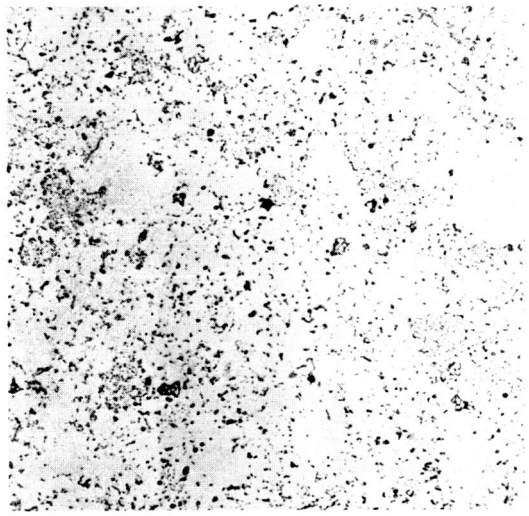

As Sintered 100 x

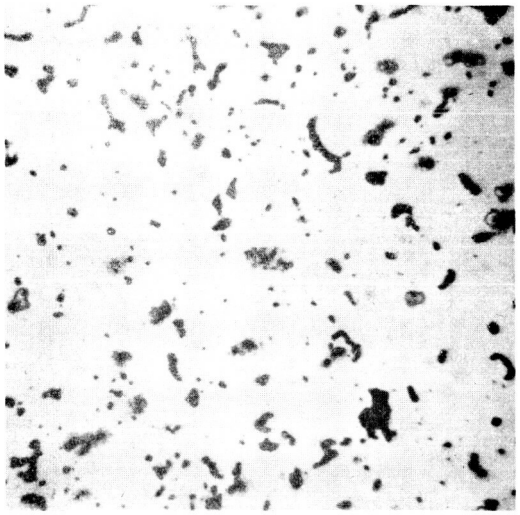

1000 x

4 V% Y_2O_3

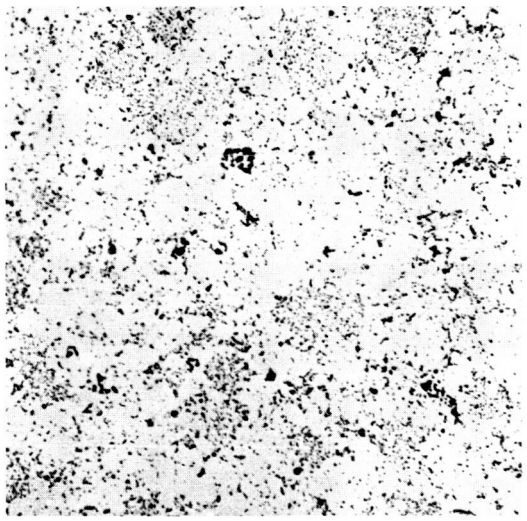

100 Hours at 1225°C 100 x

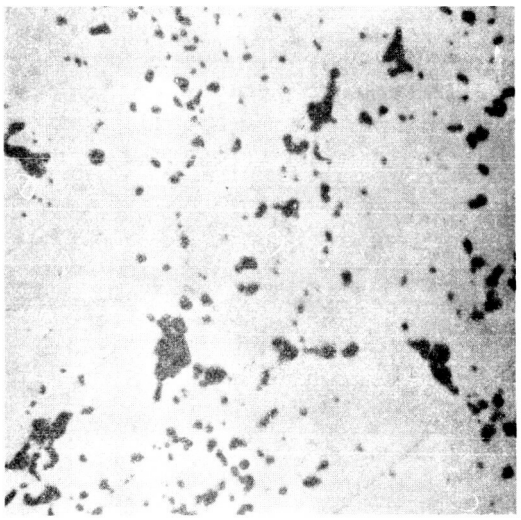

100 x

FIGURE 25

MICROSTRUCTURE OF BILLET CONTAINING
4 $^{v}/_{o}$ Y_2O_3 AS SINTERED AND AFTER 100 HOUR
THERMAL STABILITY TEST

7% Y_2O_3

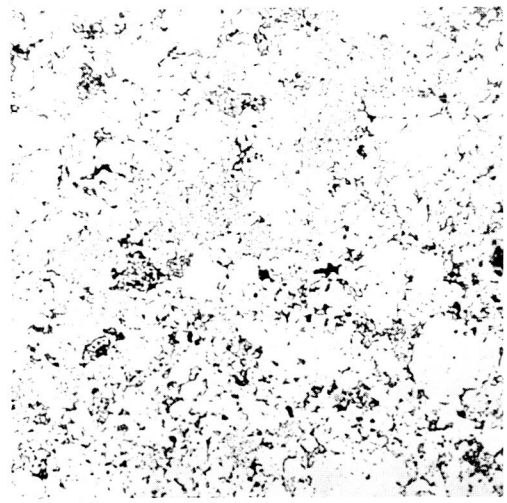

As Sintered 100x

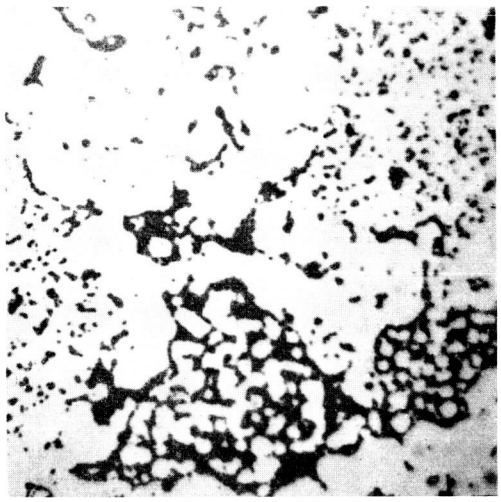

1000x

7% Y_2O_3

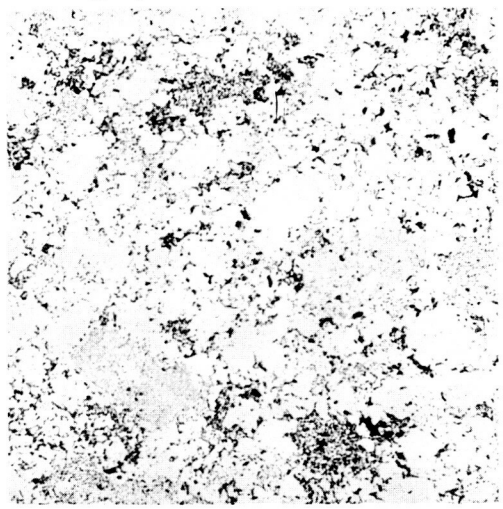

100 Hours at 1225°C 100x

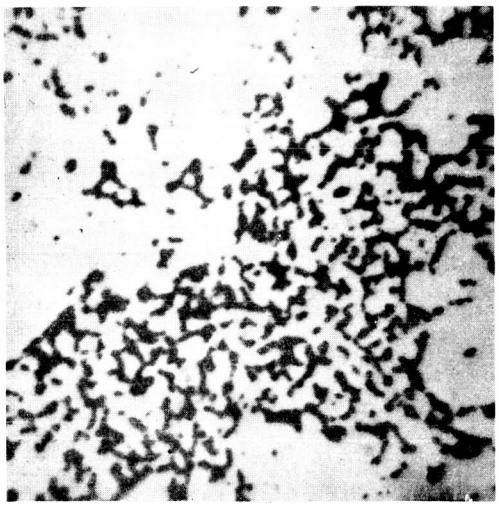

1000x

FIGURE 26

MICROSTRUCTURE OF BILLET CONTAINING
7 v/o Y_2O_3 AS SINTERED AND AFTER 100 HOUR
THERMAL STABILITY TEST

initial studies leading to the selection of Y_2O_3 as a dispersion oxide.

The ultimate dispersion particle size and particle distribution varied with thoria content, and the results were not as good as expected. Representative electron micrographs of the alloy which contained no dispersion and of the alloys containing thoria are shown in Figures 27 through 34 for both the as sintered condition and after the 100-hour thermal stability treatments. For the 2^V/o thoria alloy, very few small particles were obtained. A lineal analysis was not made because of the particle size and the limited number of particles.

The 4^V/o ThO_2 alloy, however, was considerably improved over the 2^V/o ThO_2 alloy. The great majority of the particles were less than 0.1 micron and the distribution appeared to be fairly good. Lineal analysis as described by W. Cremens[1] indicated an average particle size of 0.077 micron and an average interparticle spacing of 0.84 micron for the thoria dispersion in this alloy. Over 600 particles were counted for this determination.

The electron micrograph of the alloy containing 7^V/o ThO_2 also revealed very few small particles. It appears that some reaction may have occurred during the reprocessing of the green compact causing agglomeration of the thoria.

Figures 35 through 40 show representative electron micrographs of the alloys containing Y_2O_3. A very obvious reaction has occurred between Y_2O_3 and one or more of the alloy elements. No further evaluations were made of this material.

5.5 Extrusion of Sintered Billets

In view of the results obtained in the particle size and distribution of the dispersion oxides in the sintered billets, only the control billet and the billet containing 4^V/o thoria were considered for further processing by extrusion.

The sintered billets were machined to a nominal 1-3/4 inch diameter by approximately 5 inches long with a 1/2" x 45° taper on the nose end. The billets were vacuum canned in SAE 1018 steel, machined to an overall diameter of 2.90" and having end plugs 1/2-inch thick.

---

[1] W.S. Cremens, "Use of Submicron Metal and Non Metal Powders for Dispersion Strengthened Alloys", Ultrafine Particles, John Wiley & Sons, 1963, pp. 457-478.

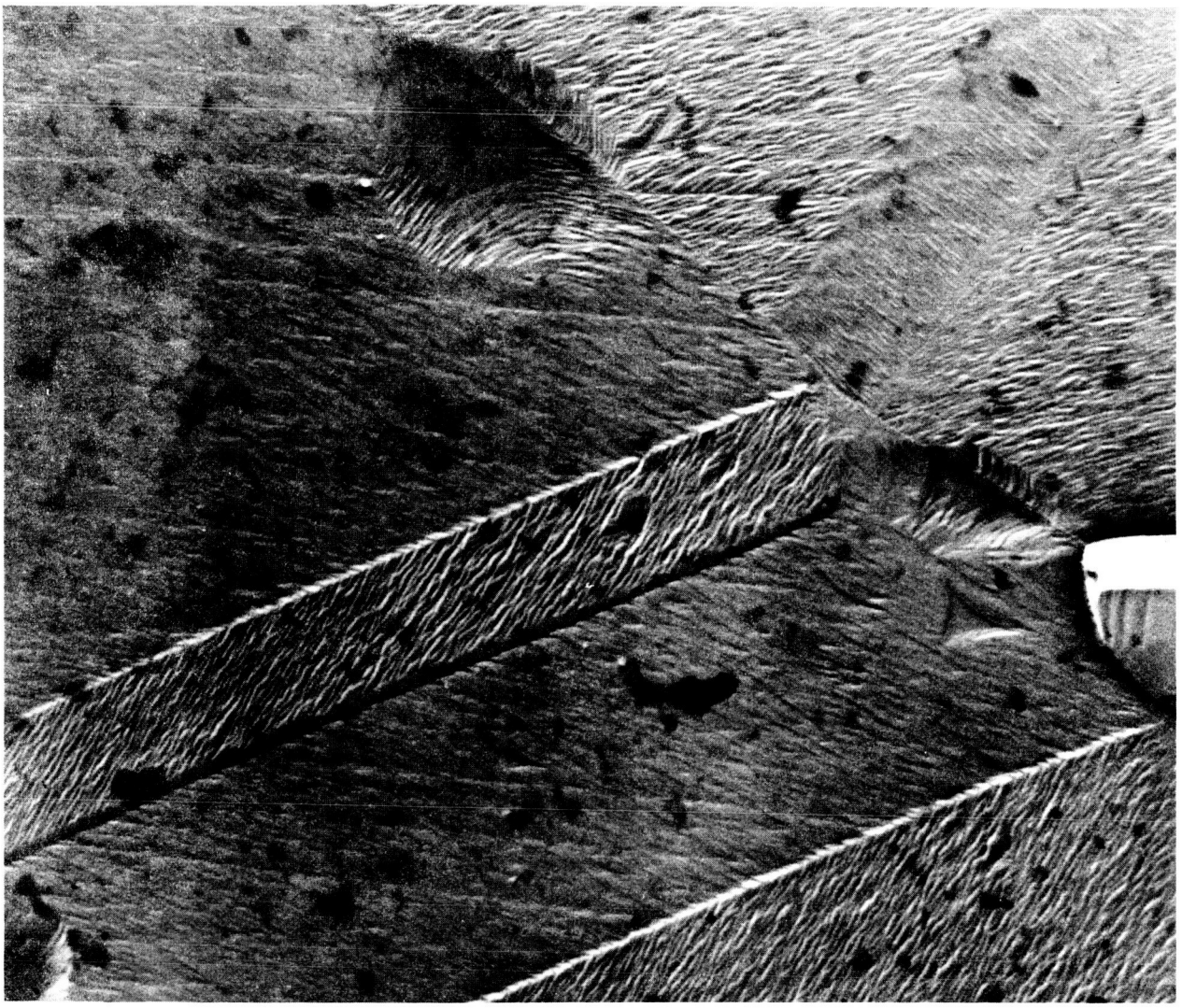

20,000×

FIGURE 27

ELECTRON MICROGRAPH OF
CONTROL BILLET AS SINTERED

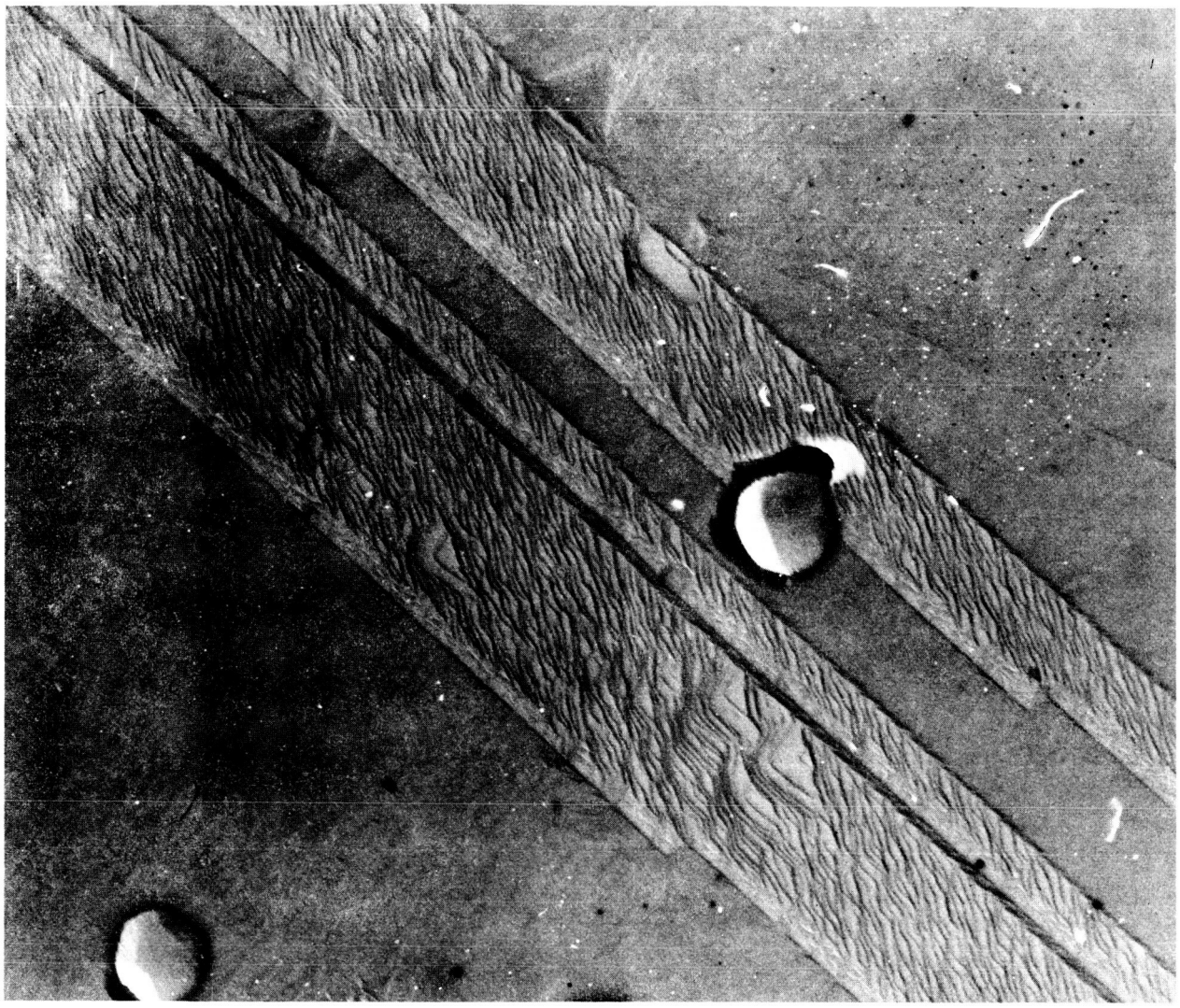

20,000×

FIGURE 28

ELECTRON MICROGRAPH OF CONTROL BILLET
AFTER 100 HOUR THERMAL STABILITY TEST

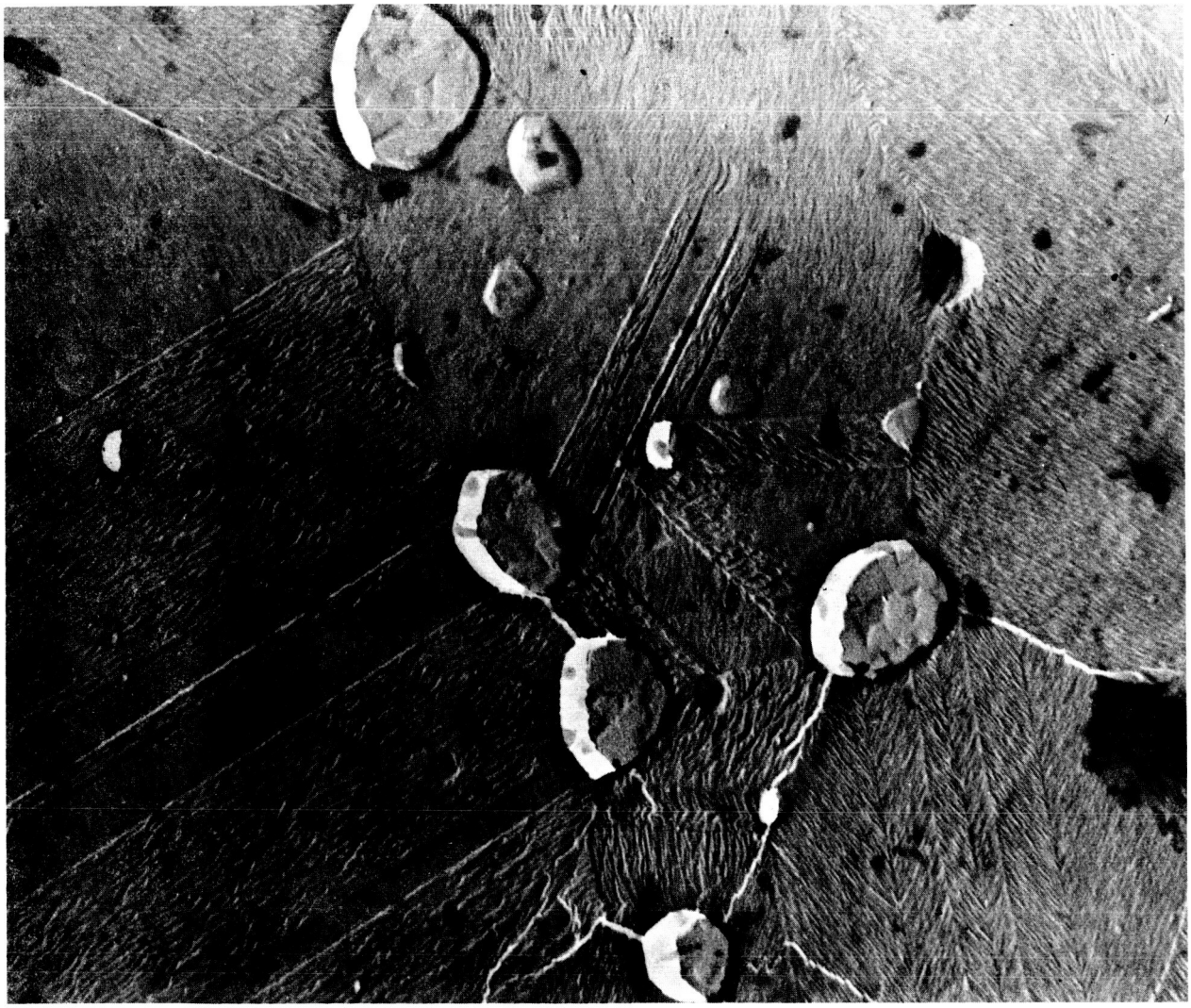

20,000×

FIGURE 29

ELECTRON MICROGRAPH OF BILLET CONTAINING
$2^{v}/o$ ThO_2 AS SINTERED

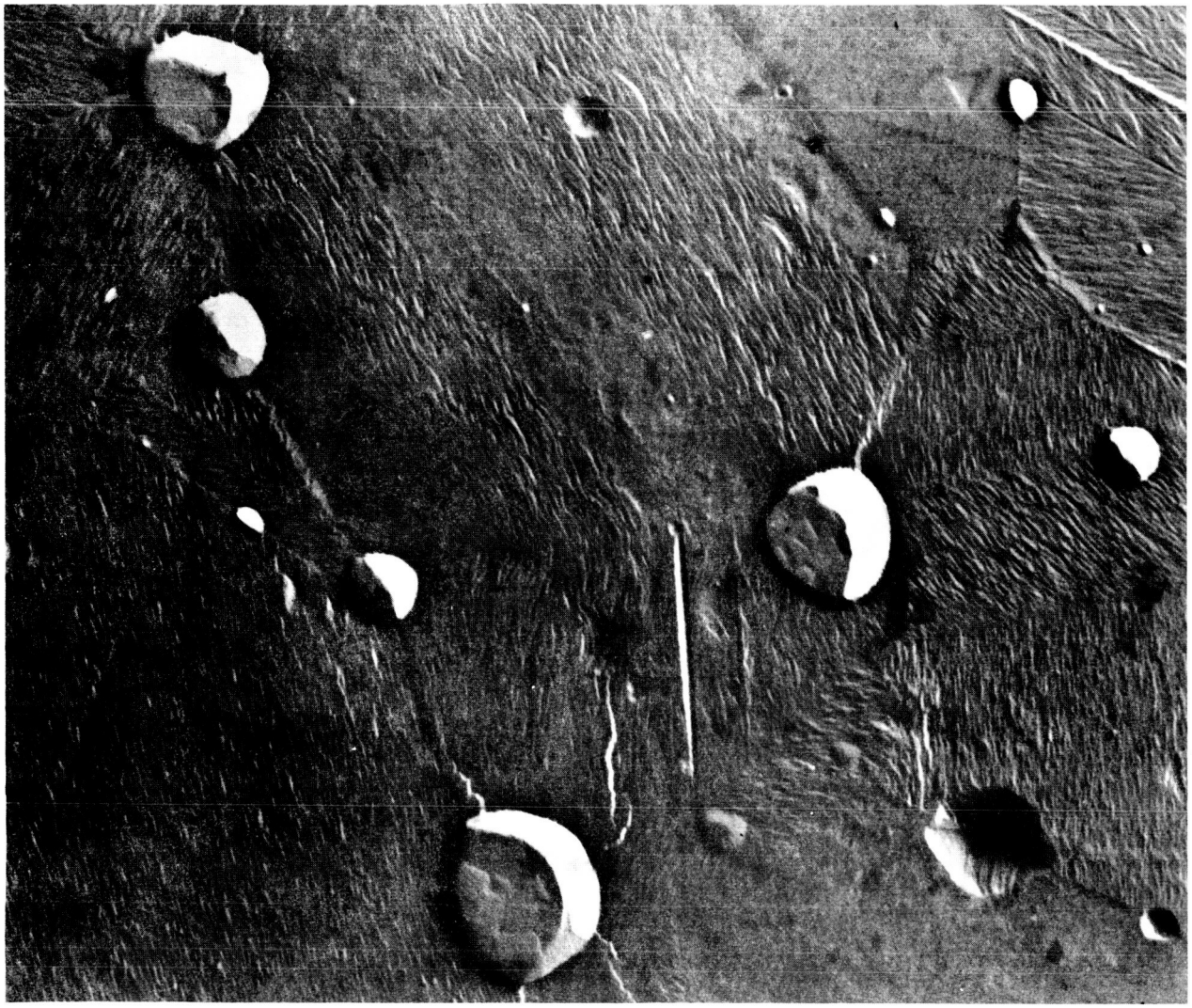

20,000×

FIGURE 30

ELECTRON MICROGRAPH OF BILLET CONTAINING
2^{v}/o ThO_2 AFTER 100 HOURS THERMAL STABILITY TEST

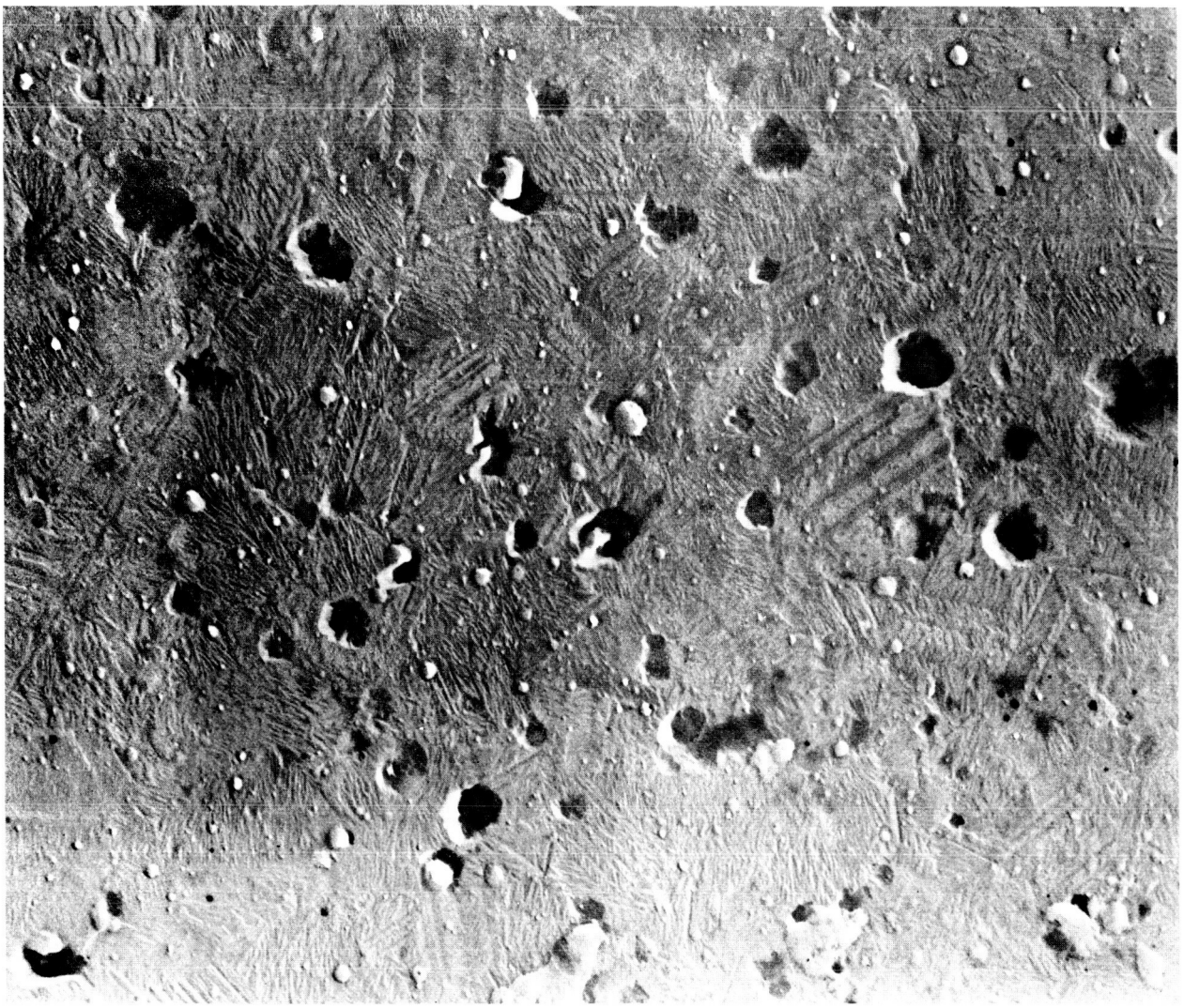

20,000×

FIGURE 31

ELECTRON MICROGRAPH OF BILLET
CONTAINING 4 $^{v}/_{o}$ ThO_2 AS SINTERED

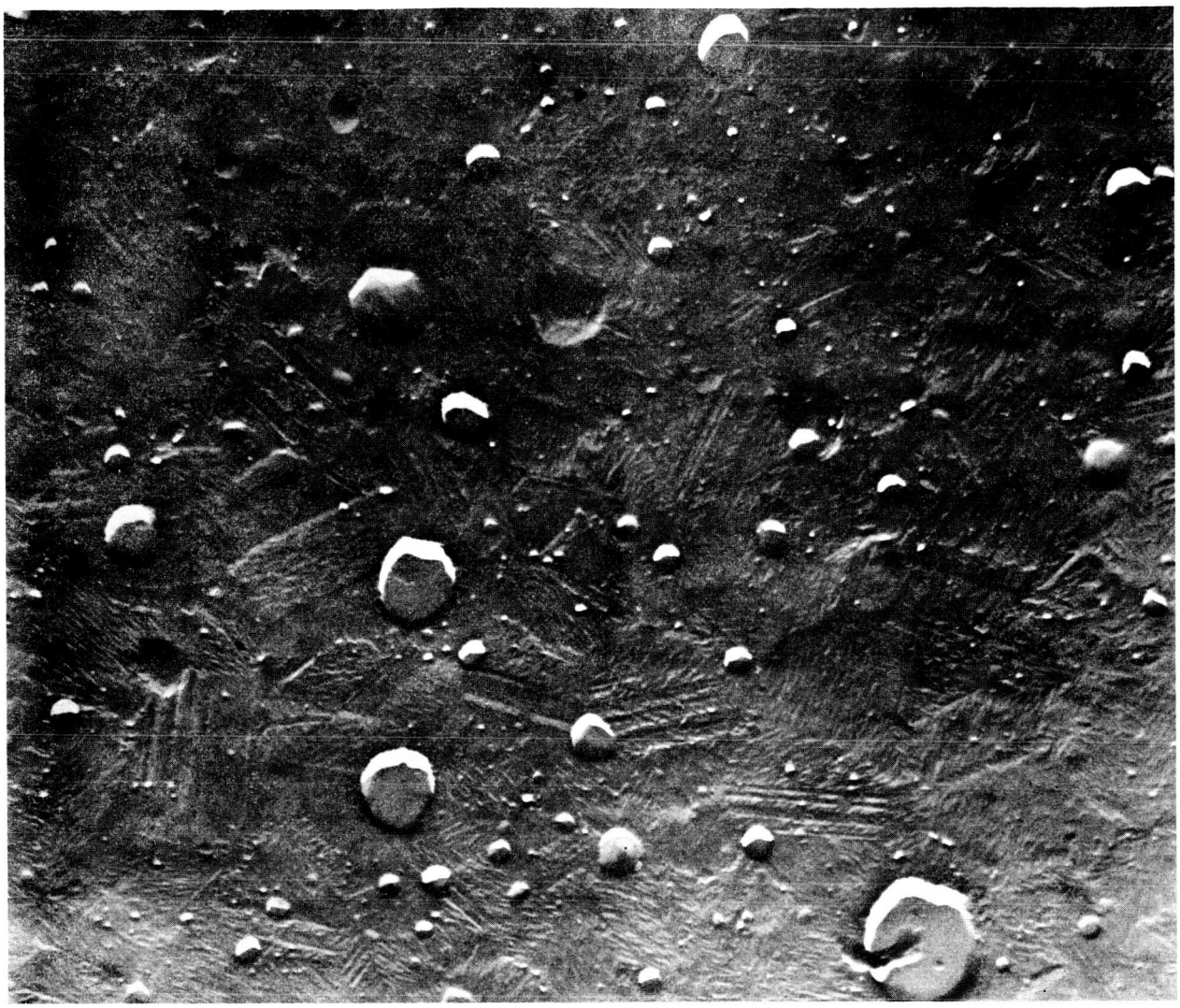

20,000×

FIGURE 32

ELECTRON MICROGRAPH OF BILLET CONTAINING
4 v/o ThO_2 AFTER 100 HOUR THERMAL STABILITY TEST

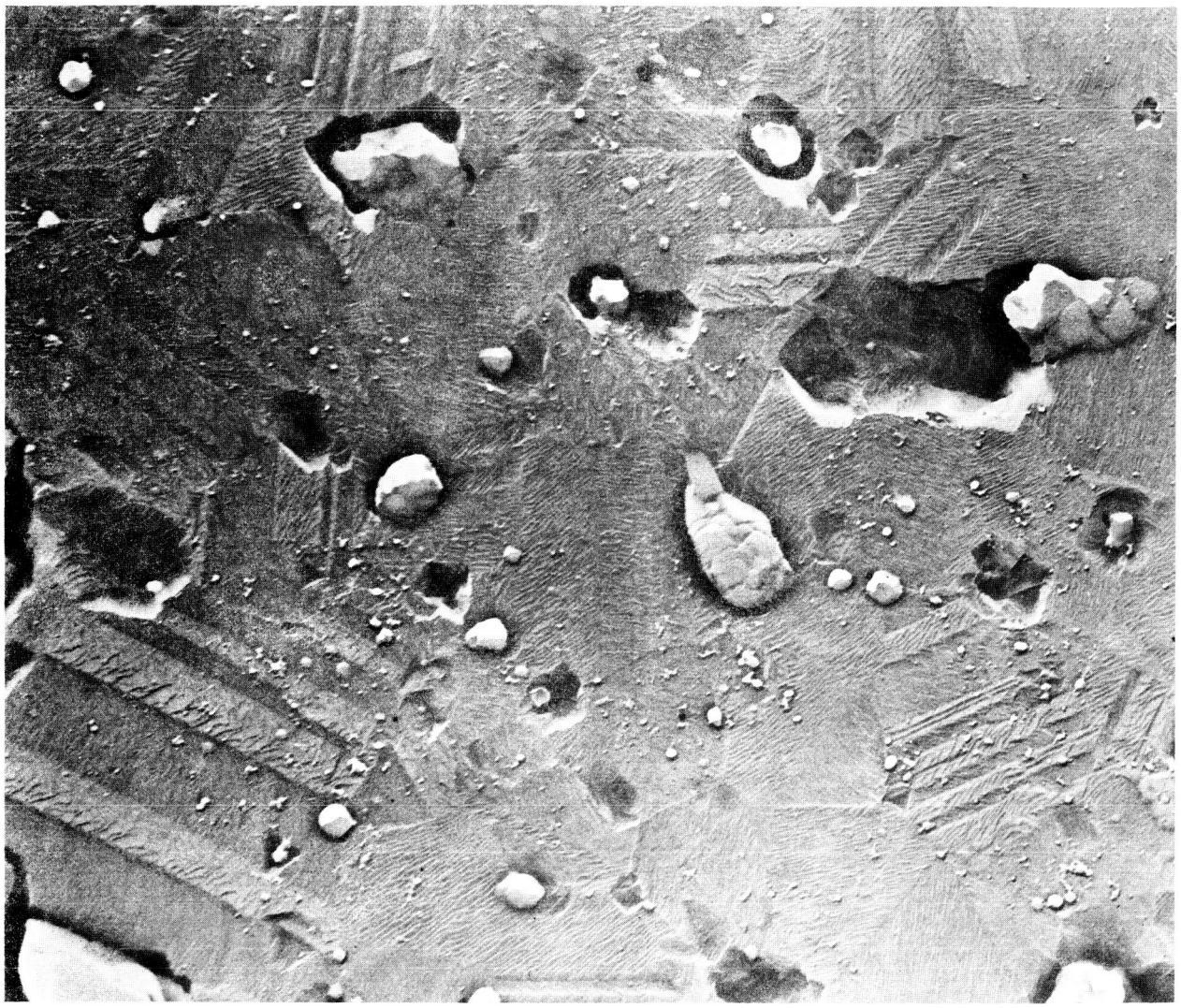

20,000×

FIGURE 33

ELECTRON MICROGRAPH OF BILLET
CONTAINING 7^{v}/o AS SINTERED

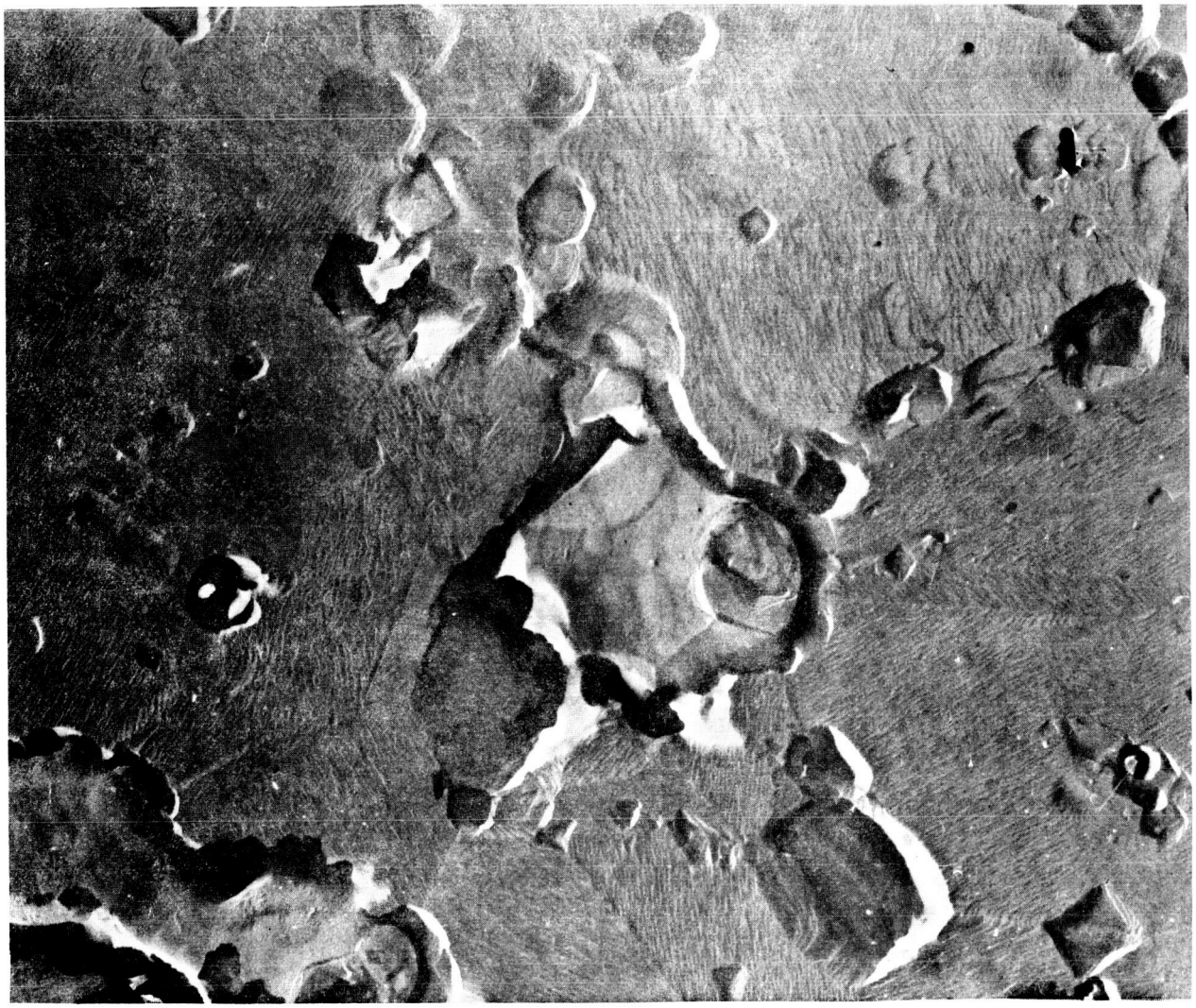

20,000×

FIGURE 34

ELECTRON MICROGRAPH OF BILLET CONTAINING
7 ^{v}/o ThO_2 AFTER 100 HOUR THERMAL STABILITY TEST

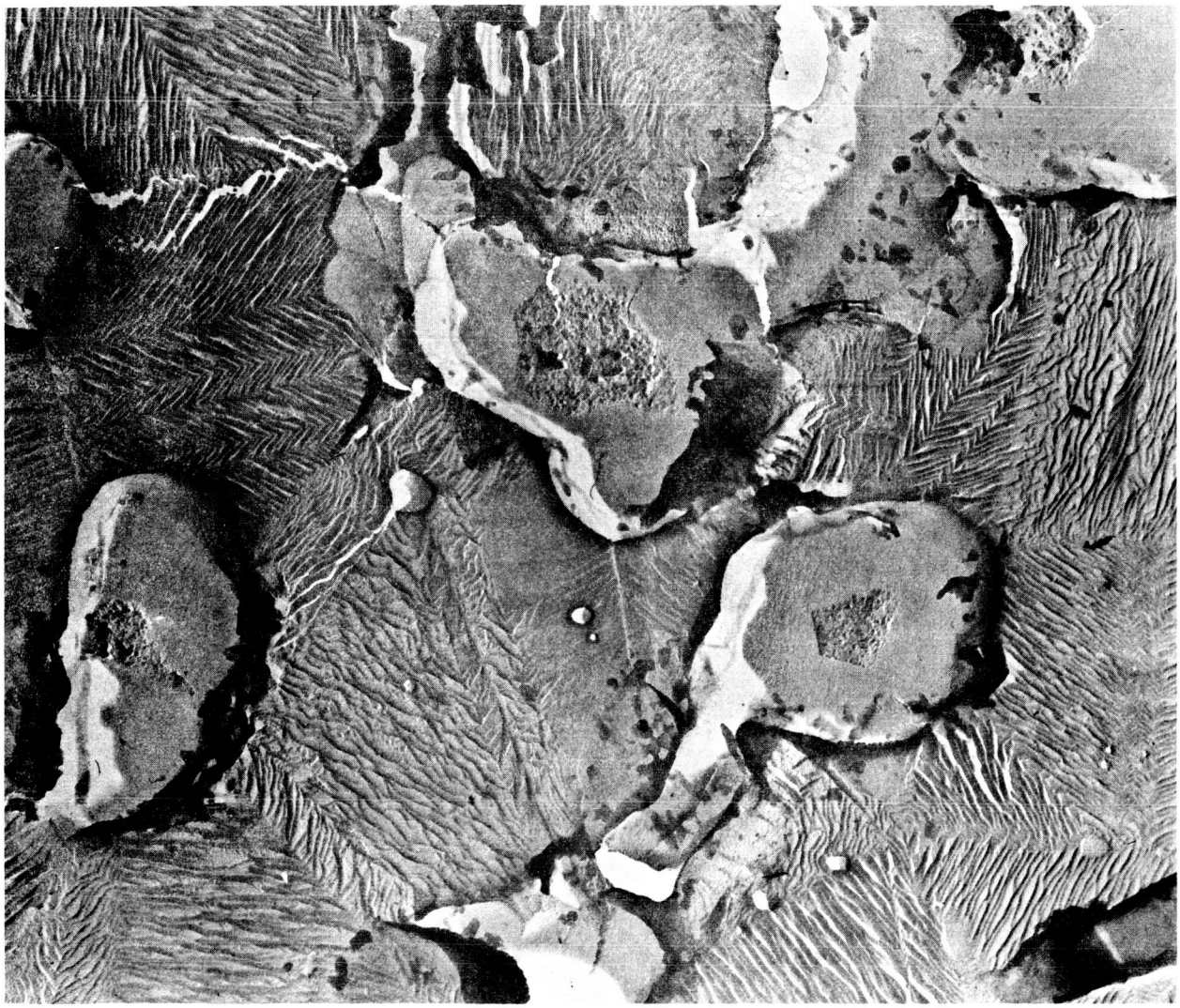

20,000×

FIGURE 35

ELECTRON MICROGRAPH OF BILLET
CONTAINING 2 v/o Y_2O_3 AS SINTERED

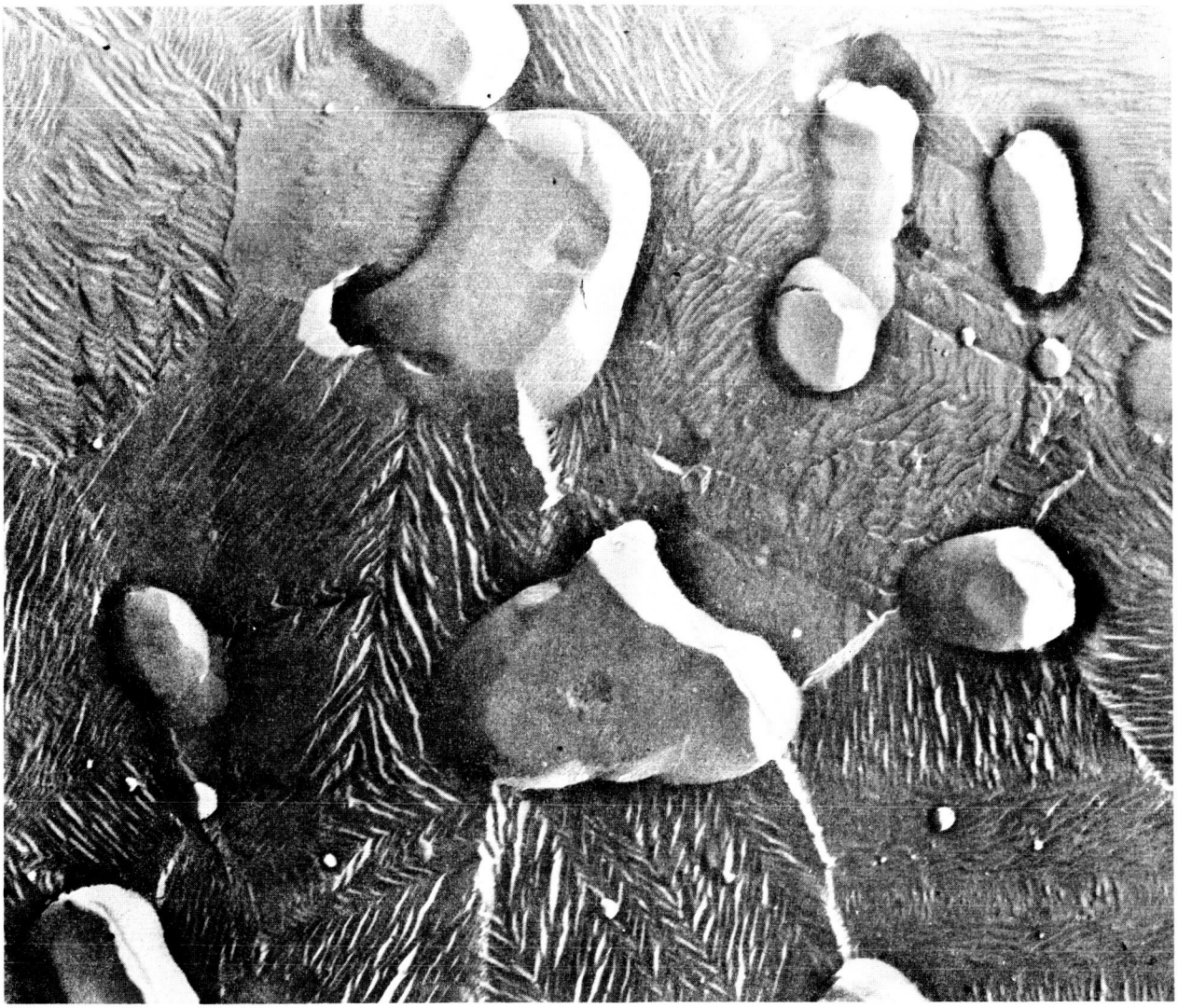

20,000×

FIGURE 36

ELECTRON MICROGRAPH OF BILLET CONTAINING
$2^{v}/o$ Y_2O_3 AFTER 100 HOUR THERMAL STABILITY TEST

20,000×

FIGURE 37

ELECTRON MICROGRAPH OF BILLET
CONTAINING 4 $^{v}/_{o}$ Y_2O_3 AS SINTERED

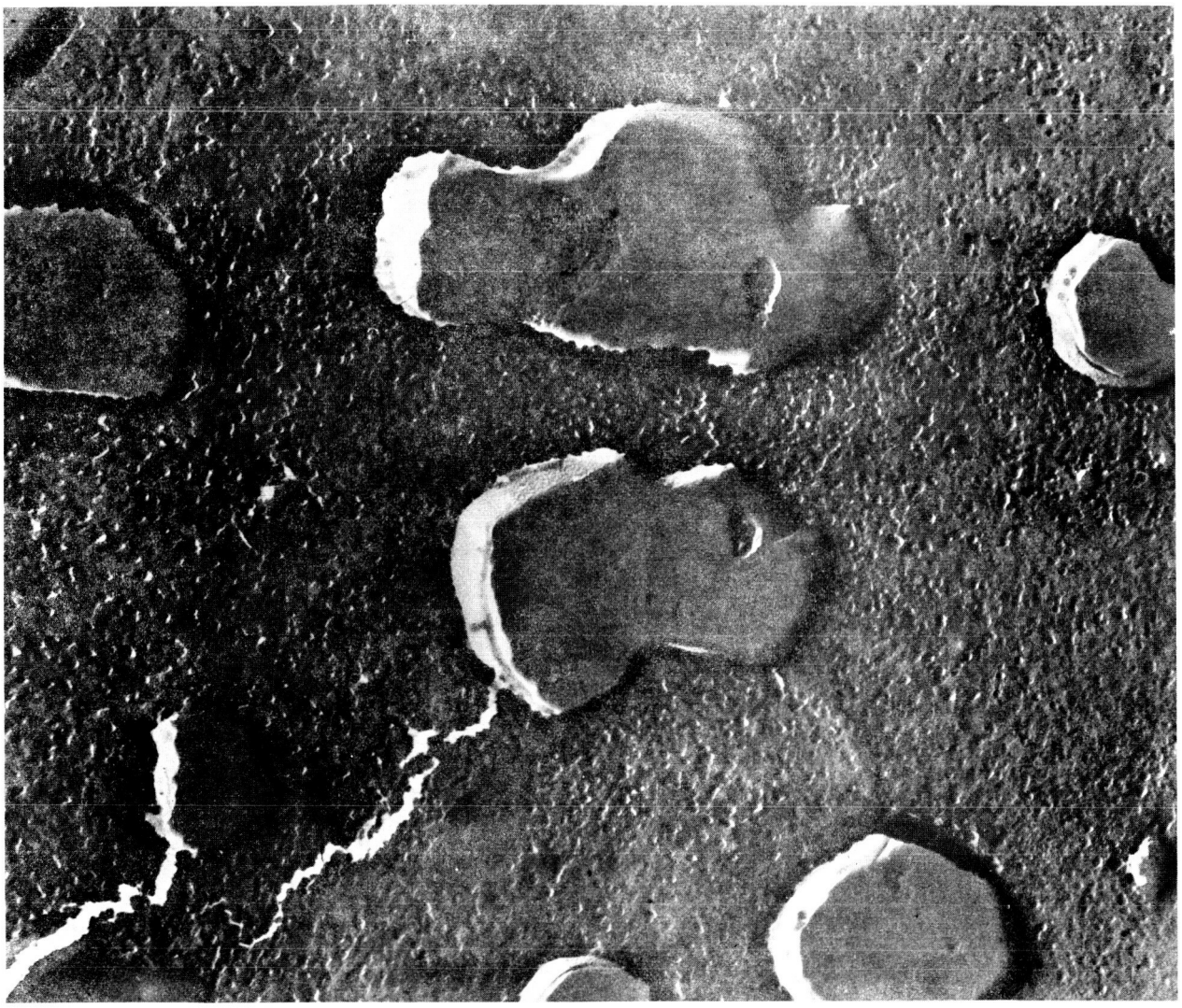

20,000×

FIGURE 38

ELECTRON MICROGRAPH OF BILLET CONTAINING
4 $^{v}/_{o}$ Y_2O_3 AFTER 100 HOUR THERMAL STABILITY TEST

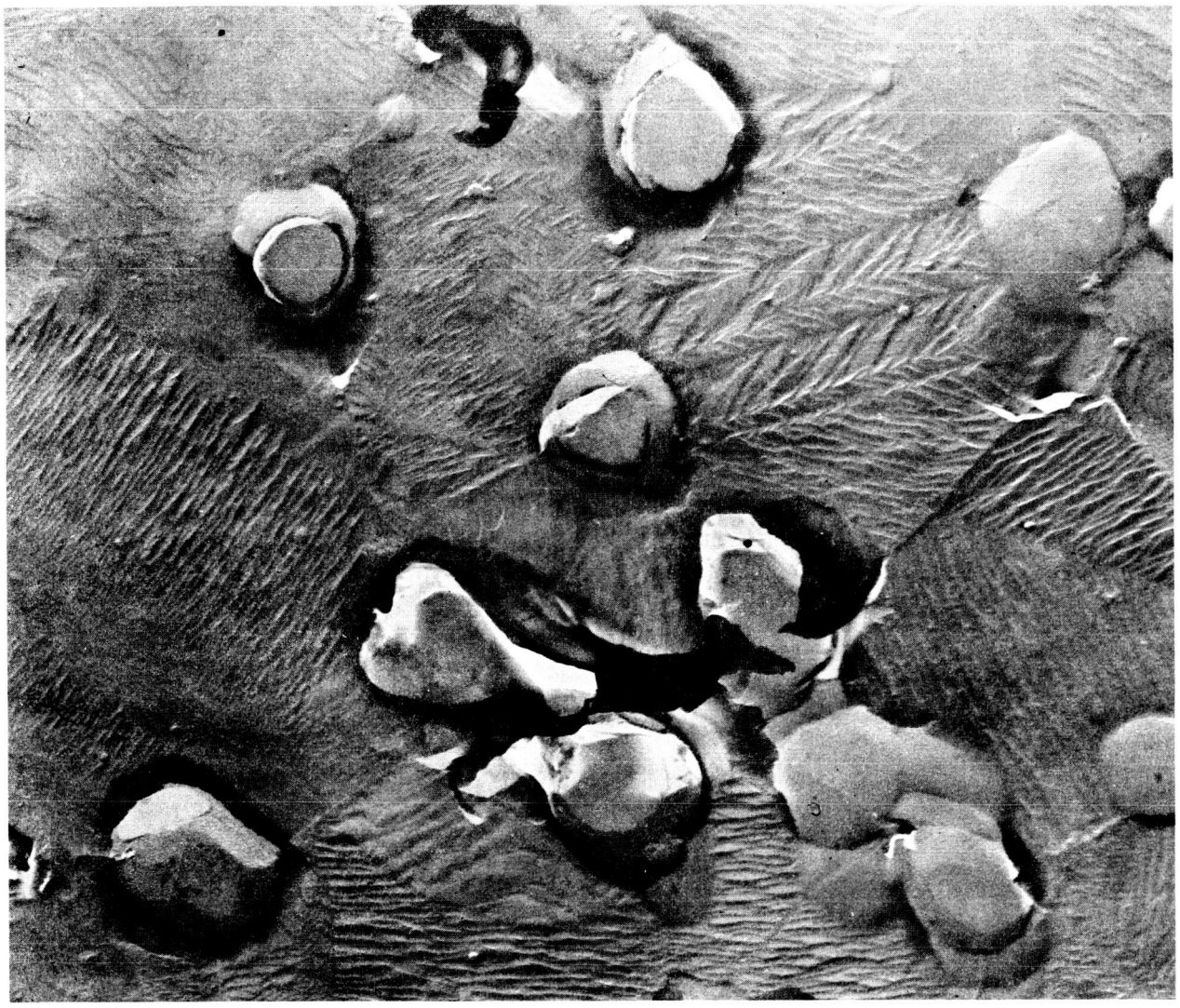

20,000×

FIGURE 39

ELECTRON MICROGRAPH OF BILLET
CONTAINING 7 $^{v}/_{o}$ Y_2O_3 AS SINTERED

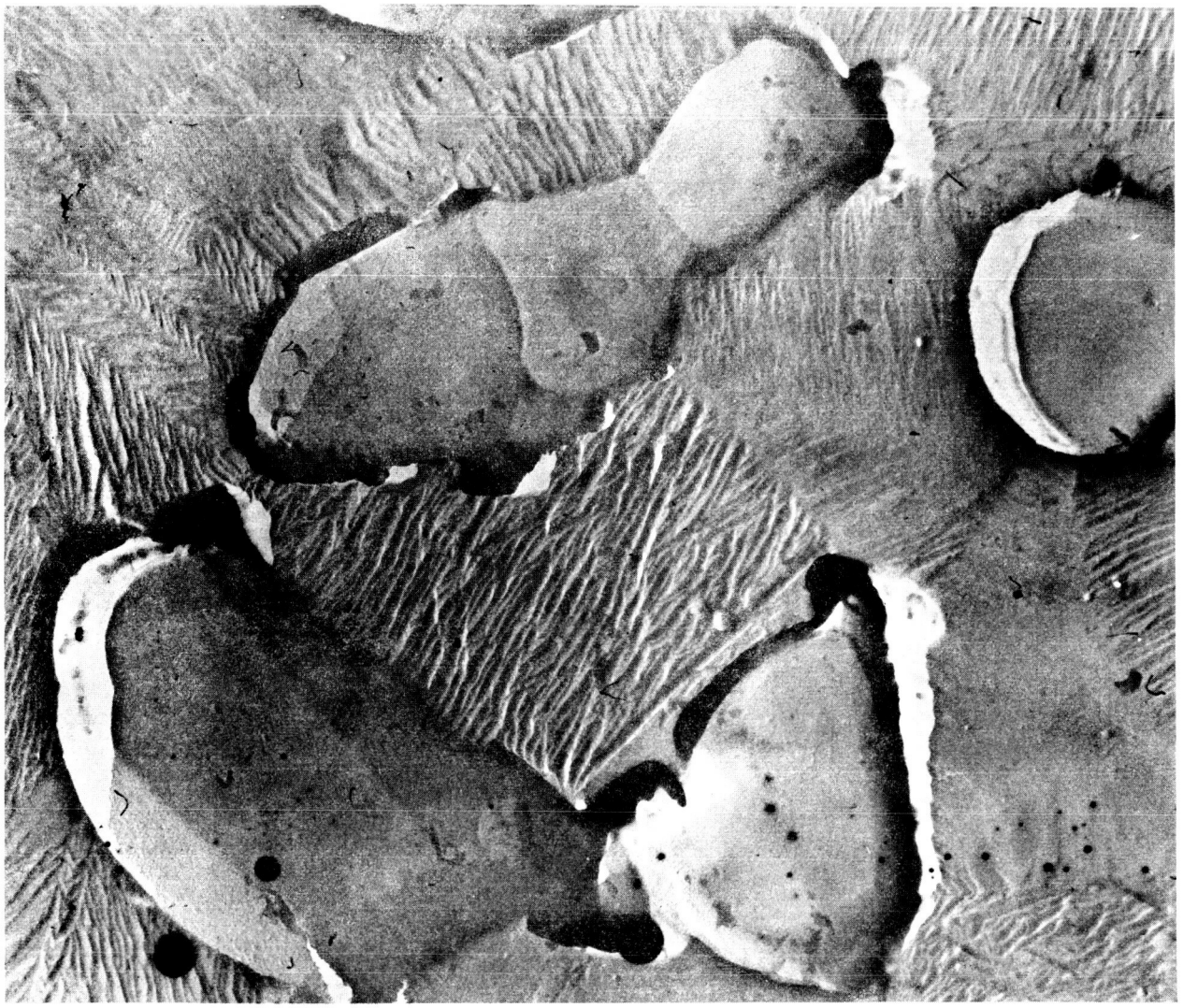

20,000×

FIGURE 40

ELECTRON MICROGRAPH OF BILLET CONTAINING
7 $^{v}/_{o}$ Y_2O_3 AFTER 100 HOUR THERMAL STABILITY TEST

The billets were extruded at the Experimental Metallurgical Plant, Research and Technology Division, Wright Patterson Air Force Base. The billets were extruded at a reduction ratio of 12.5:1 at a temperature of 2000°F through a round, 90° angle, H12 tool steel die faced with zirconium oxide. The die was preheated to 800°F. The breakthrough pressure for the control billet was 132 KSI and the continuous extrusion pressure was 103 KSI. The breakthrough pressure for the 4^{V}/o thoria alloy billet was 142 KSI and the continuous extrusion pressure was 96 KSI. The continuous extrusion pressure for both billets was very uniform. Extruded bar lengths were 70 inches. Tables 12 and 13 are copies of the extrusion data sheets, and Figure 41 is a photograph of the extruded billets.

Nose, middle, and tail sections were cut from the extrusions for evaluation. Immersion densities were determined on stripped midsections, and hardness measurements were taken on the diameter of longitudinal sections of the nose, middle, and tail. Table 14 lists the results of the density and hardness measurements.

Metallographic examination of the extrusion containing 4^{V}/o thoria revealed that the peripheral band observed in the as-sintered billet persisted in the extruded bar. This outside ring appeared to be more porous than the core. The diameter of the extruded core, however, was sufficiently greater than the gage diameter for the stress rupture specimens that no further consideration was given to this peripheral shell. Figures 42 and 43 show microstructures of the various extruded sections.

Nose, middle and tail sections of the extrusions were examined by electron microscopy. The control billet contained gross oxide inclusions in the grain boundaries. Since the as-sintered billet appeared to be essentially free of oxide inclusions, it is assumed that oxidation occurred during the extrusion process probably as the result of faulty canning. The structure of the alloy containing 4^{V}/o ThO_2 appears to be good; however, the preponderance of voids left by the extraction of ThO_2 particles and the preferential etching attack of the matrix around the remaining ThO_2 particles indicates a possible variation of matrix chemistry or submicron porosity around the particles. Figures 44 and 45 show representative electron micrographs of the two alloys extruded.

5.6 Stress Rupture Testing

Preparation of specimens and stress rupture testing was performed by Battelle. Each test specimen was located and identified as shown in Figure 46. The machined test specimen is diagramed in Figure 47.

TABLE 12

RESEARCH AND TECHNOLOGY DIVISION
EXPERIMENTAL METALLURGICAL PLANT
WRIGHT-PATTERSON AIR FORCE BASE, OHIO

EXTRUSION DATA SHEET — SERIAL NO. 2291

DATE 28 March 1967 — TIME

PURPOSE OF TEST Vitro Laboratories — H. M. McCullough (Letter 2/14/67)

BILLET — Composition Sintered Bal. Ni 20Co-10Mo-10W — Identity Control — Weight 12.2 Lbs.

Diameter 2.911" — Length 6.375" — End Shape 60° Angle x ½"

BILLET ACCESSORIES — Nose Block — Follow Block 3.0" F.B. + 3.0" Carbon

Jacket Stainless Steel - .60" thick — Other

CONTAINER — Size (I.D.) 3.072" — Temp. ≈ 800 °F — Mat'l H - 12

Condition 525

DIE — Identity W 451 Rc — Ratio ≈ 12.5:1 — Type 90° Round Angle — Mat'l H - 12 — Size

Hardness Rc 40-42 — Facing ZrO2 — No. Time Used New — Temp. ≈ 800 °F

Condition Before Newc — After Good

BILLET HEATING — Type Preheat — Time — Temp. °F

Type Final Heat Harrop — Time 1 Hour Argon Atm. — Temp. 2000 °F

LUBRICANT — Billet Precoat Mat'l — Qty. — How Applied ~~Painted~~

Billet Final Mat'l 0010 — Qty. .030" — How and When Applied 3/28/67

Container Mos2

Die Mos2

ACCUMULATOR — Start (psi) 3050 — Finish (psi)

BILLET TRANSFER (Sec) — Fce to Cont. — Cont. to Pres. — Total

HIGH PRESSURE ADMISSION — L S Setting — Manual XX — Automatic

LOAD (Tons) — Maximum 490 - 132 KSI — Minimum 380 - 103 KSI — Bottom

RAM SPEED — Valve Setting (Turns) 1.0 — Maximum (ips) 3.0 — Minimum (ips) 2.25 1.5

EXTRUDED Bar — Length 70¼" — Desc. Excellent — Yield Wt.

REFERENCES — Photo No. — X-Ray No. — Spec's

COMMENTS — N C T NB - 0 RA - 12.7:1

.862" .862" .862" SI - 5" KT - 52 KSI

≈ 90% Dense

AFML FORM 15 MAY 64

AF-WP-B-/

TABLE 13

RESEARCH AND TECHNOLOGY DIVISION
EXPERIMENTAL METALLURGICAL PLANT
WRIGHT-PATTERSON AIR FORCE BASE, OHIO

EXTRUSION DATA SHEET — SERIAL NO. 2292

DATE 28 March 1967 — TIME

PURPOSE OF TEST Vitro Laboratories H. M. McCullough (Letter 2/14/67)
Sintered Bal Nickle

BILLET — Composition 20Co-10Mo-10W-Tho2 Identity Tho2 Weight 13.0 Lbs.

Diameter 2.911" Length 6.750" End Shape 60° angle x $\frac{1}{2}$"

BILLET ACCESSORIES — Nose Block — Follow Block 3.0" F.B. + 3.0" Carbon

Jacket Stainless steel - .60" thick Other

CONTAINER — Size (I.D.) 3.072" Temp. ≈ 800 °F Mat'l H - 12

Condition 526

DIE — Identity W 451 Rc Ratio ≈ 12.5:1 Type 90° Round Angle Mat'l H - 12 Size

Hardness Rc 40-42 Facing ZrO2 No. Time Used 1 Temp. ≈ 800 °F

Condition Before Good After Good

BILLET HEATING — Type Preheat Time Temp. °F

Type Final Heat Harrop Time 1 Hour Argon Atm. Temp. 2000 °F

LUBRICANT — Billet Precoat Mat'l Qty. How Applied

Billet Final Mat'l 0010 Qty. .030" How and When Applied Painted 3/28/67

Container Mos2

Die Mos2

ACCUMULATOR — Start (psi) 3050 Finish (psi)

BILLET TRANSFER (Sec) — Fce to Cont. Cont. to Pres. Total

HIGH PRESSURE ADMISSION — L S Setting Manual XX Automatic

LOAD (Tons) — Maximum 525 - 142 KSI Minimum 355 - 96 KSI Bottom

RAM SPEED — Valve Setting (Turns) 1.0 Maximum (ips) 3.0 Minimum (ips) 2.25 1.5

EXTRUDED Bar — Length 75" Desc. Excellent Yield Wt.

REFERENCES — Photo No. X-Ray No. Spec's

COMMENTS —

N	C	T	NB - 0	RA - 12.7:1
.864"	.864"	.864"	SI - 5"	KT - 56 KSI

≈ 90% Dense

AFML FORM 15
MAY 64

AF-WP-?

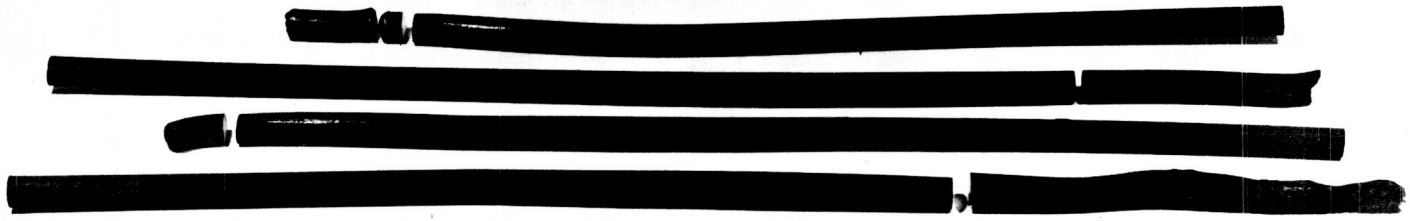

FIGURE 41

EXTRUDED BILLETS

TABLE 14

DENSITY AND HARDNESS MEASUREMENTS OF EXTRUDED SECTION

Density

	Sintered Billet		Extruded Bar
	Bulk Measured Density	Slice Immersion Density	Slice Immersion Density
Control	9.14 gms/cc	9.10 gms/cc	9.55 gms/cc
4 V/o ThO_2	9.60	9.47	9.54

Knoop Hardness, 50 gm Load

	Average	Range
Control		
As Sintered	239	216-274
Nose	292	280-292
Middle	279	273-285
Tail	303	285-309
4 V/o ThO_2		
As Sintered	404	307-517
Nose	356	356-356
Middle	467	457-477
Tail	456	426-476

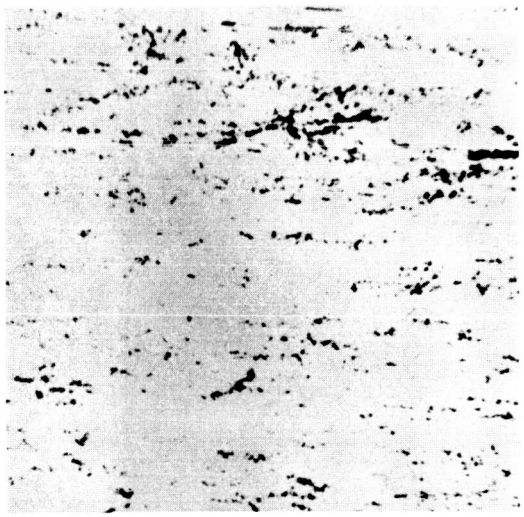

Nose 350x

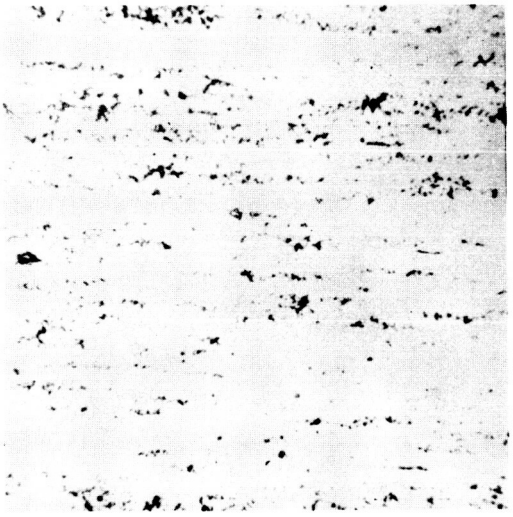

Middle 350x

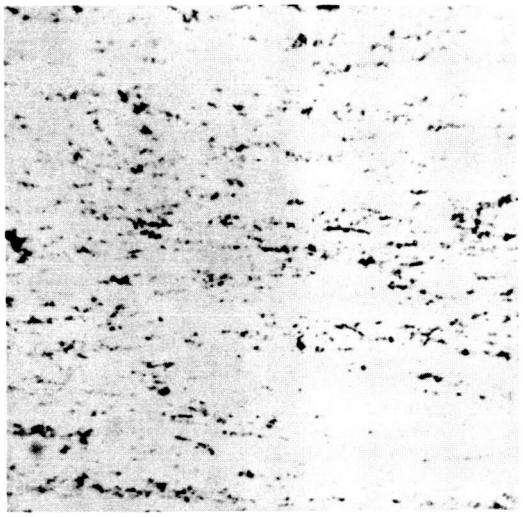

Tail 350x

FIGURE 42

MICROSTRUCTURE OF AS EXTRUDED BILLET
WITHOUT A DISPERSION OXIDE

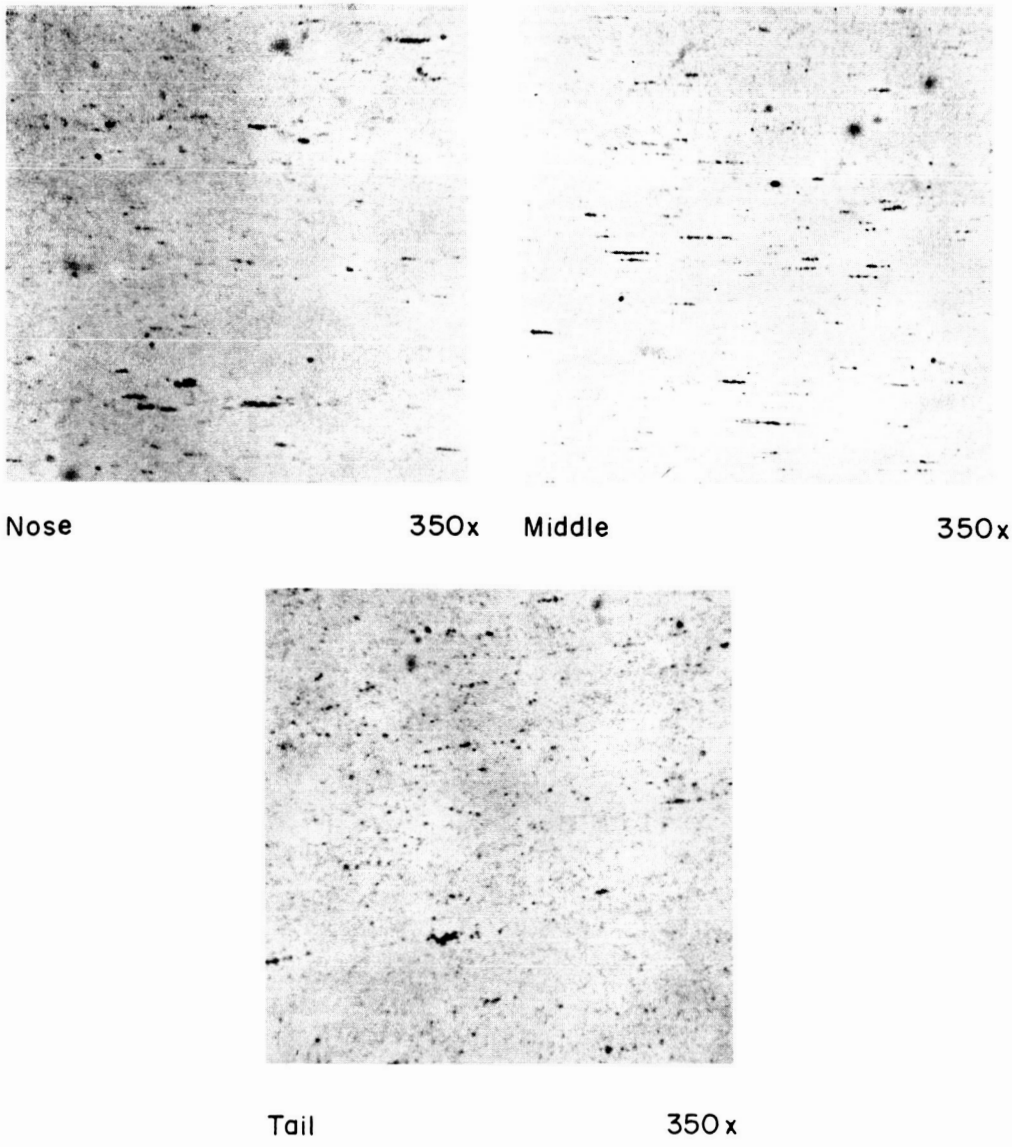

FIGURE 43

MICROSTRUCTURE OF AS EXTRUDED BILLET
CONTAINING 4% THORIA DISPERSION

20,000X

FIGURE 44

ELECTRON MICROGRAPH OF THE EXTRUDED
CONTROL BILLET WITHOUT A DISPERSION OXIDE

20,000X

FIGURE 45

ELECTRON MICROGRAPH OF THE EXTRUDED BILLET CONTAINING 4% ThO_2

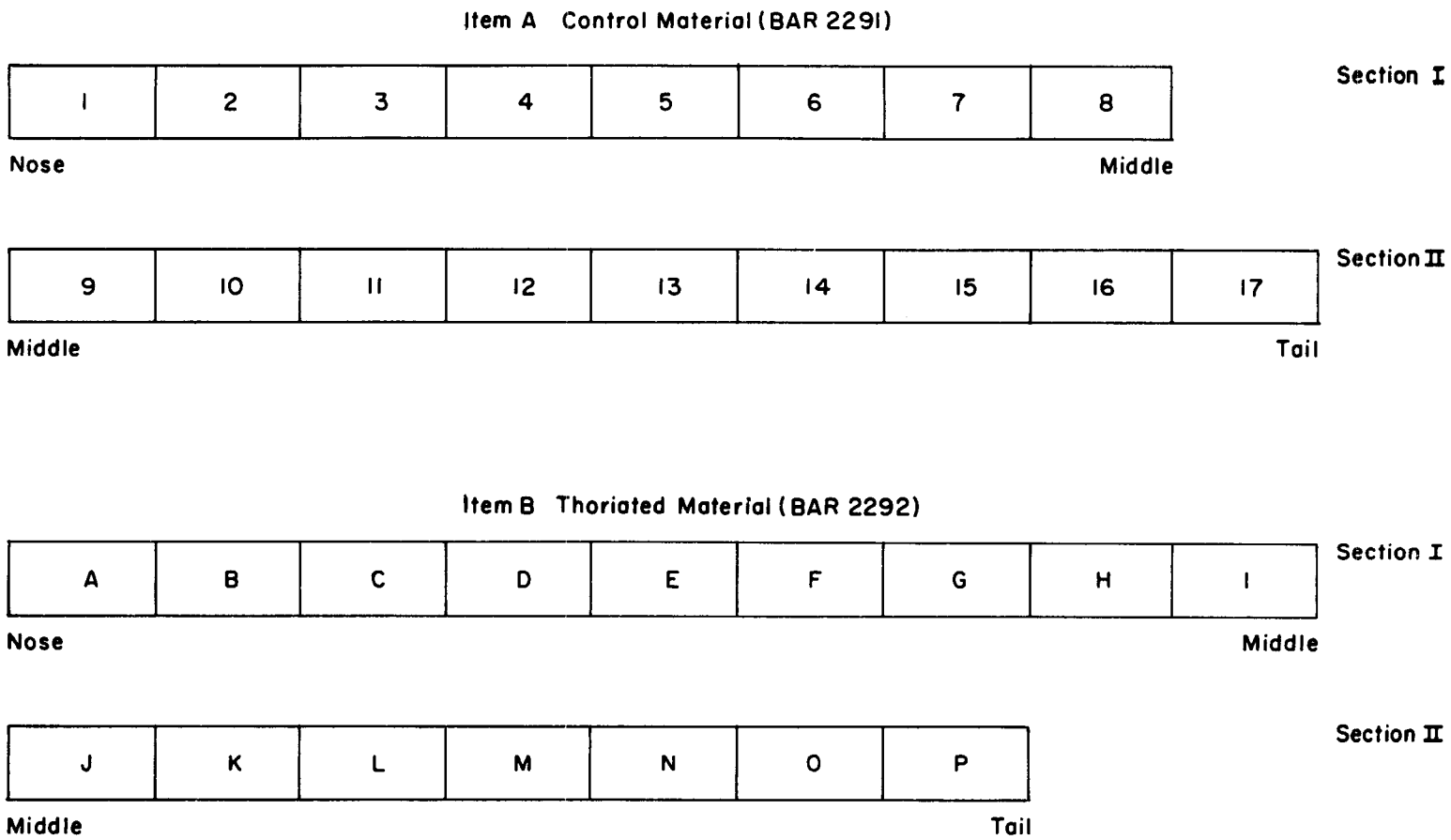

FIGURE 46

LOCATION OF SPECIMENS IN TEST MATERIAL

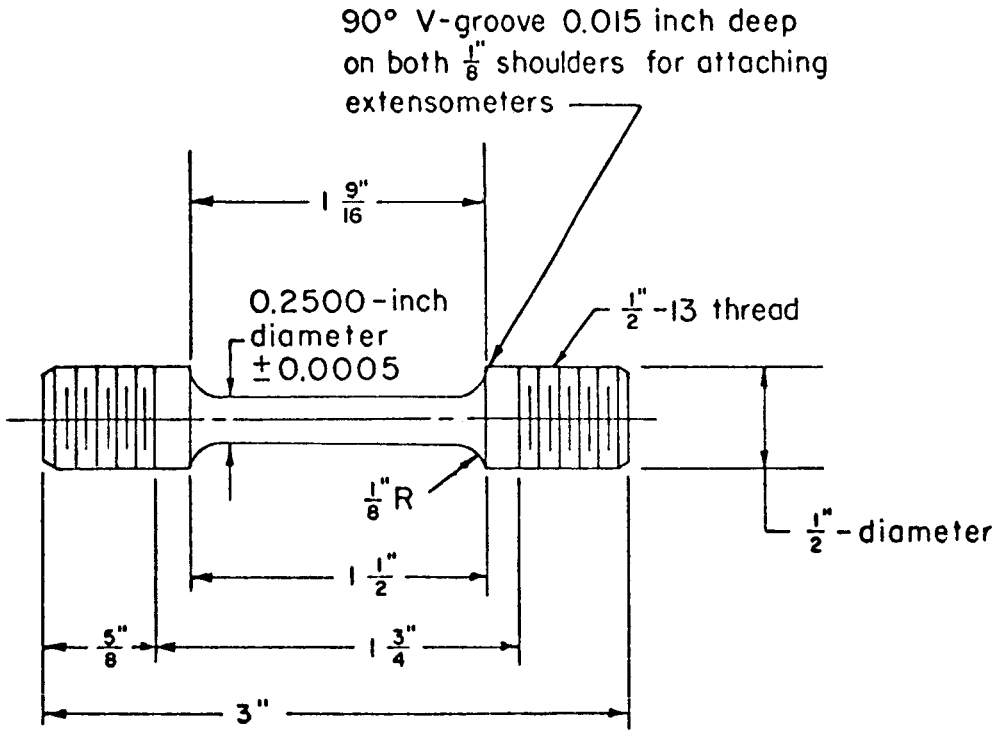

FIGURE 47

1/4-INCH CREEP - RUPTURE SPECIMEN

Stress rupture tests were conducted at 2000°F in vacuum (at 2×10^{-6} torr). The tests were made in a molybdenum-wire resistance furnace. After placing the specimens into the furnace, the chamber was evacuated and the furnace heated to the test temperature. The heating rate was maintained low enough to keep the vacuum pressure below about 5×10^{-5} torr. The test temperature was controlled within ±5°F of 2000°F.

As soon as the vacuum and test temperature were stabilized, the specimen was loaded to the desired stress level through a 9 to 1 ratio lever arm system. Specimen failure interrupted a timer which recorded the rupture time to the nearest tenth of an hour. The specimens were wrapped in molybdenum foil which remained in place during rupture testing. The foil served to prevent contamination from the thermocouple and to reduce contamination from the environment.

The test results obtained are given in Table 15 In view of the apparent oxidation of the control billet during extrusion and the low stress-rupture strengths being obtained, the testing program was discontinued.

TABLE 15

RESULTS OF STRESS-RUPTURE TESTS AT 2000°F

Specimen Number	Stress psi	Rupture Time, Hrs.	Elongation Percent	Reduction of Area, %
		Control Material		
1	2000	0.9	32.5	21.4
2	1500	5.7	47.6	28.8
3	350	105.0 (1)	85.9	47.2
7	1500	2.0	40.2	24.0
8	350	177.3	168.8	62.4
14	1500	1.3	34.1	22.1
15	350	117.0	169.6	62.2
		Thoriated Material		
A	1500	0.4	87.4	46.0
C	1000	8.3	15.6	22.8
B (2)	350	743.5	-	-
B (2)	1000	33.9	61.1	59.2
H	1500	0.50 (3)	-	-
I	1000	9.5	15.0	22.7
N	1500	0.23	105.6	64.1
O	1000	21.8	16.0	26.4

(1) Estimated rupture time. Specimen elongated to limit of machine without failing.

(2) This specimen was initially stressed at 350 psi. The test was discontinued at 743.5 hours. The same specimen was then restressed at 1000 psi.

(3) Furnace failure caused test to be terminated. Rupture time is estimated.

6. DISCUSSION OF RESULTS

One of the major problems associated with the high intensity arc vaporization of a homogeneous electrode is the preparation of an electrode which will withstand the extreme thermal shock during the vaporization parameters in order to obtain the desired product. This problem has been resolved fairly well for electrodes containing one, and in certain cases, two materials.

For the alloy system undertaken in this program, the ferrous group (Ni and Co metals, and the refractory group (Mo and W) metals are conflicting insofar as the electrode composition and vaporization parameters are concerned, at least at the present state of the art. Normally, when vaporizing nickel and/or cobalt, electrodes containing 25% carbon are vaporized at a power level of 45 kw per sq. in. of electrode cross section; whereas, in the vaporization of molybdenum or tungsten, electrodes containing 10% carbon are vaporized at 20 kw per sq. in. of electrode cross section. If the carbon content of tungsten electrodes is greater or less than 10%, excessive melting occurs at the anode face, the product drips from the electrode before it is vaporized, and thus lost from the reacting system. The vaporization is enhanced by increasing power, but the electrode then becomes subject to thermal shock. These different vaporization characteristics of the individual elements are apparent from the data on this alloy system presented in Tables 4 through 8. The ratio of the electrode to product elements shows that the ferrous group (Ni and Co) vaporizes much more readily than the refractory group (Mo, W, ThO_2), and that only a small amount of the ferrous group materials is needed in the electrode to produce a high concentration in the product. Furthermore, for this alloy, when the thoria content was increased in the electrode a greater amount of slagging occurred which necessitated an increase in the Mo and W content of the electrode to obtain the desired product composition. The reasons for these trends are only partially understood and are assso-ciated with the heats of vaporization of the electrode constituents, the reducing conditions at the anode face as a function of the carbon content of the electrode, and the arc temperature.

In all the electron micrographs of the alloys containing thoria, a number of oversized particles are present which, of course, are undesirable. These oversized particles result from the poor vaporization characteristics of the electrode and can form in two possible ways. Small

thoria particles trapped on the surface of a molten drop can agglomerate, fuse, and be blown off by the action of the arc and carried into the product stream. There is some evidence of this in particles shown in the electron micrographs of Figures 29, 30 and 33. The larger particles appear to be made up of fused agglomerates. Oversized particles can also result simply by incomplete vaporization.

From previous experiences, the utilization of submicron dispersion particles in preparing the electrode enhanced subsequent vaporization and yielded a fine submicron dispersion in the product. However, if the anode face is molten and heavy slagging occurs a limiting dispersion particle size is obtained which is larger than that of the dispersion particle size used in the preparation of the electrodes. This seems to support the thesis that agglomeration occurs at the molten face and these fused agglomerates are ejected into the product stream before being completely vaporized. Thus, it appears that the major problem in vaporization lies in the elimination of the molten anode face. If complete vaporization were achieved; as can be accomplished with individual materials, all of the resultant fume product would have particle sizes ranging up to 0-250 Angstroms. Once this condition is achieved, overall process control would be quite simple, and electrode composition would be essentially equivalent to product composition.

The difficulties encountered with the vaporization of yttria to a submicron fume product are not understood at this time. A sufficient effort could not be expended within the scope of this program to resolve the problem.

With regard to the other oxide dispersions studied, it is also believed that the anomalous results were the result of poor vaporization characteristics. An oxide-oxide reaction may have occurred on the molten face and the oversized particles ejected into the product stream before vaporization could be effected. Again, it is believed that many of the oxides can be effectively dispersed as submicron particulates in a complex alloy system by the arc process with the proper vaporization parameters.

Little can be said about the reduction, consolidation and sintering parameters other than that optimum conditions were probably not attained. This problem is a study in itself and was not within the scope of this program. Only sufficient effort was expended to determine parameters which would yield sintered billets having densities of 90% or better.

Although the stress rupture testing was not completed, an estimate of the long time rupture stress can be made by extrapolating the short time data. A log-log plot of stress versus the time to rupture is shown in

Figure 48. Even though the rupture strengths of these alloys are far below the target stress, the effect of thoria additions is evident. For very short times the addition of thoria to the base alloy appears to have a weakening effect, whereas at longer times the alloy is strengthened. This effect, however, is clouded by the fact that the control billet was oxidized during the extrusion cycle and the stress rupture data obtained may not be at all accurate.

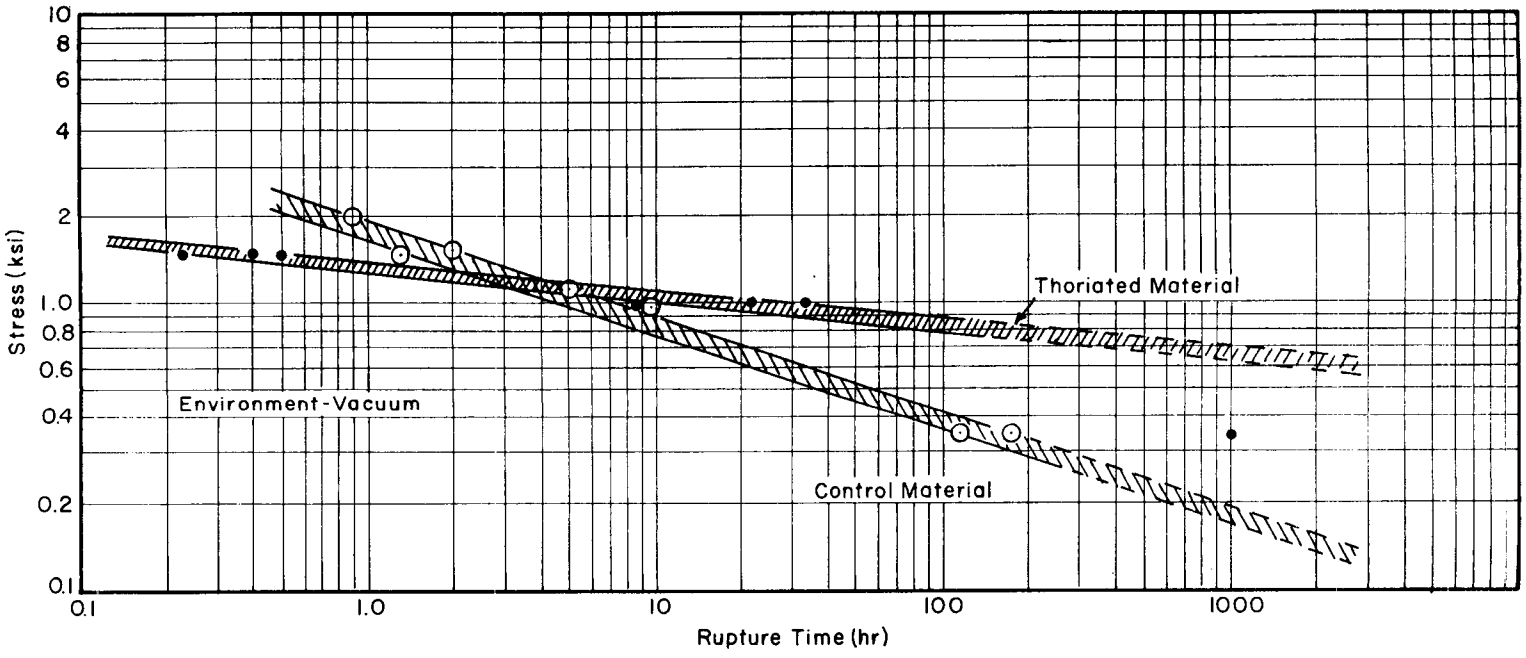

FIGURE 48

STRESS-RUPTURE RESULTS FOR THORIATED
AND CONTROL MATERIAL OF THE
60Ni-20 Co-10Mo-10W ALLOY AT 2000F

7. CONCLUSIONS

The following conclusions were established during the course of this investigation.

a. Electrodes can be made incorporating multiple components and having adequate strength to withstand the large thermal stresses associated with the vaporization process.

b. For the combinations studied in this program, the best materials for the preparation of electrodes at the present state-of-the-art are nickel and cobalt metal powders, molybdenum and tungsten oxide powders, dispersion oxide powder (ThO_2), Black Pearl carbon, and binder.

c. Complete vaporization was not achieved because of the opposing vaporization characteristics of the Ni-Co and Mo-W groups and the lack of higher power of the existing arc equipment.

d. Complete vaporization would eliminate carry-over of large dispersoid particles into the fume product.

e. Vaporization characteristics varied with carbon content, matrix composition, and dispersoid content of the electrode. An adjustment of the matrix composition of the electrode was required when either the carbon or dispersion oxide content was varied.

f. Reactions occurred between Al_2O_3, La_2O_3, and Y_2O_3 and other matrix oxides during vaporization resulting in large fused particles. No explanations for these reactions are available at the moment.

g. A possible reaction or anomalous vaporization of ZrO occurs yielding hollow particles.

h. The process was reproducible once the conditions were established for a given product composition.

i. Sulfur contents can be reduced to less than 30 ppm by calcining the fume product prior to hydrogen reduction.

j. Reduction can be carried out in a dry hydrogen atmosphere where all but the dispersoid is reduced.

k. The sintering of billets containing thoria, yttria, and without a dispersion oxide to densities in excess of 90% theoretical can be accomplished effectively by sintering in hydrogen at 1350°C for two hours.

l. The extrusion of canned billets can be accomplished successfully by extruding at a billet temperature of 2000°F.

m. The extruded material containing thoria and the control material, i.e., without a dispersion oxide, had extremely low strengths when tested at 2000°F, and it is believed that a suitable working schedule could improve the properties of the alloy.

n. The ThO_2 dispersion was not affected by the extrusion process.

o. The ThO_2 dispersion was stable in the alloy matrix after a 100 hour thermal treatment at 1225°C.

8. RECOMMENDATIONS

a. Development work should be undertaken to optimize the vaporization parameters to obtain complete vaporization of a homogeneous electrode containing multiple components. This would provide optimum control of electrode-to-product chemistry, eliminate oversized particles, and give maximum yield of product.

b. An investigation should be made of the feasibility of using multiple electrodes each of which would be composed of materials having similar vaporization characteristics, and each would be vaporized at predetermined rates into a common collector to provide the desired fume composition.

c. Investigations should be made on other dispersion oxides and means to introduce the dispersion into arc produced materials to obtain small particles and eliminate the reaction between the dispersion oxide and matrix oxides.

d. Studies should be made on the direct extrusion of powder without preliminary sintering.

e. An investigation of the working parameters should be made to obtain optimum strength of extruded material.

f. The relationships of process parameters over the entire range for alloy mixtures should be established.

APPENDIX A

RAW MATERIALS AND CHEMICAL ANALYSES

APPENDIX A

RAW MATERIALS AND CHEMICAL ANALYSES

Nickel Powder — Grade G-09
Sherritt Gordon Mines Limited
Fort Saskatchewan, Canada

Cobalt	0.090%
Copper	0.003
Iron	0.009
Sulfur	0.004
Phosphorus	<0.001
Carbon	0.023
H_2 loss	0.46
Nickel	Balance

Cobalt Powder — 300 Mesh
African Metals Corporation
New York, New York

Calcium	0.048%
Copper	0.001
Iron	0.063
Manganese	0.013
Nickel	0.085
Silicon	0.032
Sulfur	0.006
Carbon	0.021
H_2 loss	0.209
Cobalt	Balance

Molybdenum Trioxide	Reagent Matheson Company, Inc. East Rutherford, New Jersey
Ammonium	0.002%
Chloride	0.002
Heavy Metals	0.005
Insolubles in MH_4OH	0.010
Nitrate	0.003
Arsenate, Phosphate and Silicate	0.0005
Sulfate	0.020
Assay	99.5

Tungstic Oxide	Yellow Wah Chang Corporation Glen Cove, New York
Aluminum	0.001
Calcium	0.001
Cobalt	0.001
Chromium	0.001
Copper	0.001
Iron	0.001
Magnesium	0.001
Manganese	0.001
Molybdenum	0.007
Nickel	0.001
Lead	0.001
Silicon	0.001
Tin	0.001

Zirconia

Reactor Grade-Micronized
Zirconium Corporation of America
Solon, Ohio

Aluminum	100 ppm
Boron	< 1
Cadmium	< 1
Calcium	700
Chlorine	12
Chromium	10
Cobalt	<10
Copper	<10
Fluorine	<10
Hafnium	<50
Iron	170
Lead	<10
Magnesium	200
Manganese	<10
Molybdenum	<10
Nickel	<10
Silicon	300
Sulfur (SO_4)	480
Tin	<10
Titanium	<10
Vanadium	<10
Loss on Ignition	100
ZrO_2	Balance

Thoria

Grade 112H
American Potash
Rare Earth Division (Lindsay)
North Chicago, Illinois

Aluminum	< 8 ppm
Calcium	<60
Copper	< 2
Lead	10
Lithium	ND
Magnesium	200
Nickel	<0.5
Potassium	ND
Silicon	200
Sodium	23
Rare Earths	<20

Carbons

	Ash	SiO_2	Sulfur	
Philblack E	0.17%	>0.01	0.6%	(L)
G-38	0.18	0.18	<10 ppm	(L)
G-48	0.019	<0.01	<30	
Black Pearl	0.019	<0.01	800	
Thermax	0.16	0.14	70	(L)
Cathodes			30	(L)
Binder			630	(L)

(L) Analysis made by Ledoux and Company
All others made by Vitro Laboratories